

FINAL REPORT

Demonstration of ROV-Based Underwater Electromagnetic Array Technology

ESTCP Project MR-201233

MARCH 2016

Dr. Gregory Schultz
White River Technologies

Distribution Statement A
This document has been cleared for public release



Page Intentionally Left Blank

This report was prepared under contract to the Department of Defense Environmental Security Technology Certification Program (ESTCP). The publication of this report does not indicate endorsement by the Department of Defense, nor should the contents be construed as reflecting the official policy or position of the Department of Defense. Reference herein to any specific commercial product, process, or service by trade name, trademark, manufacturer, or otherwise, does not necessarily constitute or imply its endorsement, recommendation, or favoring by the Department of Defense.

Page Intentionally Left Blank

REPORT DOCUMENTATION PAGE					<i>Form Approved</i> OMB No. 0704-0188	
<p>The public reporting burden for this collection of information is estimated to average 1 hour per response, including the time for reviewing instructions, searching existing data sources, gathering and maintaining the data needed, and completing and reviewing the collection of information. Send comments regarding this burden estimate or any other aspect of this collection of information, including suggestions for reducing the burden, to Department of Defense, Washington Headquarters Services, Directorate for Information Operations and Reports (0704-0188), 1215 Jefferson Davis Highway, Suite 1204, Arlington, VA 22202-4302. Respondents should be aware that notwithstanding any other provision of law, no person shall be subject to any penalty for failing to comply with a collection of information if it does not display a currently valid OMB control number.</p> <p>PLEASE DO NOT RETURN YOUR FORM TO THE ABOVE ADDRESS.</p>						
1. REPORT DATE (DD-MM-YYYY) 05/25/2016		2. REPORT TYPE Final Report			3. DATES COVERED (From - To) April 2012 - March 2016	
4. TITLE AND SUBTITLE Demonstration of ROV-based Underwater Electromagnetic Array Technology				5a. CONTRACT NUMBER W912HQ-12-C-0075		
				5b. GRANT NUMBER		
				5c. PROGRAM ELEMENT NUMBER		
6. AUTHOR(S) Dr. Gregory Schultz				5d. PROJECT NUMBER MR-201233		
				5e. TASK NUMBER		
				5f. WORK UNIT NUMBER		
7. PERFORMING ORGANIZATION NAME(S) AND ADDRESS(ES) White River Technologies 1242 Chestnut Street Newton, MA 02464					8. PERFORMING ORGANIZATION REPORT NUMBER	
9. SPONSORING/MONITORING AGENCY NAME(S) AND ADDRESS(ES) Environmental Security Technology Certification Program (ESTCP) 4800 Mark Center Drive Suite 17D08 Alexandria VA 22350-3600					10. SPONSOR/MONITOR'S ACRONYM(S) ESTCP	
					11. SPONSOR/MONITOR'S REPORT NUMBER(S)	
12. DISTRIBUTION/AVAILABILITY STATEMENT Approved for public release; distribution is unlimited.						
13. SUPPLEMENTARY NOTES N/A						
14. ABSTRACT The objective of this project is to evaluate innovative technologies required for deploying underwater electromagnetic induction (EMI) sensors from remotely operated vehicles (ROVs). The integration of these platforms, highly accurate navigation and control systems, and a high-resolution electromagnetic array can overcome limitations of current diver-deployed, towed, and unmanned integrated underwater ordnance systems.						
15. SUBJECT TERMS						
16. SECURITY CLASSIFICATION OF:			17. LIMITATION OF ABSTRACT	18. NUMBER OF PAGES 108	19a. NAME OF RESPONSIBLE PERSON Gregory Schultz	
a. REPORT	b. ABSTRACT	c. THIS PAGE			19b. TELEPHONE NUMBER (Include area code) 603-678-8385	
U	U	U				

Page Intentionally Left Blank

Acknowledgements

This work was conducted as part of Environmental Security Technology Certification Program (ESTCP) Project MR-201233 led by White River Technologies. Dr. Gregory Schultz was the Principal Investigator. Joe Keranen of White River Technologies provided significant effort in data collection and analysis. Erik Russell, Chet Bassani, and Randall Reynolds of White River Technologies supported system engineering, mobilization, and documentation of the integrated ROV-EM system. Ben Kinnaman and Andy O'Brien of Greensea Systems provided engineering and operational expertise on the ROV navigation and control systems as well as access to and support for the implementation of the ROV systems tested. The authors wish to thank Cobalt Marine LLC for support of marine survey equipment and diving infrastructure. In particular, we would like to thank Gary Randolph for in-kind access to test facilities and the Dolores HAUV system.

Funding for this project was provided by the ESTCP. We wish to express our sincere appreciation to Dr. Anne Andrews, Dr. Herb Nelson, and Dr. Michael Richardson for providing support and guidance for this project.

This report was prepared under contract to the Environmental Security Technology Certification Program. The publication of this report does not indicate endorsement by the Department of Defense, nor should the contents be construed as reflecting the official policy or position of the Department of Defense. Reference herein to any specific commercial product, process, or service by trade name, trademark, manufacturer, or otherwise, does not necessarily constitute or imply its endorsement, recommendation, or favoring by the Department of Defense.

Page Intentionally Left Blank

Executive Summary

The overarching goal of this demonstration project was to evaluate innovative technologies required for deploying underwater electromagnetic induction (EMI) sensors from remotely operated vehicles (ROVs) in order to overcome limitations of current diver-deployed, towed, and unmanned integrated underwater unexploded ordnance (UXO) detection systems. The tests and demonstrations reported on here constitute the first for a tightly integrated hybrid AUV and EMI technology for UXO operations. The data collection and analyses we conducted were intended as an evaluation in preparation for follow-on demonstrations at a current or former Department of Defense (DoD) underwater ranges. This report summarizes the technology used, specific applications tested, and results obtained for a combined underwater ROV-EMI technology. We began our study with graduated and systematic testing in laboratory tanks and pool environments in New Hampshire, then controlled harbor sites in Massachusetts and Florida, and then demonstrated the fully integrated technology at open water test sites we established in North Carolina and Florida. Since the nature of the testing activities involved engineering integration, iterative evaluations and adjustments to optimize the system, we selected demonstration test sites that balanced tradeoffs between rigorous and representative conditions, site variability, and ease of access and control. This report focuses primarily on our final demonstration of the technology, but results from our earlier work and engineering trials are provided in an interim report contained in Appendix B.

For this demonstration we integrated and implemented a hybrid autonomous undersea vehicle (HAUV) designed to provide a stable and mobile geophysical sensing platform for seafloor investigations. The HAUV combines a vector-controlled propulsion system with a highly accurate inertial navigation and control unit in order to provide a number of controlled autonomous or manual survey missions. These include waypoint navigation, bottom following, and station keeping - all of which enable important aspects of maneuverability and positioning control in close proximity to the seafloor. This ROV platform was integrated with the multi-sensor frequency-domain digital EMI array (MFDA). This EM array employs three differential (quadrupole) receivers and acquires frequency-domain in-phase and quadrature-phase magnetic field data at discrete frequencies over the band from 400 Hz to 40 kHz.

The inertial navigation and control system used on the ROV allowed for the robust detection of small munitions (60 mm diameter) under varied conditions by providing accurate sensor positioning while executing autonomous search modes in water depths of up to 20 m. In April of 2015, we established a temporary UXO test grid site on the seafloor within the Florida Keys National Marine Sanctuary approximately 7km south of the Boca Chica Key Naval Air Station in the lower Florida keys. This site provided moderate variability in bottom conditions, currents, and had been surveyed previously using sonar and handheld magnetometer and EMI systems. The test site was surveyed and prepared by divers including the installation of 30m X 40m target grid comprised of 23 test items including 14 inert UXO simulants, 5 steel industry standard objects (ISO's), and 4 clutter items.

We successfully demonstrated a number of functions of the integrated ROV-EMI sensor system including: (i) bottom seabed following to within ± 10 cm at a commanded 50 cm standoff, (ii) system station keeping to within ± 20 cm of a commanded target location, (iii) waypoint navigation to within $<1\%$ of distance travelled and line following to within 75 cm at all times,

and (iv) UXO target detection with signal-to-noise ratios >20 dB and localization accuracy within 70 cm.

The demonstration we conducted was the first that we are know of in which a full marinized multi-sensor EMI array was tightly integrated with an ROV system capable of controlled maneuvers close to the seafloor. Despite the preliminary nature of our assessment, we were able to evaluate the prospects and potential challenges for directly transitioning and implementing the system and related procedures for operational use in MMRP production environments. The implementation prospectus is divided into three distinct type of applications or survey missions: 1) local area UXO detection search (0.5 to 2.5 acres at a time), 2) close-in anomaly characterization (full coverage dynamic characterization and localization), and 3) reacquisition and cued data collections. The ROV-EM systems was successful and effective at completing each mission type, with the close-in anomaly characterization being the most effective application of the technology.

In addition, we conducted assessments of the cost and logistical complexities for potential deployment and operations of the technology. Projected weekly rates of approximately \$7,500 for the integrated ROV-based EM system (including an ROV operator) we demonstrated lead to considerable savings relative to deployment of an EOD-trained dive team searching the seafloor for UXO. Estimation of incurred costs of labor and equipment during survey mode operations yields 100% areal coverage costs of approximately \$600/acre. We assessed potential cost savings through the use of this technology for a particular UXO site study where 500 survey contacts required reacquisition and further investigation. In this case, the ROV-EM system reveals as much as a 60% cost savings relative to conventional diver-based methods. Previous assessments have identified as many as 420 underwater ranges at over 120 different military sites comprising approximately 10 million acres of marine or lacustrine environment potentially contaminated with UXO. Of these 420 sites, it projected that 90 or more contain water depths that prohibit the use of towed geophysical survey systems or EOD divers. Where sites are shallow enough for EOD divers (<30 m) to conduct visual or handheld detector surveys, dives are highly constrained in duration and activity by strict health and safety regulations. If even as few as 1/3 of the existing sites can utilize ROV-based EM sensing, there is great potential cost savings in addition to improvements in diver health and safety. Dives generally require teams of 5 or more specialists and nominally cost \$2,000 to \$3000 per dive. ROV-EM technology can be deployed with as few as 3 operators (1 helmsman, 1 analyst, 1 EOD tech) for \$600-\$800 per dive - thus reducing the estimated daily cost (assuming ~10 dives/day) from \$25,000 to \$7,000 (~70% reduction).

Page Intentionally Left Blank

Table of Contents

1.0 INTRODUCTION	1
1.1 BACKGROUND.....	1
1.2 OBJECTIVE OF THE DEMONSTRATION	2
1.3 REGULATORY DRIVERS.....	2
2.0 TECHNOLOGY	3
2.1 TECHNOLOGY DESCRIPTION	3
2.1.1 Hybrid Autonomous Underwater Vehicle	3
2.1.2 Electromagnetic Induction Sensor Array.....	5
2.1.3 Positioning and Vehicle Control.....	7
2.1.4. ROV Platform and EM Array Position/Control Integration	9
2.2 TECHNOLOGY DEVELOPMENT	10
2.2.1 HAUV Noise Signature Characterization and Mitigation	10
2.2.2 MFDA Array Characterization	14
2.2.3 Hybrid AUV-ROV "Dolores" Integrated System.....	21
2.2.4 Topside Control and User Interface.....	22
2.2.5 Launch and Recovery Vessel: The R/V Dare	24
2.3 ADVANTAGES AND LIMITATIONS OF THE TECHNOLOGY	25
3.0 PERFORMANCE OBJECTIVES	26
3.1 OBJECTIVE: BOTTOM FOLLOWING ACCURACY.....	28
3.1.1 Metric.....	28
3.1.2 Data Requirements.....	28
3.1.3 Success Criteria.....	28
3.2 OBJECTIVE: STATION KEEPING ACCURACY.....	28
3.2.1 Metric.....	29
3.2.2 Data Requirements.....	29
3.2.3 Success Criteria.....	29
3.3 OBJECTIVE: WAYPOINT MISSION CONTROL.....	29
3.3.1 Metric.....	30
3.3.2 Data Requirements.....	30
3.3.3 Success Criteria.....	30
3.4 OBJECTIVE: DETECTION PERFORMANCE	30

3.4.1 Metric	30
3.4.2 Data Requirements	31
3.4.3 Success Criteria	31
3.5 OBJECTIVE: DETECTION LOCATION ACCURACY	31
3.5.1 Metric	31
3.5.2 Data Requirements	31
3.5.3 Success Criteria	31
3.6 OBJECTIVE: EASE OF USE	31
3.6.1 Metric	32
3.6.2 Data Requirements	32
3.6.3 Success Criteria	32
3.7 OBJECTIVE: MISSION ASSISTED AUTONOMY	32
3.7.1 Metric	32
3.7.2 Data Requirements	32
3.7.3 Success Criteria	32
3.8 OBJECTIVE: INTEGRATED SYSTEM STABILITY	32
3.8.1 Metric	33
3.8.2 Data Requirements	33
3.8.3 Success Criteria	33
4.0 SITE DESCRIPTION	33
4.1 SITE SELECTION	33
4.2 SITE HISTORY	40
4.3 SITE GEOLOGY	41
4.4 MUNITIONS CONTAMINATION	45
5.0 TEST DESIGN	48
5.1 CONCEPTUAL EXPERIMENTAL DESIGN	48
5.2 SITE PREPARATION	48
5.3 SYSTEM SPECIFICATION	52
5.3.1 Multi-Frequency Digital Array (MFDA) EM Sensor	53
5.3.2 Navigation and Control System	53
5.3.3 Remotely Operated Vehicle	54
5.3.4 Ship-based Positioning	54
5.4 CALIBRATION ACTIVITIES	55
5.5 DATA COLLECTION PROCEDURES	55

5.5.1 Basic Operational Test Instructions	56
5.5.2 Quality Checks	57
5.5.3 Characterization of Background Water Column Parameters	58
6.0 ANALYSIS AND DATA PRODUCTS	59
6.1 DATA PREPROCESSING	59
6.1.1 MFDA Data	59
6.1.2 Navigation and Control Data	59
6.2 DETECTION	59
6.3 PARAMETER ESTIMATION	59
6.4 TRAINING / DISCRIMINATION	60
6.5 DATA PRODUCT SPECIFICATION	62
6.5.1 Bottom Following, Waypoint Mission Control, and Station Keeping	62
6.5.2 Detection Accuracy	62
6.5.3 EMI Sensor Data	62
7.0 PERFORMANCE ASSESSMENT	64
7.1 BOTTOM FOLLOWING	65
7.2 STATION KEEPING	67
7.3 WAYPOINT CONTROL	68
7.4 DETECTION	70
7.5 LOCALIZATION ACCURACY	71
7.6 INTEGRATED SYSTEM STABILITY	76
7.7 OPERATIONAL EASE OF USE	76
7.8 ASSISTED AUTONOMY	80
8.0 COST ASSESSMENT	80
8.1 COST MODEL	80
9.0 IMPLEMENTATION PROSPECTUS	85
8.1 LOCAL AREA SEARCH MISSIONS	85
8.2 ANOMALY CHARACTERIZATION	87
8.3 RE-ACQUISITION AND CUED CLASSIFICATION	88
10.0 REFERENCES	89
APPENDICES	92
Appendix A: xx	92

List of Figures

Figure 1. Layout of the Dolores HAUV system. Top: Photograph of the Dolores HAUV platform with side panel exposed to show location of internal systems. Middle: Solid model showing the location of subsystems from the profile-view perspective. Bottom: Photograph of the Dolores HAUV with EMI array mounted on front.	5
Figure 2 Left: Photograph of the original equipment manufacturer MFDA EMI sensor head with a single transmitter coil (red) encompassing three differential receivers (green). The receivers are configured as oppositely wound figure-8 shaped pairs to cancel the primary field from the transmitter. Right: Photograph of the MFDA EMI sensor array and electronics encased in pressure vessels for marine operations.	6
Figure 3. Left: The MFDA array and marinized enclosure during servicing. Right: The configuration of the MFDA as installed on the HAUV. The MFDA sensor head is rigidly attached to specially fabricated solid PVC arms via fiberglass L-brackets. A ballast was added for trimming the system (aka, the "meatloaf"). It consisted of densely-packed pure silicon glass micro-beads flooded with seawater and sealed in a plastic container.	7
Figure 4. Left: Photograph of the inside of the subsea NCS pressure vessel. This processing and inertial core sensing unit works in conjunction with external aiding sensors such as DVL, USBL, altimeters, and depth sensors. Right: The NCS pressure vessel installed on the Dolores HAUV platform.	8
Figure 5. Diagram of topside and HAUV sensors and processing components.	10
Figure 6. Photographs of the dry-land noise test set up and configuration.	11
Figure 7. HAUV noise testing configuration for the static system "move-out" tests (Top Photo) and dynamic close-proximity tests (Bottom Photo).	12
Figure 8. Standoff response curves for the HAUV in the unpowered state.	12
Figure 9. Results of standoff sensitivity to forward looking sonar operation.	13
Figure 10. Results of standoff sensitivity to forward LED lights operation.	13
Figure 11. Photographs of the experimental test stand for dry characterization tests.	14
Figure 12. SNR versus standoff for several ordnance and ordnance simulants. Signals include the sum of the magnitudes of I and Q (left), the sum of I amplitudes (center), and the sum of the Q amplitudes (right). The dotted horizontal line indicates our nominal detection SNR of 9 dB.	15
Figure 13. Theoretical ROC curves (in terms of Pd versus Pfa) for SNRs of 3, 5, 6, 9 and 12 dB. Note that our revised success criteria of 95% Pd and 9 dB SNR corresponds to a Pfa of approximately 0.01 as indicated by the yellow dot.	16
Figure 14. In-phase (I) and quadrature (Q) SNR values for each frequency across each frequency set. Signals represented here are for targets in the transverse direction so as to indicate the work-case orientation of targets relative to the array (i.e., minimum coupling).	17
Figure 15. Data collection configuration for dynamic pass through tests.	17
Figure 16. Example time series EM profiles for receiver channel 2 from dynamic pass through tests.	18
Figure 17. Data collection set up as photographed on the shore of Waquoit Bay prior to in-water test stand data collections.	18
Figure 18. Time series profiles of various targets pulled under the array during in-water testing: A) Medium ISO, B) 60mm UXO, C) Large ISO, and D) 81mm UXO. The top plot for each set of target profiles represents the in-phase signals for the four frequencies recorded in the center receiver channel and the bottom plots represent the quad-phase signals.	19

Figure 19. Left: I and Q raw ADC data (no filters or gains applied) from tests when the array was raised from the seafloor to the sea surface and then back to the seafloor. No targets or metallic objects were present so as to characterize the background water column response of the sensor. As the array approached the sea surface significant oscillatory signals are observed that are consistent in frequency with wave motion at the sea surface. Right: Power spectral density of the lowest frequency (~2 kHz) I and Q signals while the array is held stationary at the seafloor (bottom: at water depths of ~2 meters) and at the sea surface. As expected wave motion at frequencies of approximately 1.5 Hz imparted a strong noise signal on the sensor response near the sea surface.....	20
Figure 20. SNR values estimated from in-water pull-through tests for two sizes of ISO targets (medium and large) and for 60mm and 81mm UXO at ranges of 40 cm from the sensor array. All target responses exceeded the minimum detection SNR of 9 dB.....	20
Figure 21. Side view (left) and plan view (right) of the Dolores hybrid AUV/ROV.....	21
Figure 22. Dolores with the side panel removed (left) and in water with the EM array mounted in the front and EM data acquisition pressure vessel mounted to the top (right).....	21
Figure 23. (Left) Conceptual drawing of the MFDA array mount. (Right) Array prior to deployment.....	22
Figure 24. Deployment (left) and trimming (right) of the Dolores HAUV with integrated MFDA EM sensor.	22
Figure 26. The standalone MFDA data UI (left figure) showing the in-phase and quad-phase color mapped array waterfall plots (left-side panel). Data anomalies are interpolated across the array (Left "L", Center "C", Right "R") and flow from top to bottom as the system moves along the seafloor. The quad-phase map is also "painted" over a map display (right-side panel) and standard pan and zoom features are accessible to the operator. A data filename and logging tool UI tool also provided. This interface was integrated as a module into the openSEA workspace and is shown in the right figure on the rightmost panel.	23
Figure 25. Software integration consisted of software components to acquire MFDA data, create and publish a UDP MFDA data message, and display MFDA data on the topside GUI.	23
Figure 27. Examples of the topside user interface. Left-to-right: Screenshot of the mission planning GUI used for the NCS, photograph of the camera display screen focused just forward of the EMI Array, and the integrated NCS and MFDA GUI showing ROV system parameters (left panel), mission control profiles (center panel: here waypoint mission plan), and EMI array data maps (right panel).	24
Figure 28. Overall topside operator interface. The two top monitors display real-time imagery from the forward-looking camera image with MFDA array in view (right-side) and downward-looking camera view with UXO in view. The bottom monitors display (from left to right) profile data of select MFDA data channels, openSEA workspace views with different system parameters shown.....	24
Figure 29. Top Left: R/V Dare - a 84-foot modified dive salvage and crew boat to which the HAUV-100 is currently dedicated. Top Right: The 17-foot Boston Whaler tender ad anchor vessel that accompanies the Dare. Bottom Left: Maine control room and ROV operations monitors. Bottom Right: Stearn ROV deployment.....	25
Figure 30. Regional bathymetry map of the West Florida Shelf relative to the Gulf of Mexico and continental North America.	34
Figure 31. Left: Google Earth map showing location of the study area in relation to primary sea bottom features. Right: Google Earth zoomed-in map showing the location of the test site	

relative to the outer reef areas juxtaposition between the Hawk Channel and Florida Straits.	35
Figure 32. The general study area is within the southern part of the Hawk Channel, ~7.5 km south of the Boca Chica Key, between the Stock Island Channel and Eastern Sambo Ecological area.	35
Figure 33. Left: Overview bathymetry of the Sambo Keys and Stock Island Channel portion of the outer reef between Hawk Channel and the Straits of Florida. Right: Extent of interferometric acoustic bathymetry data collected over the Western Sambos Ecological Reserve by NOAA in 2007. Our study area was just north and west of Middle Sambos Key, which is located in the southeast portion of the bathymetric survey area in water depths extending between 5 and 14 meters.	36
Figure 34. Underwater photographs of the mixed shell, sand, mud bottom during preliminary site clearance in the demonstration area.	37
Figure 35. Underwater photograph of the fine sandy carbonate sediments that cover dominate the demo area. Intermittent areas of sea grass and patch reef are also observed throughout the area.	38
Figure 36. Photographs of the NOAA Sand Key National Buoy Station at 24.456 N 81.877 W .	39
Figure 37. Surface METOC weather data from our demonstration period in April 2015: WSPD is wind speed, WDIR is wind direction relative to north, and the bottom plot shows the surface air temperature.	39
Figure 38. Schematic of the marine morphologic features in the study area (from Lidz et al., 2003).	43
Figure 39. Isopach map of sediment thickness around the study site. A relatively large degree of variability in the sediment thickness is mapped around the study site - indicated by yellow outline (modified from Lidz et al., 2003).	44
Figure 40. Data from the USGS/NOAA geophysical data collection campaigns in the study site area. Top : Map of the seismic profiles including the Lines 1 and 2, which correspond to the seismic profile interpretations shown in the Bottom figures (from Lidz et al., 1991)....	45
Figure 41. Map of DOD training areas within the Key West Range Complex.	46
Figure 42. Map of DOD munitions dumping grounds and facilities in and around the Lower Keys.	46
Figure 43. Photographs of AN-MK 5 Mod 1 practice bomb uncovered during salvage operations near our proposed site area. Left: Dummy bomb test item; Right: Tail section of dummy bomb detected with the ROV-EM system and recovered from the sea bottom.....	47
Figure 44. Photograph of the dry-run target layout and planning with divers. Divers and crew practiced the deployment strategy in a soccer field the day prior to sea-based deployment in order to work out the best practices and process for deployment of the target grid.	49
Figure 45. Photograph of our Industry Standard Objects, configured with floating marine rope lines for easy diver-based deployment and attaching to anchor systems or tie-downs.	49
Figure 46. Photograph and table of the UXO stimulants and other targets used.....	50
Figure 47. Photographs of the global positioning survey method for surveying in the grid corners and spar buoy locations. A) Trimble SPS dual antenna GPS system on the abaft beam, B) winch system for used for establishing and fine maneuvering of the 3-point anchor system, and C) the gravity line extending down from below the GPS antenna.....	50
Figure 48. Photographs of divers clearing the grid area prior to target installation.	51

Figure 49. Target grid layout with UXO simulants, ISO and clutter objects oriented along perpendicular transects. Targets are spaced along grid points and surveyed using the grid corners as a global reference. This set up contains 17 distinct targets, with 12 UXO simulants, 5 ISOs, and 4 clutter objects.	52
Figure 50. Left-to-Right: Photographs of the spar buoy, a 60mm simulant target, and 155mm projectile installed in the target grid.	52
Figure 51. Photograph of the Onset HOB0 environmental monitoring device used to sample background water column conductivity and temperature during ROV-EM tests.....	58
Figure 52. Sample of background water column property observations during ROV-EM tests. Left: 14 April 2015 data; Right: 15 April 2015 data.....	58
Figure 53. Processing flow used to create target classification features from raw EM sensor and navigation data.	60
Figure 54. Comparison of the forward model output to observed data at each of the four EM sensor frequencies for a MK118 rocket (top) and a 60 mm mortar (bottom). The sample index represents a non-sequential data scan number. Each frequency I and Q value is demodulated and digitally acquired simulataneously so that the first 62 sample indices associated with 1.5 kHz I and Q values correspond to those acquired at the same time for the other 3 frequencies (i.e., samples 63-124 for 4.5 kHz data, samples 125-186 for 13.5 kHz, and samples 187-248.....	61
Figure 55. Example of frequency-domain inverted polarizabilities using the ortho-normalized volume magnetic source model that was modified to address EM propagation through a conductive seawater medium. This example shows that nearly identical axial polarizabilities for both In-Phase and Quad-Phase components are derived as expected for the axi-symmetric sphere target tested.....	62
Figure 56. Example data product to be supplied along with the detection location accuracy metric.	63
Figure 57. Example data product to be supplied along with the EMI array data quality checks.	63
Figure 58. Still shots of the integrated ROV-EM system (left) and the EM sensor (right) performing bottom following operations.	65
Figure 59. Plots showing desired versus actual ROV altitude, roll, and pitch during a 45 m transect.	66
Figure 60. Summary of atlimiter, roll, and pitch control errors.....	66
Figure 61 Example of station keeping data collected while keeping station for 5 minutes over an individual target. Data zoom-in plots show the local position error found by subtracting the commanded northing and easting position from the northing and easting position reported by the navigation system.....	67
Figure 62 Reported Easting and Northing data over the 5-minute station keeping data collection.	68
Figure 63 Left: Summary of station keeping stability and accuracy. Right: Example bullseye plot of the station keeping error from groundtruth locations from the four corners and center of our test grid.	68
Figure 64. User interface for waypoint mission control. The center portion of the screen illustrates the waypoints input by the user to which the ROV-EM system is commanded to navigate. Multiple waypoints can be entered to configure a multi-point mission plan.	69

Figure 65 Desired line defined by waypoints (black circles), line beginning (green) and line ending (red) waypoints, and the reported location (magenta) of the ROV as it traveled between waypoints.	70
Figure 66. Raw (red) and calibrated (black) USBL Easting and Northing locations are shown. Each corner target location (green circle) were DGPS surveyed. The USBL transducer locations (magenta) are also shown. The zoom-in on the bottom left shows the effect of the calibration. Calibrated locations are centered around the surveyed location.....	72
Figure 67 The slant range is provided by the USBL. The USBL estimates a depth estimate using the slant range and the vertical angle of arrival. The USBL depth and slant range are used to estimate the horizontal range. Horizontal ranges were adjusted using the more accurate depth estimate from the INS sensor onboard the ROV along with the USBL slant range. ..	73
Figure 68 USBL (green) and Fused (black) position estimates for a transect with large target responses in the center of the EMI array indicating ROV travel directly over the targets. In this example the Fused locations provide a better estimate of the true ROV position during the transect.	74
Figure 69. Coverage map created using EMI data integrated with filtered USBL position information.....	75
Figure 70. Detection location errors for USBL (red circle) and Fused (blue x) location estimates.	76
Figure 71. Dolores HAUV-1000 integrated ROV-EM system launch and recovery operations. The system requires sufficient deck space and hoist capability to deploy over the side of the vessel.....	77
Figure 72. Various screen captures of the integrated HAUV-EMI graphical user interface. The top left image shows one of system configuration windows. The top right shows system configuration information and map display of waypoints set up during mission planning of grid surveying. The bottom left image shows a screen grab during operation waypoint missions with system configuration and status information on the left, waypoint map information and mission plan data in the middle, and MFDA real-time data display on the right. The bottom right image shows a similar view with a different set of real-time system data displayed on the lefthand portion of the UI.....	78
Figure 73. Photograph of the main control cabin are showing the layout of joystick control and flat panel displays for real-time awareness during operations. The bottom images show the myriad of camera, data, and user information displays and zoom-in of the MFDA data display and map tracking UI.	79
Figure 74. Left is the estimated error after 50 m distance traveled for DVL/IMU systems with a MEMS IMU (Greensea Bolton), FOG IMU (CDL TOGS/NAV), and a RLG IMU (Kearfott 6053). Also included for comparison are the Tritech MicronNav USBL system and the IXSEA GAPS USBL system. Right is the same figure with the Tritech MicronNav removed.....	82
Figure 75. Survey activities relevant to underwater UXO detection include local area search (left), anomaly characterization (center), and anomaly re-acquisition (right).	85
Figure 76 Positional accuracy estimates over a 50 m x 50 m survey area (black square) for four scenarios. Top left: USBL system with the USBL transceiver (white circle) located 50 m East of the center of the survey area. Top right: USBL system with the USBL transceiver (white circle) positioned directly over the center of the survey grid. Note the improved accuracy over the survey area due to the reduced ranged from the USBL transceiver to the	

survey area. Bottom left: INS position system accuracy on a survey platform starting the survey in the southwest corner of the survey area and following 1 m spaced lines (white) in a lawn mower pattern across the survey area. Without calibration from a secondary positioning system INS error increases with distance traveled. Bottom right: LBL error is constant across an area encompassed by calibrated LBL transceivers (white circles). 86

List of Tables

Table 1. Performance Objectives	27
Table 2. Daily tidal levels as measured from the Key West monitoring station during the demonstration period.	40
Table 3. Potential military expended material in the Key West Range Complex.	47
Table 4. Summary of target objectives, metrics, and results.	64
Table 5. Waypoint and line following performance in meters.	69
Table 6. Detection performance results.	71
Table 7. USBL and Fused detection location accuracy metrics	75
Table 8. Cost Model for a Detection/Discrimination Survey Technology	80
Table 9. ROV lease and purchase data.	81
Table 10. Inertial core navigation systems.	82
Table 11. Support Equipment Costs	83

List of Acronyms

°C:	Degrees Celsius
ADC:	Analog to Digital Conversion
ACM:	Air Combat Maneuvers
AFTT:	Atlantic Fleet Training and Testing
ATCAA:	Air Traffic Control Assigned Airspace
AUV:	Autonomous Underwater Vehicles
CERCLA:	Comprehensive Environmental Response, Compensation and Liability Act
CH:	Channel
cm:	Centimeter
COTS:	Commercial Off The Shelf
CPU:	Central Processing Unit
CST:	Conductivity, Salinity, Temperature
dB:	Decibels
DC:	Direct Current
DoD:	Department of Defense
DVL:	Doppler Velocity Log
E:	Easting
EOD:	Explosive Ordnance Disposal
EM:	Electromagnetic
EMI:	Electromagnetic Induction
EMF:	Electromotive Force
ESTCP:	Environmental Security Technology Certification Program

FA:	False Alarms
FDEM:	Frequency Domain Electromagnetic
FFWCC:	Florida Fish and Wildlife Conservation Commission
FKMNS:	Florida Keys Marine National Sanctuary
FOG:	Fiber Optic Gyro
FREQ:	Frequency
GUI:	Graphical User Interface
GPS:	Global Positioning System
HAUV:	Hybrid AUV
HD:	High Definition
HDOP:	Horizontal Dilution of Precision
HP:	Horsepower
Hz:	Hertz
I:	In-phase
IMU:	Inertial Measurement Unit
INS:	Inertial Navigation Unit
IVS:	Instrument Verification Strip
ISO:	Industry Standard Objects
kg:	Kilogram
kHz:	Kilohertz
kW:	Kilowatt
LAR:	Launch and Recovery
LCM:	Lightweight Communications and Marshalling
LED:	Light Emitting Diode
LBL:	Long Baseline
m	Meter
MEMS:	Micro Electro-Mechanical Sensor
MFDA:	Multi-Frequency Detection Array
MHz:	Megahertz
MMRP:	Military Munitions Response Program
MSK:	Minimum Shift Keying
N:	Nothing
NAS:	Naval Air Station
NCS:	Navigation and Control System
NMEA:	National Marine Electronics Association
NOAA:	National Oceanic and Atmospheric Administration
NTP:	Network Time Protocol
OEM:	Original Equipment Manufacturer
ONVMS:	Ortho-Normalized Volume Magnetic Source
OPENSEA:	OPEN Software and Equipment Architecture
OPERA:	Operating Area
Pd:	Probability of Detection
PDBS:	Phase Differencing Bathymetric Sonar
PDOP:	Position Dilution of Precision
Pfa:	Probability of False Alarm
ppt:	parts per thousand

Q:	Quadrature
RLG:	Ring Laser Gyro
ROI:	Region of Interest
ROV:	Remotely-Operated Vehicles
RPM:	Revolutions Per Minute
RTK:	Real-time Kinematic
Rx:	Receiver
S:	Siemens
SBAS:	Satellite-Based Augmentation System
SDGPS:	Satellite Differential Global Positioning System
SNR:	Signal to Noise Ratio
STMR:	Single Transmit Multiple Receive
SWAP:	Size, Weight, and Power
TACTS:	Tactical Aircrew Combat Training System
TDOP:	Time Dilution of Precision
TOI:	Target of Interest
UDP:	User Datagram Protocol
UI:	User Interface
USBL:	Ultra-Short Baseline
UUV:	Unmanned Undersea Vehicle
UXO:	Unexploded Ordnance
VBES:	Vertical Beam Echosounder
VDOP:	Vertical Dilution of Precision
VHF:	Very High Frequency
WWII:	World War II

1.0 INTRODUCTION

Current methods for detecting and characterizing underwater ordnance rely heavily on explosive ordnance disposal (EOD)-trained divers for visual inspection and handheld metal detector surveys. These dive teams are highly constrained in duration, depth, cost, and activity by health and safety regulations. While autonomous underwater vehicles (AUVs) provide an alternative, those currently available for marine munitions response operations require well-trained operators and do not allow for real-time awareness of the benthic environment. Additionally, the hydrodynamics and propulsion configurations of commercial AUVs preclude hovering for cued interrogation and very slow or adaptive operation at, or very near, the sea floor.

The objective of this project is to evaluate innovative technologies required for deploying underwater electromagnetic induction (EMI) sensors from remotely operated vehicles (ROVs). The integration of these platforms, highly accurate navigation and control systems, and a high-resolution electromagnetic array can overcome limitations of current diver-deployed, towed, and unmanned integrated underwater ordnance systems. Specifically, ROV-based sensing enables the positioning of array-based sensors directly over targets of interest.

To meet the objectives of the project, we have developed a series of graduated demonstrations. This test report summarizes the technologies, procedures, metrics, and results from our final demonstration of the ROV-based EMI integrated sensing platform.

1.1 BACKGROUND

Demonstration of ROV-based EMI array sensing may provide several direct benefits for future marine munitions operations. Effective, practical, and defensible methods for detecting and characterizing underwater ordnance are recognized as one of the key advances required to reduce the cost and time required for clean-up of contaminated marine and lacustrine sites (SERDP, 2007). At many sites, ROV-based EMI sensing may reduce the cost and health and safety burden currently placed on diver surveys while enhancing the overall awareness of the benthic environment from high quality EMI data collected in conjunction with supporting visual and acoustic sensor modalities. Successful deployment of ROV-based EMI sensing will demonstrate: 1) close and well-controlled standoff from the seafloor, 2) real-time operator situational awareness and dynamic repositioning of sensor arrays, and 3) implementation of EMI sensor arrays capable of detecting and discriminating small munitions to greater depths than manned, surface towed, or fully autonomous sensing systems.

In this project we demonstrated the ability to collect high quality EMI data from a commercial inspection class ROV. Although the performance of the system depends on the type of environment, bathymetry and bottom characteristics, currents, and target type and distribution, this demonstration project showed that the system can provide critical capabilities of precise data collection, sensor positioning, and terrain following, resulting in high probabilities of detection of underwater munitions.

Throughout the scope of this project, we employed a multi-sensor frequency-domain digital EMI array that utilizes three differential (quadrapole) receivers mounted to an ROV. This EMI system was mounted directly to a commercially available inspection class ROV system utilizing an advanced inertial navigation and control system. This ROV provides a stable operating platform for deployment of the marine EMI array and is capable of highly accurate positioning and close and well-controlled standoff from the sea floor. The inertial navigation and control system used on the ROV allows for the precise detection of small munitions (<60mm diameter) under varied conditions by providing precise sensor positioning in moderate water depths (>20m), bottom following, station keeping, and autonomous search modes.

1.2 OBJECTIVE OF THE DEMONSTRATION

The primary objective of this demonstration was to quantify the performance of an integrated EMI array sensor, precision navigation and control system, and hybrid AUV/ROV platform through testing in a realistic underwater environment. Performance was assessed through analyses of the integrated EMI array, position, and attitude data collected during execution of multiple underwater unexploded ordnance (UXO) detection operations: 1) wide area coverage, 2) anomaly characterization, and 3) anomaly reacquisition. Another objective was to quantify improvements in UXO detection using precise control by comparing EMI sensor data registered with positioning methods of varying degrees of accuracy. Potential underwater UXO operations could benefit significantly by utilizing autonomous ROV behaviors, such as bottom-following, line-following, and station keeping. These operating modes were analyzed for effectiveness in UXO operations during this demonstration. We tracked the cost and time of using the demonstrated system to complete the various missions for comparison against the cost and time efficiency of currently used methods. The final objective of this demonstration was to identify shortcomings and areas of improvement in the hardware, software, and operation of the integrated system.

1.3 REGULATORY DRIVERS

The Department of Defense (DoD) is responsible for assessment and remediation of numerous munitions sites, many containing in-water areas, in the United States. When the transfer of responsibility to other government agencies or to the civilian sector takes place, the DoD lands fall under the compliance requirements of the Superfund statutes. Section 2908 of the 1993 Public Law 103-160 requires adherence to Comprehensive Environmental Response, Compensation, and Liability Act (CERCLA) provisions. The basic drivers are related to assumption of liability for ordnance contamination on the previously DoD-controlled sites.

Site cleanup is performed using the Superfund CERCLA process, which provides the liability of persons responsible for waste at these sites and provides details on the steps required for site cleanup from initial assessment to redevelopment. EMI and magnetic detection sensors are standard technology used in various stages of the CERCLA process in cleanup of ground sites. The technology demonstrated is towards implementation of a similar technology set for the cleanup of in-water sites.

There are no explicit regulatory drivers or considerations associated directly with this preliminary demonstration. All demonstration activities were conducted in waters regulated by federal and state (Florida) laws and outside of any military areas or regulated by special munitions contamination provisions.

2.0 TECHNOLOGY

In this project, we demonstrated an EMI sensor integrated with an ROV platform capable of accurate positioning and control. The ROV and positioning control system combines the Dolores Hybrid AUV (HAUV) 1000 with the commercial Balefire navigation and control system developed by Greensea Systems. The primary EMI sensor payload technology is the Multi-sensor Frequency-domain Digital Array (MFDA) modified by White River Technologies for underwater UXO detection and tightly-integrated with the high performance AUV control system in addition to auxiliary sonar and environmental sensors (i.e., high-definition video and imager, electrical conductivity, salinity, and temperature).

2.1 TECHNOLOGY DESCRIPTION

2.1.1 Hybrid Autonomous Underwater Vehicle

The Hybrid AUV (HAUV-1000) was originally designed and built by Greensea Systems in 2011. This AUV system, known commonly as "Dolores", is permanently installed on an operations vessel and is equipped with forward-looking sonar, side-scan sonar, a low-grade inertial navigation system, and is powered by two 5.35 kW-hour lithium-iron (LiFePO₄) rechargeable batteries. The system was commissioned by Cobalt Marine LLC and is dedicated to marine geophysical survey and archeological salvage operations.

The Dolores HAUV vehicle body is constructed of non-ferrous materials and was specifically designed for metallic object detection operations. As a hybrid system, it provides remote control typical of traditional ROVs using a fiber-optic tether as well as a fully autonomous mission execution with or without the tether. Similar to most other ROVs, when deployed with a tether, Dolores allows for direct operator-in-the-loop control and provides full bandwidth data to and from the HAUV including video, sonar data, payload data, and systems monitoring. A full autopilot suite provides for higher performance control than is typical with traditional inspection class ROVs by augmenting the remote control operation with waypoint navigation, station keeping, attitude control, precision bottom following, and fly-by-wire joystick features. When deployed as an AUV with or without the tether, Dolores is capable of conducting pre-planned missions, moderate-scale surveys, search patterns, and high-resolution interrogation surveys via station keeping.

The hydrodynamically stable body is propelled by two fixed forward thrusters, one lateral thruster, and one vertical thruster. The thrusters are fixed but provide powerful bollard thrusts of over 35 kgf each. They are composed of brushless DC motors actuated by the HAUV control system. This allows the 300 kg (in air) HAUV system to remain stable in moderate currents (2.5 knots). This means that the system can hold station in terms of attitude, depth, and lateral position even with the forward mounted EM array platform (discussed in the following sections).

A significant advantage that this HAUV system configuration has over traditional tethered ROVs for operating UXO detection technologies is that it is battery powered, eliminating noisy umbilical and power distribution systems. The on-board subsea power management system provides up to 14 continuous hours of operation in ROV mode and over 18 hours in AUV mode.

Dolores is equipped with standard ROV awareness sensing and instrumentation including 1) Tritech Micron scanning sonar, 2) low-light black and white downward-looking (belly-cam) video camera, 3) forward-looking color video camera for navigation, 4) and low-power LED lights. Additionally, Dolores has a payload bay for mission-specific instrumentation such as high-definition cameras, EMI UXO sensors, magnetometers, and side-scan sonar. Our demonstration system is also equipped with a LinkQuest TrackLink 1500 Ultra-Short Baseline (USBL) positioning system as well as the inertial navigation and positioning system (as described below).

Greensea has previously demonstrated their inertial navigation and autonomous control package on the Dolores HAUV. This demonstration was completed in June 2014 and included demonstration of station-keeping, autopilots, precise positioning, and autonomous search execution. During this demonstration, the capabilities of the vehicle to operate in current, pulling over 200 m of tether, and carrying a large payload were demonstrated.

The EMI array is mounted directly to the non-metallic ROV structural frame chassis. It is positioned slightly below the ROV in order to minimize potential standoff distances from the seafloor. The EMI array electronics are mounted under the chassis and away from any obstructions or hazards. Photographs of the HAUV and solid model of the subsystems configuration are shown in Figure 1.

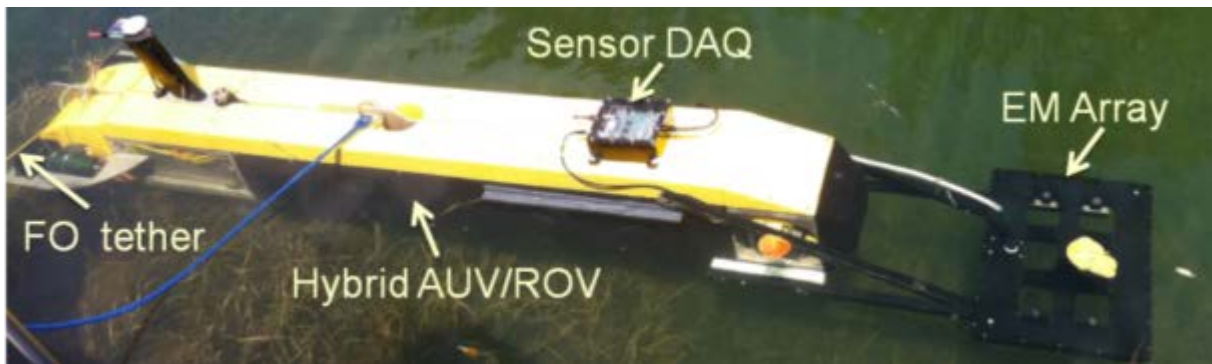
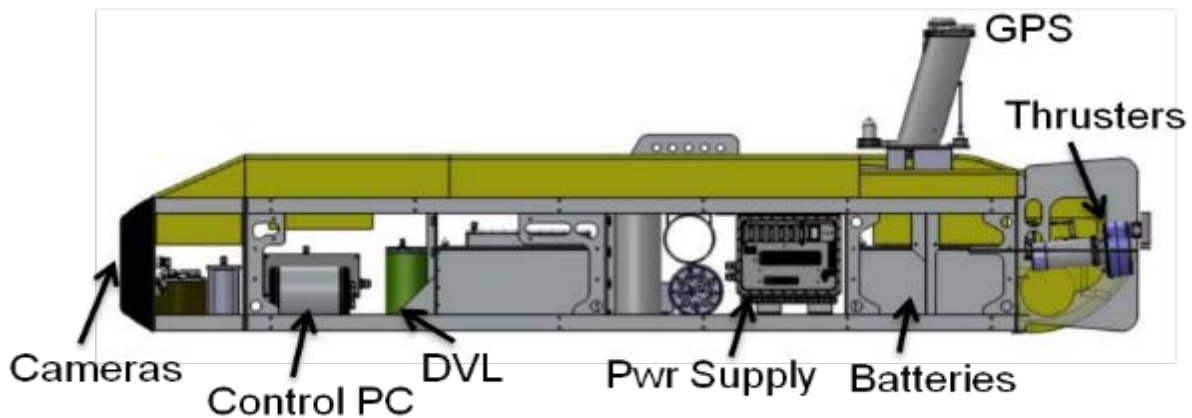


Figure 1. Layout of the Dolores HAUV system. Top: Photograph of the Dolores HAUV platform with side panel exposed to show location of internal systems. Middle: Solid model showing the location of subsystems from the profile-view perspective. Bottom: Photograph of the Dolores HAUV with EMI array mounted on front.

2.1.2 Electromagnetic Induction Sensor Array

The MFDA was developed from a marriage between multi-frequency technology originally incorporated in Minelab's handheld metal detectors and the differential receiver design used in the US Army vehicle-mounted Single-Transmit Multiple-Receive (STMR) system (Stamatescu and Schultz, 2007). In contrast to similar frequency-domain EM (FDEM) instrumentation (e.g.,

Geophex GEM-3), the MFDA employs a single transmitter and three single-axis (z-oriented) differential receivers. This multi-static configuration provides multiple measurements of the sampled scattered magnetic field that in turn yields information about the spatial distribution of the scattered field from targets of interest.

The sensor head is constructed of very lightweight (1.4 kg) high density foam and windings of litz wire. It comprises a 45 cm x 65 cm transmitter and three figure-8 shaped (quadrupole) receiver coils (Figure 2). The three quadrupole receivers form oppositely wound coils (monoloops) that create an equal and opposite electromagnetic field (EMF) from the transmitter on each monoloop coil. When the signals from each coil are added in series, the primary field EMF disappears leaving only the secondary field response. This arrangement has the advantage of canceling the net primary field from the transmitter and reducing vehicle noise as well as providing relatively accurate 3-dimensional target localization. The digital data acquisition and processing electronics are housed in a small pressure vessel and weigh about 0.24 kg. The system currently transmits 4 frequencies simultaneously, but can transmit and receive up to 8 frequencies over a range of 400 Hz to 70 kHz. Communication with the host at a rate of 10 Hz provides in-phase and quadrature-phase signals for each frequency and for each coil. As well as the raw in- and quad-phase readings, the sensor supplies a set of ground-compensated data based on a simple normalization method (Bruschini, 2004). The digital demodulation procedures utilized in this array are unique among frequency-domain detectors in that they do not require sequential (or stepped) detection of each frequency component, but utilizes a continuous wave demodulation such that higher frequency harmonics are nearly eliminated (Stamatescu and Nesper, 2012). This is achieved through the application of an optimally designed 3-level waveform through two half-bridge amplifier circuits.

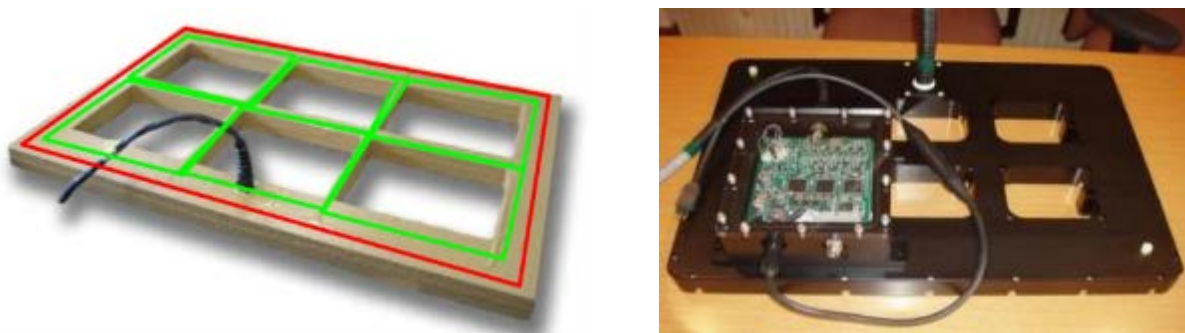


Figure 2 Left: Photograph of the original equipment manufacturer MFDA EMI sensor head with a single transmitter coil (red) encompassing three differential receivers (green). The receivers are configured as oppositely wound figure-8 shaped pairs to cancel the primary field from the transmitter. Right: Photograph of the MFDA EMI sensor array and electronics encased in pressure vessels for marine operations.

This frequency-domain sensor has the advantage of superior control of selection and power in the frequency content of received signals. In marine applications where conduction currents influence the quadrature-phase signal, the FDEM approach provides additional in-phase information that may be important for characterizing targets of interest (Schultz et al., 2011). Additionally, this system is less band-limited than similar pulsed induction arrays and, thus offers a greater equivalent time range of response, particularly at very early times (or equivalently high frequencies) and at sufficiently late times where information on the asymptotic limits of scattering may reveal important discriminating information.

The MFDA sensor array was first integrated on a small, unmanned robotic ground vehicle and successfully demonstrated in 2009. Detection and discrimination capability was assessed over a series of buried munitions where the MFDA detected all targets over which it passed. Subsequently, in 2010, the system was encased in a ruggedized pressure vessel and tested in the underwater environment. Before integration with a Seabotix mini-ROV (LBV-300-5), a series of vehicle signature tests were conducted to determine the noise effects of the ROV platform and to specify a mounting configuration that best minimizes those effects. Signature testing revealed that the in-phase data were more sensitive to the magnetic moment (permanent and induced) of the vehicle. Analysis of standoff measurements revealed the noise produced by the Seabotix mini-ROV was below the ambient noise floor at distances >60 cm behind the ROV. Dynamic noise generated primarily by the brushless DC thruster motors was also observed to affect both the in-phase and quadrature-phase data. This noise is relatively narrow band and can be mitigated by appropriate selection of EM frequencies. Pulsed induction EM systems generally provide less configurability to adjust for narrow band dynamic noise sources emitted from the ROV vehicle. Prior to the demonstration described in this report the MFDA sensor was serviced and integrated with the Dolores HAUV (Figure 3).



Figure 3. Left: The MFDA array and marinized enclosure during servicing. Right: The configuration of the MFDA as installed on the HAUV. The MFDA sensor head is rigidly attached to specially fabricated solid PVC arms via fiberglass L-brackets. A ballast was added for trimming the system (aka, the "meatloaf"). It consisted of densely-packed pure silicon glass micro-beads flooded with seawater and sealed in a plastic container.

2.1.3 Positioning and Vehicle Control

Positioning and navigation for ROV applications occurs through solutions that yield varying degrees of accuracy and precision. These include: 1) acoustic navigation from Ultra-Short BaseLine (USBL) or Long BaseLine (LBL) systems, 2) dead reckoning, or 3) integrated solutions based on inertial navigation systems aided by Global Positioning Systems (GPS), Doppler Velocity Logs (DVLs), pressure sensors, subsea positioning systems such as USBL and LBL, altimeters, and magnetic attitude sensors. Positional accuracy varies depending on the method used and quality of the sensors implemented (e.g., type of gyros used in the inertial

measurement unit) as well site and deployment conditions. Practical experience with USBL positioning of ROV systems in a number of environments has yielded accuracies of approximately 1 m in less than 25 m water depths but larger positioning errors are typical. Although USBL is relatively simple to operate, bearing accuracies exceeding ~3 degrees lead to unsuitable positional errors for UXO detection operations that increase with range from the USBL transducer.

Our demonstration required a more accurate navigation and positioning capability for UXO site mapping relative to commercial-grade USBL systems alone. This enabled the integrated ROV-EM sensing system to maneuver with a high degree of control – including close terrain following. The Navigation and Control System (NCS) provides an attitude, positioning, and navigation solution for the ROV and EMI sensor. This technology is a compact and stand-alone vehicle control system integrated with an inertial navigation capability for ROVs and provides a complete solution for underwater vehicle navigation, positioning, control, and automation. The NCS is based on a high-performance inertial core sensor, mounts to any underwater vehicle, and requires relatively little integration. The NCS fuses the data from aiding sensors with the core inertial measurements and continuously calculates vehicle position and orientation. This system provides vehicle tracking in coordinates relative to a known starting location or in absolute navigation coordinates if an initial or even periodic GPS position estimate is provided. Figure 4 shows internal and external photos of the NCS "Balefire" pressure vessel.

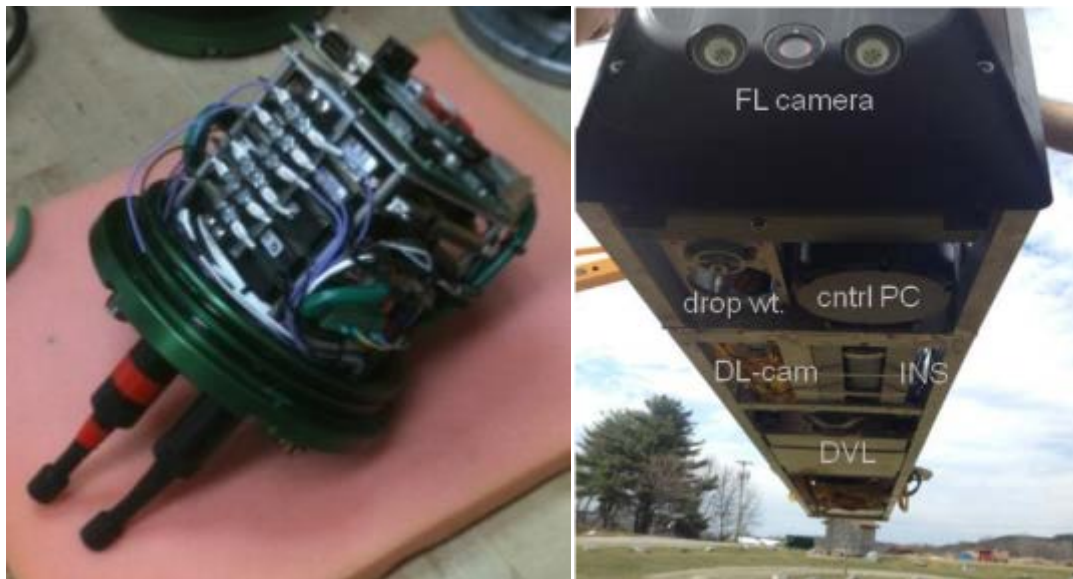


Figure 4. Left: Photograph of the inside of the subsea NCS pressure vessel. This processing and inertial core sensing unit works in conjunction with external aiding sensors such as DVL, USBL, altimeters, and depth sensors. Right: The NCS pressure vessel installed on the Dolores HAUV platform.

Greensea Systems has previously integrated their Balefire inertial navigation system to a streaming high-definition video payload similar to that planned for this demonstration, to produce geographically accurate photo mosaics of shipwreck sites in more than 5500 m of water. With no GPS data available and very unreliable USBL data, this technology allowed archeologists with no previous ROV experience to navigate the high definition (HD) video suite

around sites of interest with 10 cm accuracy. The fusion of navigation and payload data correlated each frame of HD video to vehicle position enabling very accurate site surveys.

This system fuses state data from several reference frames and from several sensors to form an estimate of local position and orientation. By integrating data from Earth-centered measurement sources such as USBL and a GPS receiver, we correlate the vehicle position and orientation to Earth coordinates. The system uses a stable gyro and magnetic compass in an integrated unit as the core inertial sensor and an optimal Kalman-derived state filter to fuse the aiding sensor data such as speed over bottom, depth, GPS position, and altitude with the inertial data.

With an accurate state estimate of the position and orientation of the vehicle, the EMI sensor array can be precisely located and geo-referenced to Earth coordinates. This system also features a closed-loop control system around the navigation solution in order to control the vehicle position, EM sensor attitude, and EM sensor height off bottom and significantly improve the quality and consistency of UXO survey data collected. This control methodology should allow pilots with very basic skill levels to accurately maneuver the ROV-EM system while station-keeping, hovering, transiting to waypoints, and bottom following. This tight coupling of a reliable navigation estimate to the sensor data is also intended to help eliminate inaccuracies and process noise generated by navigation referenced to the vehicle.

2.1.4. ROV Platform and EM Array Position/Control Integration

The ability of the ROV EM system to perform UXO remediation applications requires integration of the EMI sensor and position data into the previously-developed navigation and control system. Figure 5 is a diagram of the topside and bottomside ROV processing components. ROV processing components consist of a central control processor to read and timestamp ROV sensor data from the inertial navigation unit (INS/DVL) and communicate control commands to the ROV thrusters. Topside, the system control graphical user interface (GUI) communicates with the subsea processor via User Datagram Protocol (UDP) communications through the ROV tether. The EMI sensor electronics pressure vessel is connected to the subsea network via Ethernet through an auxiliary sensor connector available on the subsea processor pressure vessel. This connection enables EMI sensor configuration and control using a dedicated topside laptop computer. The sole function of the MFDA topside computer is to receive EMI data in the sensor's native format, convert the data to a UDP message, and send the UDP message to the ROV topside GUI for timestamping and logging. Measurement of the execution time required to: 1) read the raw sensor data, form the UDP message, and transmit the UDP message was less than 100 ms. Upon receipt of the EMI data UDP message by the topside GUI it is time-stamped with a time common to all other subsea data messages enabling synchronization of the MFDA data with navigation and control data during post-processing.

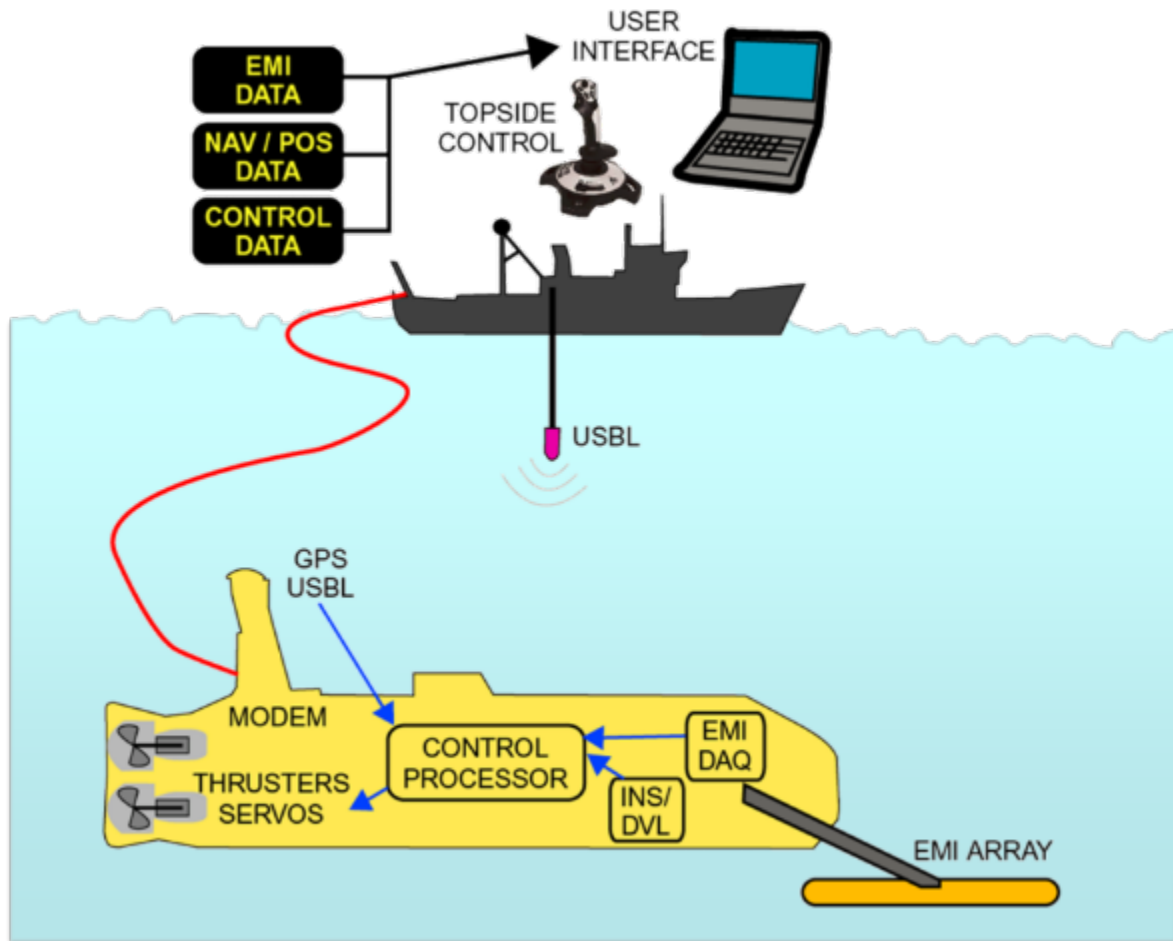


Figure 5. Diagram of topside and HAUV sensors and processing components.

2.2 TECHNOLOGY DEVELOPMENT

2.2.1 HAUV Noise Signature Characterization and Mitigation

We characterized the electromagnetic and magnetic signature of the HAUV system by collecting MFDA sensor data in several different configurations relative to the platform located. Three basic tests were conducted to help constrain the electromagnetic signature of the platform: 1) static signature of the platform at varying standoff distances, 2) power-on sequence to isolate and assess noise from individual HAUV components, and 3) dynamic testing of various actuators, thrusters, and instruments on the HAUV platform. The HAUV was taken to a low noise dry land area and elevated on wood stands (dunnage). Prior to emplacement of the HAUV in the test area, we performed a survey to assess the ambient electromagnetic background signature including spatial and temporal variability in MFDA signals in the general study area. The MFDA sensor was then positioned in close proximity to the platform to mimic mounting placement on the HAUV. Data were acquired from both the HAUV control system and the MFDA sensor control system using wired connections to laptop computers. A few photos of the test configuration are shown in Figure 6.



Figure 6. Photographs of the dry-land noise test set up and configuration.

Static tests were conducted with the HAUV in both powered and unpowered states for comparison. For these tests, the MFDA array was first positioned with its rear edge directly adjacent to leading edge of the nose of the HAUV in the horizontal plane and at an elevation 23.5cm below the bottom-most edge base of the platform. Data were acquired for approximately 5 seconds at this position and then the sensor was moved 20cm away from the nose and measurements were repeated at each position between 0 and 200 cm from the nose. Following these tests, we repositioned the array at 10cm increments from 0 to 90cm from the nose of the HAUV and performed systematic tests of various components. Lastly, we positioned the array in very close proximity to potential noise sources. Figure 7 shows the test configuration for both static standoff measurements and dynamic close-proximity measurements.

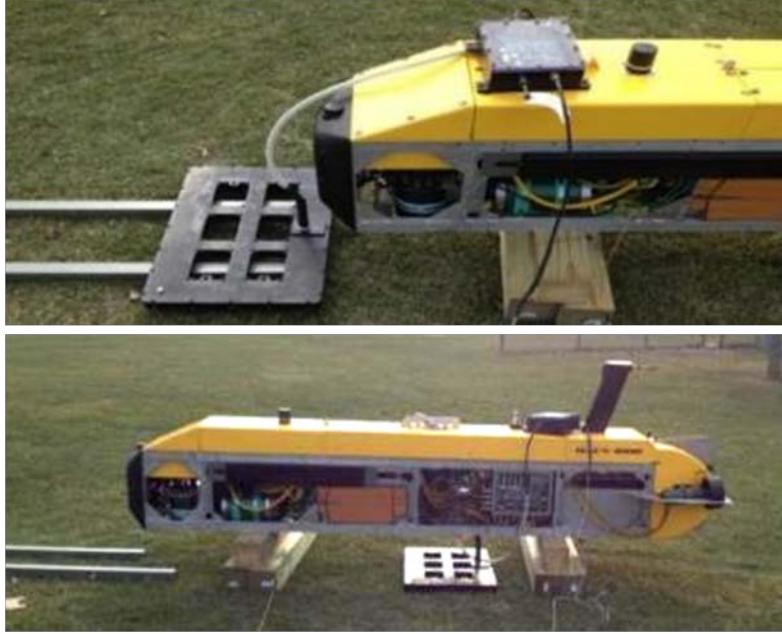


Figure 7. HAUV noise testing configuration for the static system "move-out" tests (Top Photo) and dynamic close-proximity tests (Bottom Photo).

The plots in Figure 8 show the MFDA response to the unpowered HAUV as a function of the standoff distance from the platform leading edge (aka, "the nose"). No data post-processing has been applied beyond the raw, background-subtracted demodulated values that are reported by the sensor. The spectral characteristics vary to some degree depending on the spatial offset from the platform, but overall we observed a general log-linear type attenuation with distance. The quadrature phase data drifts considerably over the time elapsed during data collection events, especially at higher frequencies. This drift produces standoff plots that are not log-linear. In previous studies, we have found that it is difficult to summarize the source as a single dipole or even a few dipoles and estimating a physical model based on the data does not seem warranted. Intrinsic sensor noise free from the HAUV platform was characterized and generally yielded raw ADC counts of $9,900 \pm 420$ with variability dependent on frequency (the noise and noise variation increasing with frequency). If we take 10,000 counts signal as a nominal raw ADC background sensor noise floor level, it appears all signals are below background levels at approximately 75cm from the nose of the HAUV. The 10,000 count noise floor estimated from in-air testing was comparable to noise levels found in-water by the HAUV and MFDA system.

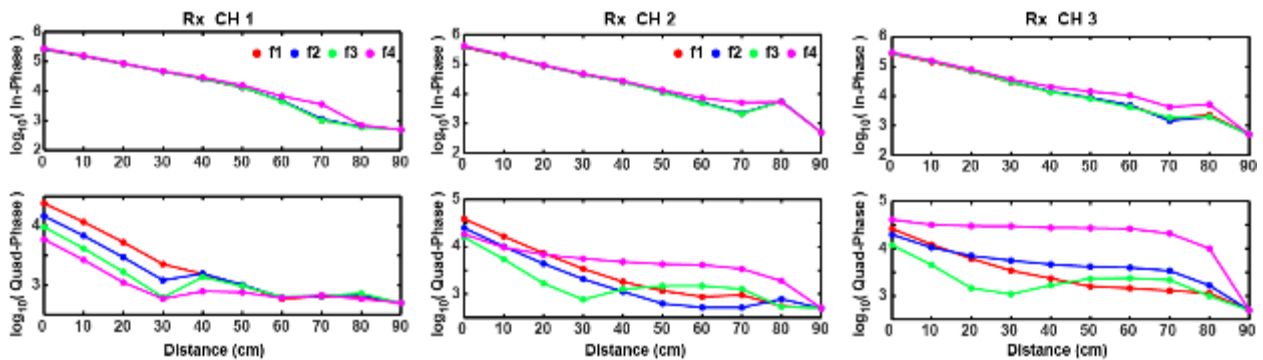


Figure 8. Standoff response curves for the HAUV in the unpowered state.

Repeating these standoff measurements while exciting independent components of the system was also useful to help isolate noisy subsystems or function. The HAUV subsystems we assessed include:

- Forward-looking Sonar
- Forward LED lights
- Aft thrusters
- Lateral and vertical mid-ship thrusters
- Downward looking lights
- Downward looking camera

The standoff measurements for the forward-looking sonar and forward lights are shown in Figure 9 and Figure 10 below. Those subsystems were observed to have the most significant noise effect when powered on. These two subsystems had very similar signatures relative to the background static noise level.

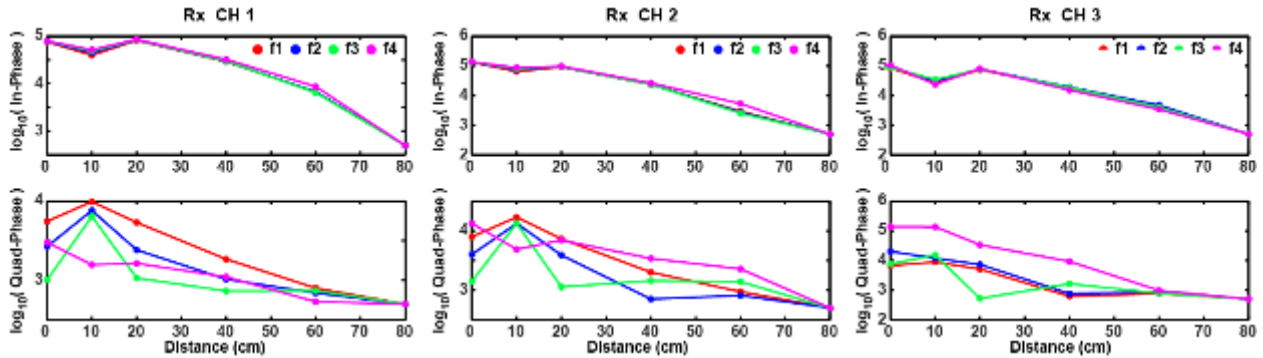


Figure 9. Results of standoff sensitivity to forward looking sonar operation.

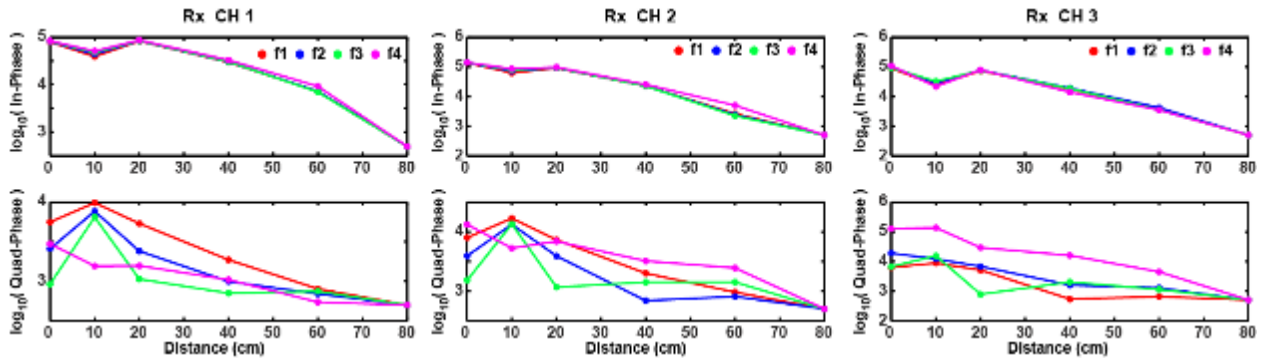


Figure 10. Results of standoff sensitivity to forward LED lights operation.

The standoff measurements yield a relatively rapid attenuation with distance from the HAUV platform with signals at background sensor noise levels between 70 and 80 cm from the nose of the HAUV. Therefore, we took 70 cm as the minimum distance from the nose for the array mount. Further discussion of the array mount can be found later in Section 2.2.3.

2.2.2 MFDA Array Characterization

In addition to noise characterization of the HAUV, we also performed separate measurements to characterize the MFDA independently. This included both in-air dry and submerged test stand data collection and analysis. In-air test stand measurements were conducted over two intervals during times when the MFDA array was being serviced (i.e., for maintaining o-ring seals and other components that require periodic maintenance or calibration verification).

In our initial set of MFDA in-air experiments, we set out to assess the baseline sensitivity to different targets. For these tests, the MFDA was placed on a non-metallic test stand and targets were positioned at various lateral and vertical offsets from the array. Figure 11 depicts the test set up and configuration. Targets tested include: small steel ISO and similar sized aluminum pipe section, medium ISO and similar sized aluminum pipe section, a 2.5-inch solid steel sphere (denoted as FeSphere) and 3-inch spherical shell (denoted as mdFeSphere), 81mm mortar, 60mm mortar, and 37mm projectile. Targets were oriented in both the longitudinal and transverse directions relative to the array transmitter.



Figure 11. Photographs of the experimental test stand for dry characterization tests.

To determine the optimal signal for detection SNR values were calculated using three types of integrated signals across all frequencies: 1) the sum of the in-phase (I) components, 2) the sum of the quadrature (Q) components, and 3) the sum of the magnitudes $\sqrt{I^2 + Q^2}$. Figure 12 shows these SNR values versus standoff distance for the different targets tested. The SNR analysis shown here is for the worst-case transverse target orientation (minimally coupled with the transmitter). The combined I and Q magnitude generally produces the largest SNR values at depth and thus have the best depth sensitivity. As expected the 81mm UXO had the largest SNR values for the summed I and Q magnitude, summed I , and summed Q amplitudes of the targets we tested. The combined I and Q magnitude response from the medium aluminum pipe section (designated mdAlISO) had a relatively large SNR due to its relative size, surface area, and conductive nature.

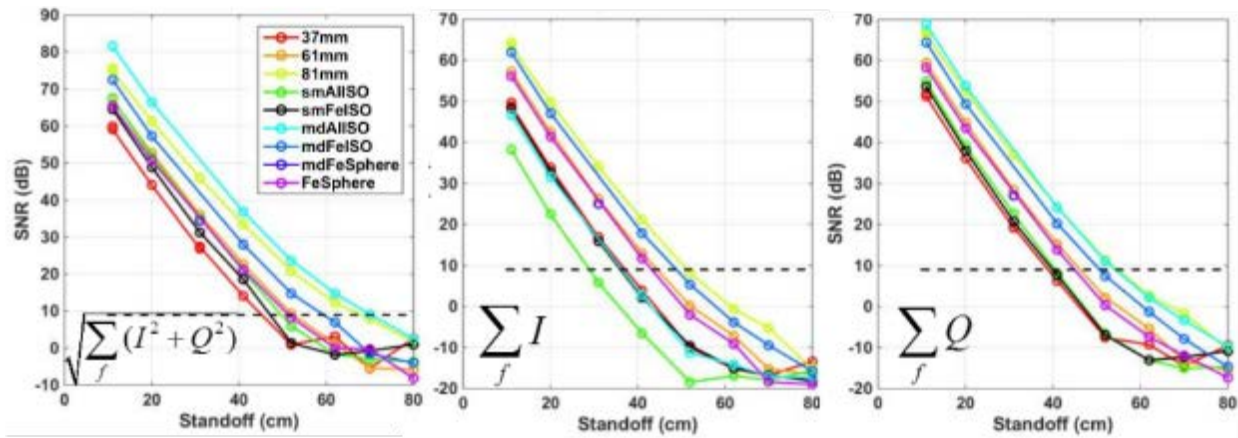


Figure 12. SNR versus standoff for several ordnance and ordnance simulants. Signals include the sum of the magnitudes of I and Q (left), the sum of I amplitudes (center), and the sum of the Q amplitudes (right). The dotted horizontal line indicates our nominal detection SNR of 9 dB.

Based on these results, we suggested a minimum detection SNR threshold of 9 dB (as indicated by the dashed lines in Figure 12). This SNR threshold corresponds to a probability of detection of 95% at a probability of false alarm of approximately 0.01. Figure 13 below shows the theoretical form of the receiver operating characteristic (ROC) curve (i.e., the P_d versus P_{fa} curves) for various SNR levels assuming a nonfluctuating target in Gaussian noise.

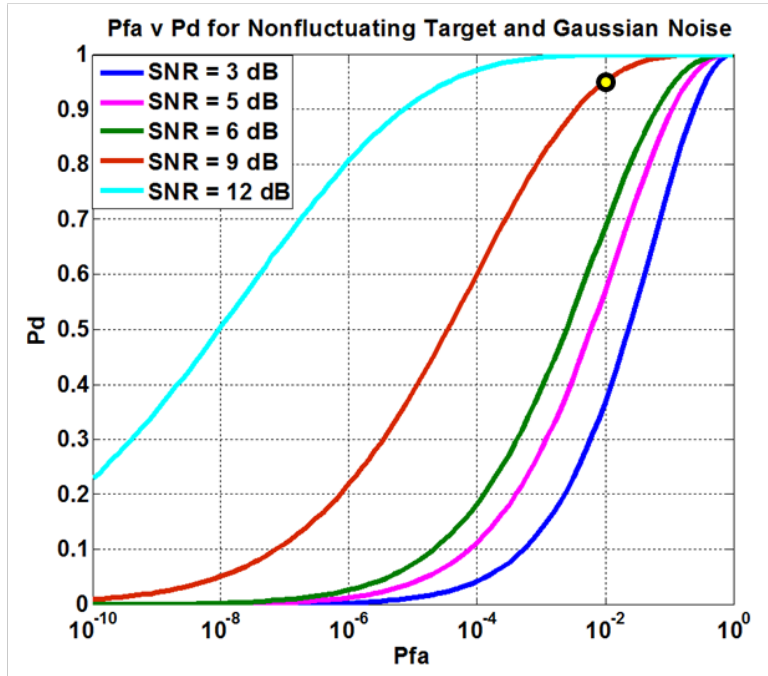


Figure 13. Theoretical ROC curves (in terms of P_d versus P_{fa}) for SNRs of 3, 5, 6, 9 and 12 dB. Note that our revised success criteria of 95% P_d and 9 dB SNR corresponds to a P_{fa} of approximately 0.01 as indicated by the yellow dot.

We also assessed the selection of frequency sets amongst the 21 available settings for the MFDA. The primary objective was to guide selection of data acquisition and detection parameters that would lead to optimal data collection during our final demonstrations. Optimality for these tests was generally characterized in terms of maximizing the signal-to-noise ratio. The signal was determined using a calibration item (solid Ferrous sphere) placed directly underneath the center of the array. A noise estimate was measured without the calibration target in place. Data were collected in this manner over the 21 frequency sets available to the sensor operator. The SNR results for each frequency set are shown in the Figure 14. Analysis of these data reveals high noise in frequency sets 1 and 15 with the rest of the frequency sets exhibiting similar noise characteristics. Frequency set 5 was selected based on its combination of low in-phase and quadrature noise characteristics.

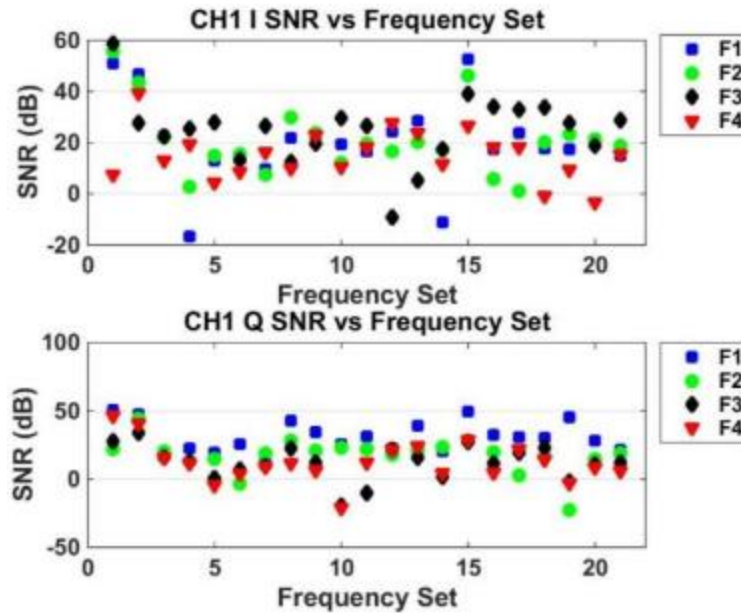


Figure 14. In-phase (I) and quadrature (Q) SNR values for each frequency across each frequency set. Signals represented here are for targets in the transverse direction so as to indicate the worst-case orientation of targets relative to the array (i.e., minimum coupling).

To assess the dynamic response of various targets in the sensor we collected data with the sensor stationary while targets were passed underneath the sensor at various standoffs. Figure 15 shows the data collection configuration for these tests. We utilize a nonmetallic stand with fiberglass rails over which each target is pulled under the array.



Figure 15. Data collection configuration for dynamic pass through tests.

Example "pull through" profiles are shown for two targets in Figure 16 for a medium ISO and a 60mm, both at 37 cm standoff range from the array. The signal amplitude in the Figures is the filtered raw time series ADC values reduced by a gain factor of 1/1000. For the target set we tested (medium-sized standardized targets and relatively small to medium UXO simulants), SNR values in-air were between 30 and 55 dB at 40 cm range from the sensor array.

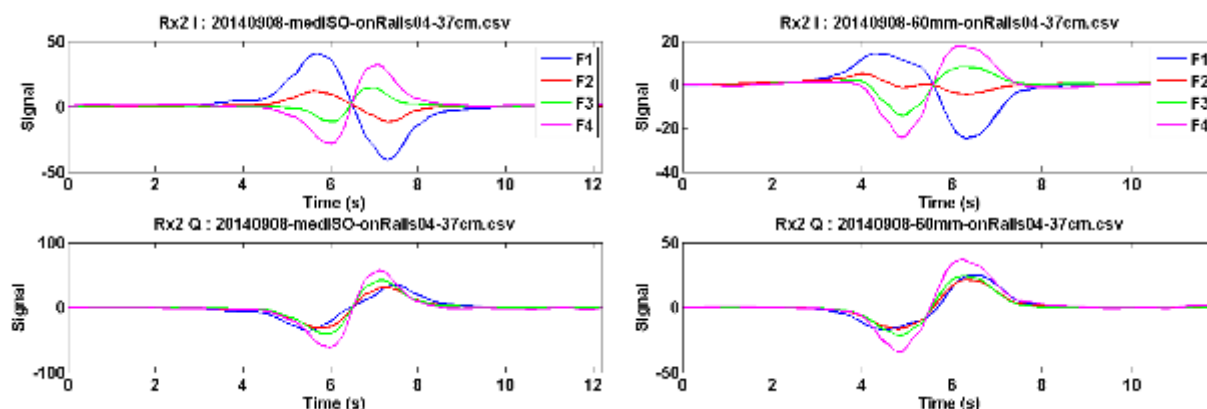


Figure 16. Example time series EM profiles for receiver channel 2 from dynamic pass through tests.

A similar series of tests were performed at the Waquoit Bay National Estuarine Research Reserve on Cape Cod in shallow water with the array submerged. We utilized a small non-metallic test stand that was placed in the water from shore and anchored the seafloor (see Figure 17). The array was elevated approximately 35 cm above the seafloor and targets were placed on the stand above the array in the water column. Nominal water depth was 180 cm, although it varied approximately ± 20 cm due to wave action and tides during our data collection period. We conducted target sensitivity dynamic "pull through" tests, static target tests, and background data collection at various positions in the water column.



Figure 17. Data collection set up as photographed on the shore of Waquoit Bay prior to in-water test stand data collections.

Dynamic target response tests were conducted using a similar set up and process to those conducted in-air. Figure 18 shows time series profiles of various ISO and UXO simulant targets as they are moved under the array. The standoff distance for these profiles was 37 cm so as to compare directly with data that were collected in a similar fashion in-air.

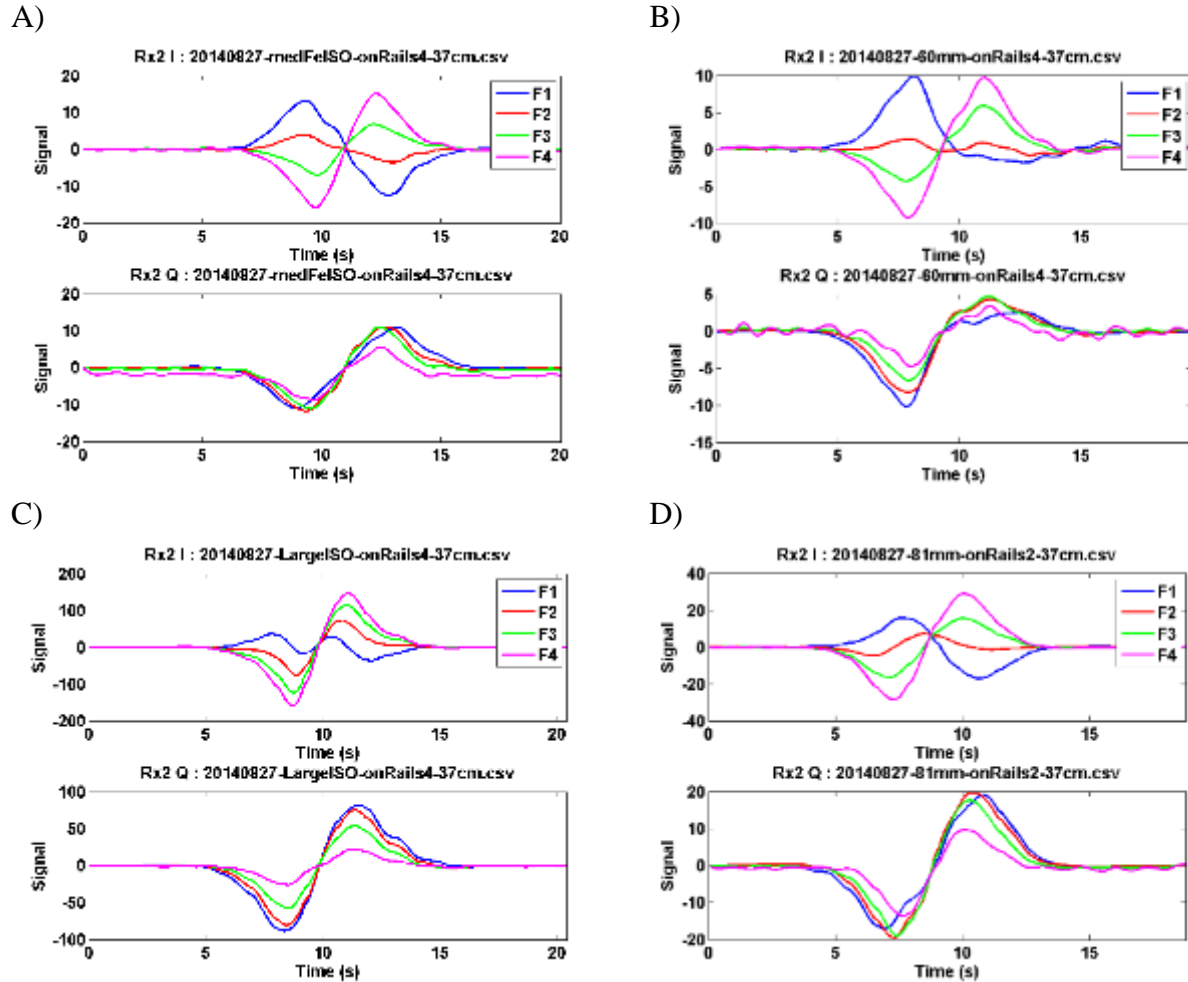


Figure 18. Time series profiles of various targets pulled under the array during in-water testing: A) Medium ISO, B) 60mm UXO, C) Large ISO, and D) 81mm UXO. The top plot for each set of target profiles represents the in-phase signals for the four frequencies recorded in the center receiver channel and the bottom plots represent the quad-phase signals.

There are two notable differences in the in-water data compared to that collected in-air. First, the signals are attenuated below those we observed during in-air tests. This is expected due to the added exponential attenuation with range and wavenumber in the conductive seawater environment, where the wavenumber is a function of the electrical conductivity of the medium surrounding the sensor (at Waquoit Bay, conductivity was measured to be approximately 4.6 S/m). The attenuation represents approximately 45-67% reduction relative to the measured in-air signals. The second notable difference in the profile data relative to that we collected in-air was a low frequency signal of approximately 1.5 Hz superposed atop the target response signal. This low frequency noise signal is likely attributed to interaction of the sensor with the oscillating sea-air interface (i.e., wave motion). This effect is evident in both the I and Q data profiles.

Addition qualitative tests were conducted to gain further insight into the origin of this low frequency signal. In these tests, the array was first lowered to the seafloor, then raised slowly to the sea-air interface and then lowered again to the seafloor (Figure 19).

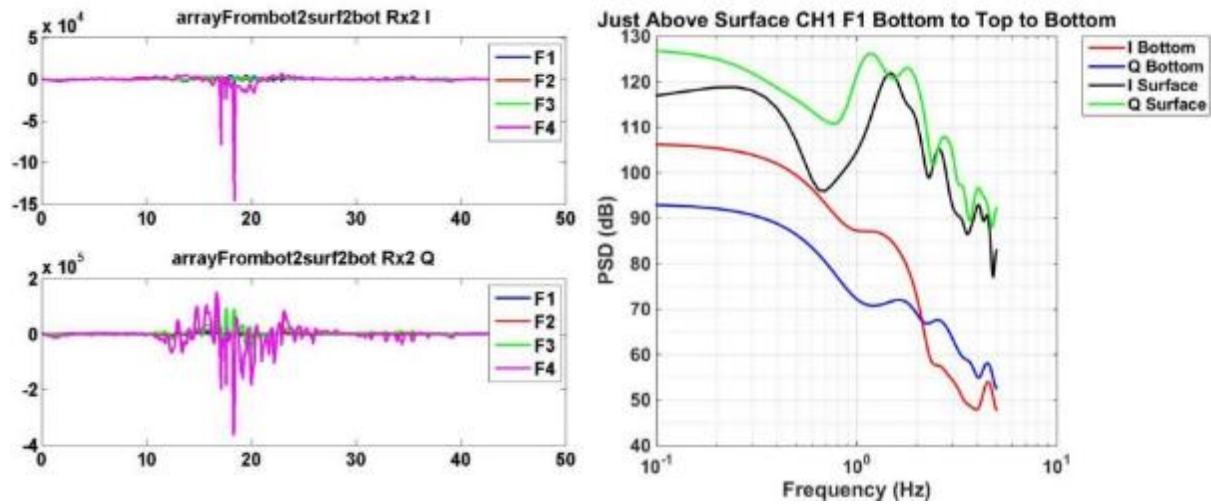


Figure 19. Left: I and Q raw ADC data (no filters or gains applied) versus time (s) from tests when the array was raised from the seafloor to the sea surface and then back to the seafloor. No targets or metallic objects were present so as to characterize the background water column response of the sensor. As the array approached the sea surface significant oscillatory signals are observed that are consistent in frequency with wave motion at the sea surface. Right: Power spectral density of the lowest frequency (~2 kHz) I and Q signals while the array is held stationary at the seafloor (bottom: at water depths of ~2 meters) and at the sea surface. As expected wave motion at frequencies of approximately 1.5 Hz imparted a strong noise signal on the sensor response near the sea surface.

To estimate the performance of the MFDA for underwater ROV operations, we analyzed pull through data in order to compute SNR values. Specifically, we analyzed raw ADC SNR values at 40 cm from the sensor array for 4 different target types in seawater: medium and large ISO targets and a 60mm and 81 mm UXO. The SNR assessment is shown in Figure 19. All target SNR values exceeded the prescribed 9 dB threshold detection level at the 40 cm standoff measured.

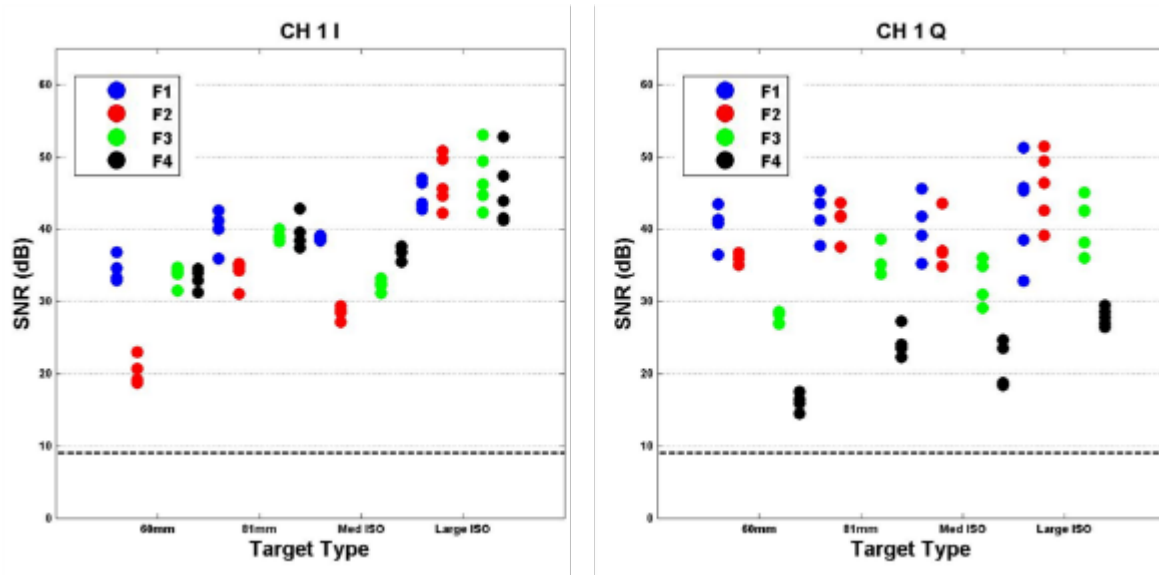


Figure 20. SNR values estimated from in-water pull-through tests for two sizes of ISO targets (medium and large) and for 60mm and 81mm UXO at ranges of 40 cm from the sensor array. All target responses exceeded the minimum detection SNR of 9 dB.

2.2.3 Hybrid AUV-ROV "Dolores" Integrated System

For this demonstration we utilized a hybrid AUV/ROV system for integration with the MFDA EM array system. The "Dolores" HAUV is a fiber-optic tethered hybrid AUV system built for wide area archeological assessments to depths of up to 1000 m. The system was developed by Greensea Systems in collaboration with Cobalt Marine and Mel Fisher Salvage Group using original equipment manufacturer (OEM) components (Figure 21 and Figure 22).

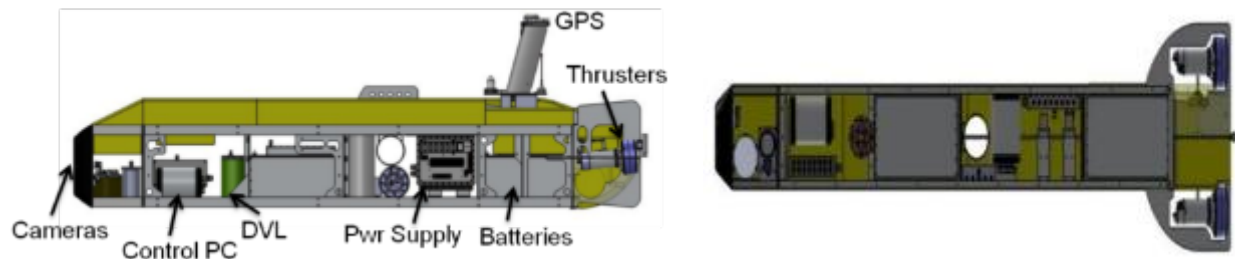


Figure 21. Side view (left) and plan view (right) of the Dolores hybrid AUV/ROV.



Figure 22. Dolores with the side panel removed (left) and in water with the EM array mounted in the front and EM data acquisition pressure vessel mounted to the top (right).

Hardware integration was done using a pair of specially fabricated PVC arms attached to the front of the HAUV and to the EM sensor via a pair of fiberglass angle brackets. This mounting configuration provided a stable means of positioning the sensor in front and below the HAUV platform. The location of the array forward of the vehicle enabled viewing of the sensor through the forward HAUV camera. Positioning of the sensor below the HAUV enabled the sensor to be positioned in close proximity to the bottom or even on the bottom while maintain HAUV bottom standoff of greater than 30cm; the height required by the DVL for maintaining bottom lock. The array mount allowed for movement of the array vertically to decrease the likelihood of sensor damage upon sensor contact with the seafloor. Figure 23 and Figure 24 show the mounting concept and realization as well as images of the EM sensor-equipped HAUV during and after deployment.

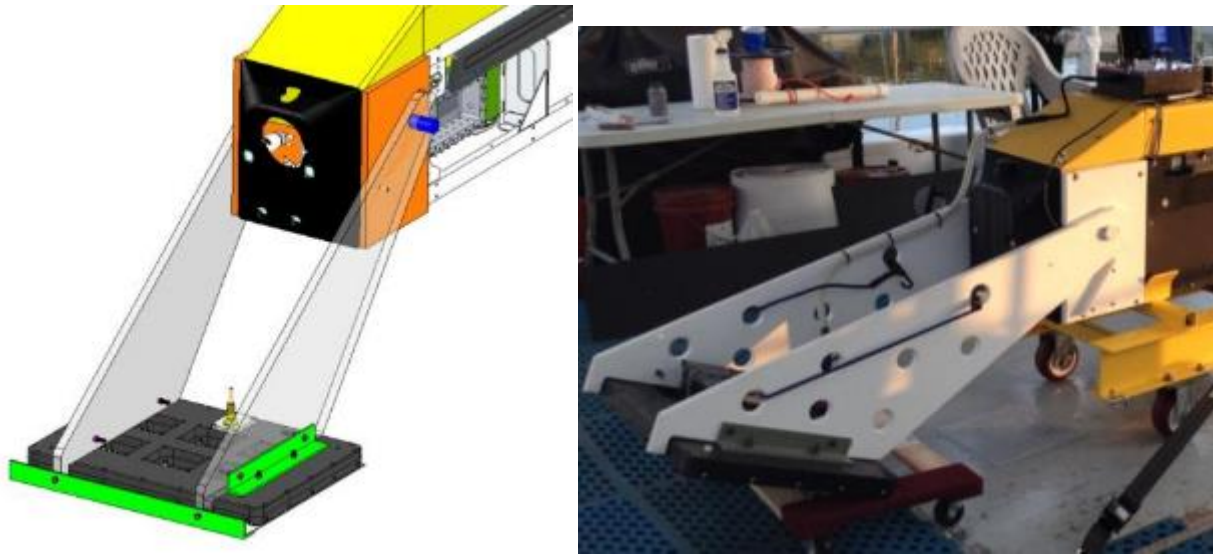


Figure 23. (Left) Conceptual drawing of the MFDA array mount. (Right) Array prior to deployment.

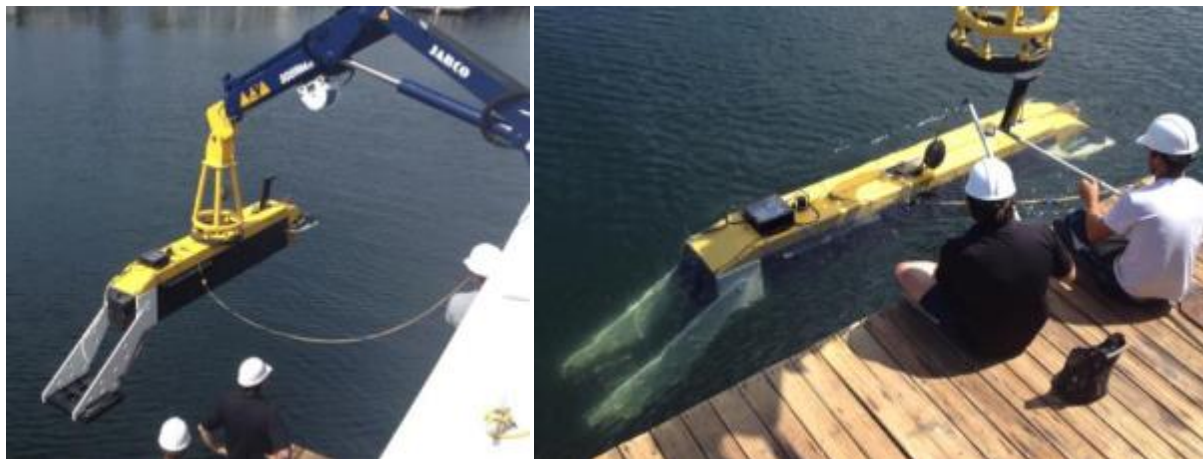


Figure 24. Deployment (left) and trimming (right) of the Dolores HAUV with integrated MFDA EM sensor.

2.2.4 Topside Operator Interface

The topside interface for the HAUV is focused around the operator workspace and user interface. This contains both a joystick control box and extensive ROV workspace software environment that provides correlation of navigation, control, and EM sensor data on a common screen. Data is distributed and shared over an ethernet-based network via the topside ethernet switch. This provides a common network such that all subsea and topside networked devices can communicate, synchronize, share resources, and access common data.

The workspace environment enables real-time data acquisition and logging and mission pre-planning. The workspace also supports playback of previously recorded data sets. It is comprised of a fully distributed network workspace that utilizes a local area network and centralized data framework based on the Greensea Systems openSEA (Open Software and Equipment Architecture) operating platform architecture. openSEA is common software

architecture designed to enable integration into any and all ROV platforms. It is based on a set of applications supported by a software library that contains modules for inertial navigation, device management, vehicle control, and mission management.

For our demonstration, we modified the HAUV operator workspace to include real-time feedback from the MFDA EM array. Otherwise, the HAUV operator interface was used in its standard configuration. In order to integrate the MFDA sensor functions and data display with this operator workspace, we developed additional modules so that the data could be

synchronously displayed with alongside other vehicle data, camera feedback, and overlaid on map information. We developed a C++ application using the QT framework in order to format MFDA array data, display both in-phase and quad-phase data in a waterfall type plot that interpolates and maps array data, track the array position and overlay on a map, and provide alarm indications if sensor data metrics exceed a given threshold. Mission planning capabilities, including the creation and editing of waypoints to follow during wide area coverage, resided on the navigation and control GUI panels on the display (Figures 26-28).

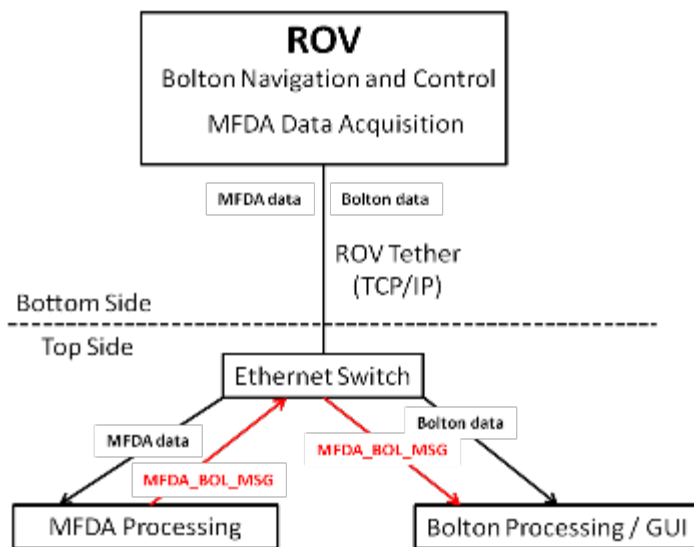


Figure 25. Software integration consisted of software components to acquire MFDA data, create and publish a UDP MFDA data message, and display MFDA data on the topside GUI.

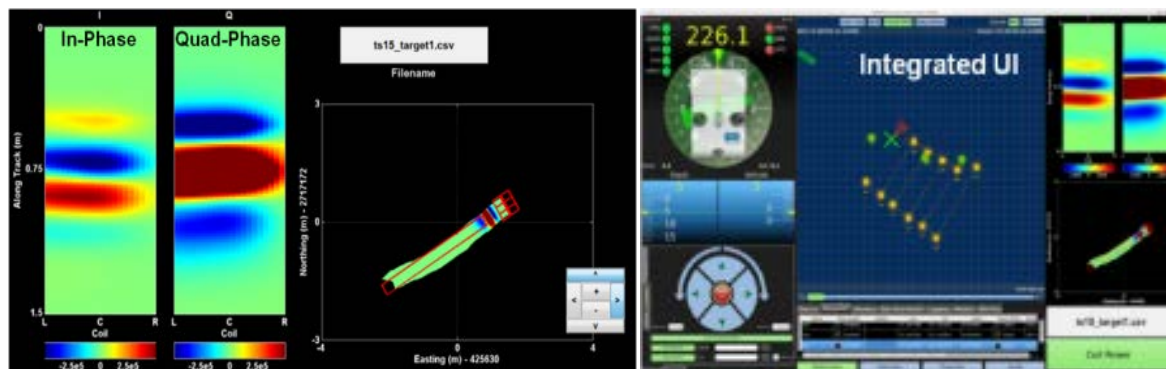


Figure 26. The standalone MFDA data UI (left figure) showing the in-phase and quad-phase color mapped array waterfall plots (left-side panel). Data anomalies are interpolated across the array (Left "L", Center "C", Right "R") and flow from top to bottom as the system moves along the seafloor. The quad-phase map is also "painted" over a map display (right-side panel) and standard pan and zoom features are accessible to the operator. A data filename and logging tool UI tool also provided. This interface was integrated as a module into the openSEA workspace and is shown in the right figure on the rightmost panel.

The user interface workspace environment operates on a Linux CPU server system is exposed to the operator via an array of flat panel monitors. Mission planning modules, HAUV real-time camera display, sonar data, as well waypoint maps, system status and configuration, and the EM data display are shown in Figure 27.



Figure 27. Examples of the topside user interface. Left-to-right: Screenshot of the mission planning GUI used for the NCS, photograph of the camera display screen focused just forward of the EMI Array, and the integrated NCS and MFDA GUI showing ROV system parameters (left panel), mission control profiles (center panel: here waypoint mission plan), and EMI array data maps (right panel).



Figure 28. Overall topside operator interface. The two top monitors display real-time imagery from the forward-looking camera image with MFDA array in view (right-side) and downward-looking camera view with UXO in view. The bottom monitors display (from left to right) profile data of select MFDA data channels, openSEA workspace views with different system parameters shown.

2.2.5 Launch and Recovery Vessel: The R/V Dare

The R/V Dare is a welded aluminum hull vessel that was originally specialized for fast transport of offshore personnel, deck cargo, and below-deck cargo. The vessel is propelled by 3 Detroit 12-71 diesel engines with twin disk transmissions providing 715 HP each at 2100 RPMs. These engines also supply two 3-71 Detroit diesel generators for 30 kW of power. The Dare was built in 1981 and has registered length of 84 feet, breadth (beam) of 22 feet and draft of 7 feet. She has a gross tonnage weight of 90 tons.

This vessel has been significantly modified from the original configuration and optimized for salvage dive operations and later for deployment of ROV systems. The bridge contains Raymarine color multifunction navigational display systems with additional depth displays, an ICOM VHF radio, SDGPS chartplotter and radar overlay, and dual digital depth sounders. Below deck are cabin quarters and births for up to 11 people. Aft of the bridge is a co-pilot bosun's bridge with vessel network and control room. Aft of the bosun's bridge is the main enclosed control room, where ROV operators and operations managers can command wet or dry missions. Toward the midship and stern are the diver and ROV preparation and storage areas.

The very aft part of Dare houses deskpace for LAR operations including a Jabco 12.5 ton knuckleboom hoist crane. This system attaches directly to the mounting hook atop of the HAUV for relatively simple deployment. The HAUV is uncoupled from the hoist once in water by a

diver, then rocked to expel any trapped air to aid in submerging and generating the proper buoyancy. The R/V Dare, Boston Whaler, knuckleboom, and ROV control center are shown in Figure 29.



Figure 29. Top Left: R/V Dare - a 84-foot modified dive salvage and crew boat to which the HAUV-100 is currently dedicated. Top Right: The 17-foot Boston Whaler tender and anchor vessel that accompanies the Dare. Bottom Left: Maine control room and ROV operations monitors. Bottom Right: Stearn ROV deployment.

2.3 ADVANTAGES AND LIMITATIONS OF THE TECHNOLOGY

The ROV-based EMI technology has particular advantages over EOD-trained divers equipped with handheld detectors or EM or magnetometer arrays towed from surface vessels. Divers are highly constrained in terms of the mobility, depth and duration during dives due to strict health and safety regulations as well as physics. Towed systems as well as fully autonomous unmanned undersea vehicles (UUVs) place sensors 2-5 m above the sea floor, and thus restrict detection capabilities to large UXO only. The ROV-based EMI technology to be demonstrated has particular advantages that can be leveraged for marine UXO operations:

- Tightly integrated vehicle position and control with high resolution active source EMI data. This will lead to improved detection and a reduction in false alarm rate through improved classification resulting from high resolution EM sensor data collected synchronously with high resolution position data.
- Real-time operator situational awareness and dynamic repositioning capability. This affords the operator both a dynamic mapping mode and a detailed reacquisition or static characterization mode with data collection over suspected targets.
- Precise navigation and positioning of the sensor array in close proximity to the seafloor. This provides accurate positioning, tracking, and bottom following, which leads to improved survey efficacy and efficiency. Because signal levels drop off quickly with

range from a target, it is critical to accurately and precisely position the sensor in varying conditions.

- Tele-operation removes the operator from the water column and allows for accurate operations in both shallow (<3m) and deep water (>20 m). The endurance of an ROV system is only limited by the tether length and not power supply (UUVs) or safety (divers). This enables extended time on the seafloor as well as significant cost savings relative to deployment of dive teams.

Throughout the project we have worked to systematically reduce the limitations and demonstrate the most optimal configuration of an integrated system. Based on our Year 1 engineering tests and demonstration (see Appendix B), we made a series of modifications and enhancements to the system. Among the specific issues we addressed for the final demonstration included the following:

- Potential degradation of the heading accuracy due to interference of the compass with other components including the EMI array. We mitigated this by performing a thorough compass calibration and follow-on verification with the integrated system before the demonstration.
- Loss in positional accuracy when the sensor is at close range (<0.3 m) to the seafloor. This situation may result in a loss of DVL ‘bottom lock’ that quickly corrupts the navigation solution. We worked to mitigate this by mounting the EMI array lower than the DVL mount on the bottom of the ROV.
- Although the thrust force available from Dolores HAUV is sufficient to provide stable powered thrust in up to 2 knot currents, it may not be well-suited for operation in very high currents (>3 knots). Although, we were not able fully assess the limitations of the system under relatively strong currents during the demonstration, we project that operations during maximum ebb and flood tidal currents in some areas may be significantly affect stability.
- Limitations on the range of operation due to limited tether lengths (nominally 1000 m) may constrain wide area coverage operations. We have developed mission plans that utilize a mobile base from a surface vessel to mitigate this limitation. Another potential solution is longer fiber optic tethers that have significantly less drag impact and have been configured up to lengths of 14 km for various applications (e.g., aqueduct inspections, riverine operations, etc.).

3.0 PERFORMANCE OBJECTIVES

The performance objectives (Table 1) were focused on demonstration of precise system positioning and control required for execution of UXO detection and characterization missions. The functions we demonstrated include station keeping, bottom following, and waypoint navigation while achieving correlated EMI data quality metrics during area coverage and mapping and detailed area or reacquisition surveys.

Table 1. Performance Objectives

Performance Objective	Metric	Data Required	Success Criteria
Quantitative Performance Objectives			
Bottom Following Accuracy	Average error between desired altitude and true altitude of system, standard deviation of true system altitude	<ul style="list-style-type: none"> Beginning and End waypoint coordinates Desired altitude Altitude reports from the navigation and control system 	$\Delta A < 0.15 \text{ m}$ $\sigma A < 0.15 \text{ m}$
Station Keeping Accuracy and Precision	<p>Average error and standard deviation in northing, easting, and altitude between true position and desired position of the system</p> <p>Average error and standard deviation in heading, roll, and pitch</p>	<ul style="list-style-type: none"> Anomaly location (desired position), within 10 cm Desired altitude Desired heading, roll, and pitch Position and orientation reports from the navigation and control system 	$\Delta N \text{ and } \Delta E < 0.35 \text{ m}$ $\sigma N \text{ and } \sigma E < 0.35 \text{ m}$ $\Delta A < 0.15 \text{ m}$ $\sigma A < 0.15 \text{ m}$ $\Delta H < 1 \text{ degree}$ $\sigma H < 2 \text{ degree}$ $\Delta R < 1 \text{ degree}$ $\sigma R < 2 \text{ degree}$ $\Delta P < 1 \text{ degree}$ $\sigma P < 2 \text{ degree}$
Waypoint Mission Control	<p>Average error in distance between line defined by waypoints and recorded position</p> <p>Standard deviation of error between linear path followed and recorded position</p>	<ul style="list-style-type: none"> Beginning and End waypoint coordinates (true line position), Position reports from the navigation and control system and calculated deviations from a best-fitting straight line path to the points along travel 	$\Delta D = (\Delta N^2 + \Delta E^2)^{0.5}$ $\Delta D < 1.5\% \text{ distance travelled}$ $\sigma D < 0.5 \text{ m}$
Detection of all munitions greater than 60 mm	Signal to Noise Ratio (SNR) of signal produced by munition in EMI sensor to noise in EMI sensor	<ul style="list-style-type: none"> Signal received during anomaly interrogation Noise estimate during anomaly interrogation Position reports from the navigation and control system 	$\text{SNR} > 9 \text{ dB}$ $\text{Pd} > 0.95$ (assuming a nonfluctuating target and Gaussian noise a 0.95 Pd at 9 dB corresponds to a pFA of approximately 0.01)
Detection Location Accuracy and Precision	Average error in northing and easting between true position and estimated target position	<ul style="list-style-type: none"> MFDA data Navigation data True Target Locations 	$\Delta \text{TN and } \Delta \text{TE} < 1.0 \text{ m}$ $\sigma \text{TN and } \sigma \text{TE} < 1.0 \text{ m}$
Qualitative Performance Objectives			

Ease of use	Operator observations	• Field notes recorded during setup and testing	Ease of use comparable to alternate standard marine surveying procedures
Mission Assisted Autonomy	Operator observations	• Comparisons of manual and automated control	Value of assisted autonomy functions
Integrated System Stability	Operator observations	• Time and effort spent trimming system	Valuation of time and effort to stabilize

3.1 OBJECTIVE: BOTTOM FOLLOWING ACCURACY

The ability of the system (ROV with the EMI sensor attached) to autonomously maintain a programmed height from the seafloor directly affects the SNR, and therefore the detection range, of metallic objects on or below the seafloor.

3.1.1 Metric

Here we compared the desired altitude of the system to the actual altitude reported by the navigation and control system. The altitude is measured relative to the lowest altitude component of the system, which is the MFDA sensor array. Average error, defined as the mean of reported altitudes minus the desired altitudes, and the standard deviation of the reported altitudes were calculated.

3.1.2 Data Requirements

We calculate bottom following accuracy while the system travels from one waypoint to another. Waypoints are placed so that no abrupt elevation changes or large obstacles are encountered. If abrupt changes in seafloor elevation or large objects are encountered, requiring fast altitude changes, we record their time and location for removal of these data during analysis. We also record the desired altitude (constant) and the altitudes reported by the navigation and control station at 1 Hz or faster rate. We collect bottom following data along a minimum of 100 meters of travel at desired altitudes between 25 and 100 cm. The system traverses the seafloor at nominal operating speeds (1-2 knots). For our tests, transects were repeated to estimate variability.

3.1.3 Success Criteria

Our objective is to achieve an average altitude error less than 15 cm with the standard deviation of altitude reports less than 15 cm. We anticipate variation of seafloor bathymetry on the order of 0.05 to 0.3 m/m depending which part of the site we are traversing.

3.2 OBJECTIVE: STATION KEEPING ACCURACY

In our demonstration station keeping refers to the system's ability to maintain a commanded three-dimensional position and orientation over time. The ability of an ROV to autonomously

keep station is a function of the underwater environment (current), the accuracy and precision of the navigation sensors, and control algorithms.

3.2.1 Metric

Our station keeping demonstration, compared the desired position (northing, easting, and altitude) of the system to the actual position reported by the navigation and control system. Average northing, easting, and altitude error, defined as the mean of reported position minus the desired position, and the standard deviation of the reported positions is calculated. Average heading, roll, and pitch error, defined as the mean of reported orientations minus the desired orientation, and the standard deviation of the reported heading, roll, and pitch is also measured or estimated.

3.2.2 Data Requirements

We command the system to keep station over various seeded items at a commanded Northing, Easting, altitude, heading, pitch, and roll. During the demonstration, we focused on maintaining heading so the commanded pitch and roll were generally set to 0 degrees. We record the commanded location and orientation and logged navigation reports during time durations between 1 and 5 minutes. Data were recorded at a rate of 1 Hz or higher in all cases. We collected station keeping data on over 12 different anomaly locations. We attempted to sample anomaly locations that contained some degree of varying current conditions to the degree possible by conducting surveys over different times of the day (over the tidal cycle) and over different parts of the study area.

3.2.3 Success Criteria

Our objective was to achieve an average northing and easting error less than 35 cm with the standard deviation of easting and northing reports less than 35 cm. Our objective vertical control was to achieve an average altitude error less than 15 cm with the standard deviation of reported altitude less than 15 cm. The average roll, pitch, and heading errors were intended to be less than 1 degree, with the standard deviation of reported orientation data less than 2 degrees.

3.3 OBJECTIVE: WAYPOINT MISSION CONTROL

The system's ability to transit from one point to another and follow a given line affects the quality and completeness of UXO survey map data collected by the EMI array mounted to the ROV. Additionally, the capability to accurately navigate and survey between waypoints is required to carry out the wide area EM coverage mission. Therefore, we assessed waypoint mission control accuracy using two distinct analysis methods and associated metrics. The first metric (ΔD) relates the global positional accuracy of the navigation solution and is defined as the mean of the distances between the line defined by surveyed waypoints and navigation solution locations recorded while traveling between waypoints. The second metric (σD) relates the system's ability to navigate on a linear path and is defined as the standard deviation of the distances between the reported system positions and the best line fit to the reported system positions.

3.3.1 Metric

The two metrics we used to assess waypoint mission control included: (1) average error from the global waypoints and (2) average relative deviation from a straight line through the measured navigation points. The system's ability to follow a line comprised of global waypoints was created by comparing the desired position (northing, easting) of the system at equally spaced intervals along a line defined by two waypoints to the actual position reported by the navigation and control system. Average distance error, defined as the mean of the distance from the reported position to the desired position was calculated.

The system's ability to navigate on a linear path was determined using the standard deviation of the error between individual navigation reports and the best line fit to the recorded data. Heading, roll, and pitch reports were also analyzed simultaneously in order to shed light on trends in the position data.

3.3.2 Data Requirements

We calculate the survey path following accuracy while the system travels from one waypoint to another. We record the commanded position and log navigation reports during system transit between waypoints. In order to assess path following capability, data should be acquired over a minimum of 200 m total distance with at least 2 different headings.

3.3.3 Success Criteria

Our objective was to achieve an average northing and easting error less than 1.5 m over 100 m of distance travelled. This corresponds to waypoint position accuracy of 1.5% distance traveled.

3.4 OBJECTIVE: DETECTION PERFORMANCE

The ability of an ROV-mounted EM system to detect relevant UXO test objects yields quantification of a key system metric. To produce detections, the EMI array must be functioning properly, data must be processed in order to improve signal-to-noise characteristics, and positioning of receivers must provide the resolution required to delineate individual targets larger than 60 mm diameter.

3.4.1 Metric

To assess detection performance, we compare the total number of target encounters to the actual number of targets detected. A target encounter is determined by any part of the EMI sensor have an easting and northing coordinate within 0.5 m of the recorded position of a seeded test item while at a reported altitude less than 0.5 m. The metric that we measure is the Signal-to-Noise Ratio (SNR) of signal produced by a munition target to noise recorded in EMI sensor. Our signal estimate is the maximum value of the processed data when overpassing an object. Our noise estimate is the standard deviation of the processed signal when no targets are present.

3.4.2 Data Requirements

Georeferenced EMI sensor and navigation data correlated in time are required for input into custom detection algorithms.

3.4.3 Success Criteria

Our objective was to achieve an average SNR of 9 dB or greater over all target encounters against targets that are larger than 60 mm in diameter. We also endeavor to achieve a probability of detection of 0.95 or better. The probability of detection is defined as the number of detections divided by the number of emplaced targets that pass within 0.5 m of the sensor coverage footprint while the sensor is at an altitude less than 0.5 m. Utilizing a SNR of 9 dB approximately corresponds to a probability of false alarm of 0.01. This SNR was selected based on previous testing (see Section 2.2.2 for further explanation).

3.5 OBJECTIVE: DETECTION LOCATION ACCURACY

The ability of an ROV-mounted EM system to produce accurate anomaly locations is critical to UXO survey and detection missions. To produce accurate detection locations, the position of the EMI sensor must be accurate during target investigations.

3.5.1 Metric

For location accuracy analysis, we compare the estimated position (northing, easting) of each target detected by the MFDA to the true position of each target. Average northing and easting error, defined as the mean of reported position minus the true position, are calculated. Separate metrics are reported for detection surveys along generally East-West transect and generally North-South transects in order to segment any potential directional biases.

3.5.2 Data Requirements

Georeferenced EMI sensor and navigation data correlated in time are required for input into custom detection algorithms.

3.5.3 Success Criteria

Our objective was to achieve an average northing and easting error less than 1.0 m.

3.6 OBJECTIVE: EASE OF USE

The ease of use of the integrated system including ROV, EMI sensor, and navigation and control system is important to determine the level of training required for use of this equipment in a production environment. Ease of setup, calibration, and operation were determined. We assess launch and recovery of the system in terms of required equipment, personnel, and specialized skills required to deploy and recover the system.

3.6.1 Metric

There were no specific quantitative metrics for this objective. The qualitative metric was determined based on notes and observations from operators and crew.

3.6.2 Data Requirements

Observations and field notes taken by test personnel are reviewed to determine the qualitative ease of use of each component in the system and identify any shortcomings of each component's operation.

3.6.3 Success Criteria

Success is relative to other similar survey systems in the experience portfolio of the operators. If the system is considered significantly more complex, difficult, or unwieldy relative to similar or comparable marine survey systems, it was not considered successful.

3.7 OBJECTIVE: MISSION ASSISTED AUTONOMY

Mission assisted autonomy is comprised of automated control missions that the system undergoes without direct and continuous control by the operator. These missions can be initiated with a button click and run with minimal or no action or management by an operator. Auto-station keeping is one example of this. When the system has transited to, or close to, a directed station keeping point, the operator will set the mission to start and the system will autonomously attempt to hold station over the point.

3.7.1 Metric

There were no specific quantitative metrics for this objective. The qualitative metric is determined based on notes and observations from operators and crew.

3.7.2 Data Requirements

Observations and field notes taken by test personnel were reviewed to determine the effectiveness of automated mission control relative to skilled operator control.

3.7.3 Success Criteria

Success is evaluated relative to skilled operator control. A comparison of which automated missions perform equal to, better than, or worse than those conducted by a skilled operator was assessed.

3.8 OBJECTIVE: INTEGRATED SYSTEM STABILITY

The ability to stabilize the system through mechanical means in variable underwater environments before beginning a survey affects its overall usefulness and range of sites where it will be applicable. Specifically, we assess the time and effort required to trim and level the system using passive ballasting and configuration. This may be necessary when moving from one operating area (e.g., freshwater to saltwater; or cold water to warm water) to another.

3.8.1 Metric

There were no specific quantitative metrics for this objective. The qualitative metric include notes and observations from operators and crew.

3.8.2 Data Requirements

Observations and field notes taken by test personnel were reviewed to assess the level of effort (number of personnel and amount of materials required) and time needed to stabilize the system under hydrostatic and hydrodynamic conditions.

3.8.3 Success Criteria

Success was qualitatively assessed based on overall system logistics and mobilization time and effort.

4.0 SITE DESCRIPTION

The site for this demonstration was located in the offshore areas just south of Boca Chica Key, Florida in the Lower Florida Keys on the south Florida shelf. We have identified and pre-surveyed a data collection site over an approximate 250 x 200 m area near the Sambo Keys and Sambo reef. The site provides a mix of conditions and appropriately balanced cost effectiveness for our demonstration with thorough testing under representative conditions. The following sections describe the site selection and site areas in more detail.

4.1 SITE SELECTION

Preferred site conditions contain a range of water depths and variety of bottom types and current conditions. The desired site should also be amenable to boat and diver access as well as seeding of surrogate targets and standard test objects (e.g., ISO's). Site that have some prior marine surveying conducted are advantageous in pre-characterizing site conditions and survey areas. This may be in the form of bathymetric surveys, multi-beam or side-scan sonar surveys, or other types of marine geophysical surveys.

The demonstration site we selected was within the Florida Keys Marine National Sanctuary (FKMNS) about 7 km south of the Boca Chica Key and approximately 250 m north/northwest of Middle Sambo Key on the southern part of the West Florida shelf area off the Lower Florida Keys. The FKMNS site is administered by the Department of Commerce National Oceanic and Atmospheric Administration (NOAA) and is managed by both NOAA and the state of Florida's Board of Trustees of the Internal Improvement Trust Fund through the Florida Department of

Environmental Protection. We received an exclusive permit to conduct testing in the area from the NOAA FKMNS superintendent (see Appendix for copy of permit) prior to our demonstrations.

Since this demonstration was intended as an evaluation of the integrated system in a realistic survey environment, we selected a site area that balanced the tradeoff between representative site conditions, site variability, previous survey information, and logistical ease and cost effectiveness. An regional overview bathymetric map of the Gulf of Mexico and Straits of Florida regional area is shown in Figure 30 and Figure 31 to provide mesoscale context for the site. Given the time frame for the demonstration in early 2015, the lower Florida Key general area provided water conditions (i.e., temperature, wave/tide, clarity) with adequate days of continuous weather amenable for operations than other potential areas.

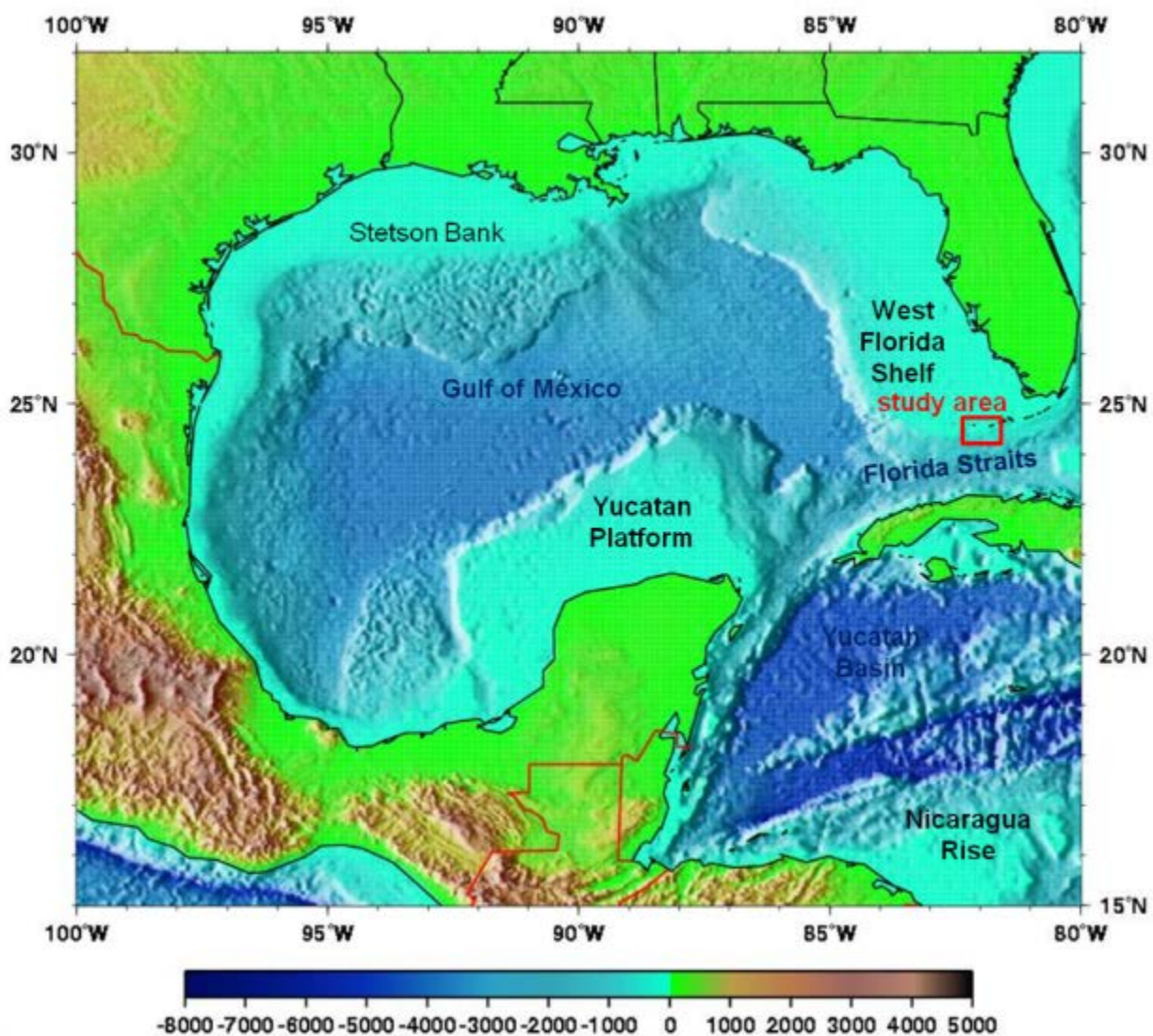


Figure 30. Regional bathymetry map of the West Florida Shelf relative to the Gulf of Mexico and continental North America.



Figure 31. Left: Google Earth map showing location of the study area in relation to primary sea bottom features. Right: Google Earth zoomed-in map showing the location of the test site relative to the outer reef areas juxtaposition between the Hawk Channel and Florida Straits.

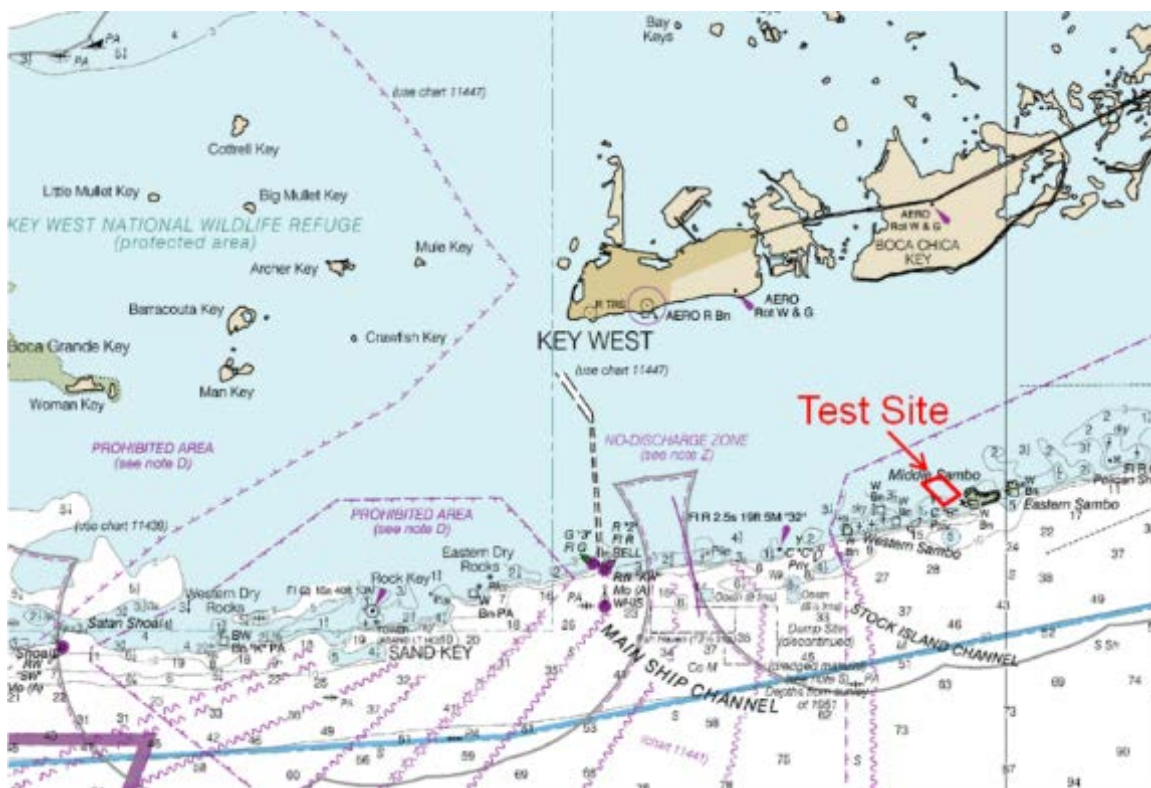


Figure 32. The general study area is within the southern part of the Hawk Channel, ~7.5 km south of the Boca Chica Key, between the Stock Island Channel and Eastern Sambo Ecological area.

The selection of the particular study site in the region was based on logistical considerations and cost effectiveness of the operating support infrastructure. This included taking advantage of on-going operations of the vessel that the selected ROV platform is dedicated to. These considerations are described further below.

The specific areas identified for ROV-EM demonstrations are within the larger area identified. Previous surveys have established spar buoy anchor points and other sea surface or sea bottom

fiducial markers to use as survey baselines. The use of these sites allowed us to configure, test, and assess system validation results from realistic conditions without incurring logistics and DoD intrusive site investigation expenses that would be required for demonstration at a live site during this stage.

The Sambos Keys are located approximately 7 km due south of the Boca Chica Airfield at the Key West Naval Station on Boca Chica Key, Florida in the lower Florida Keys. Middle Sambo, Western Sambo, and the Eastern Dry Rocks are Holocene reefs located along the shelf edge between the reefs at Eastern Sambo and Eastern Dry Rocks. A single outlier reef occurs along the seaward edge of the upper-slope terrace off Eastern and Western Sambos. The study site is on the shoaling sands just north of the reef that separates the inner Hawk Channel from the deeper Florida Straits. The Hawk Channel is a shelf lagoon trough that extends to the south and southwest, deepening off the lower Keys, and continuing to deepen as the main reef track arcs westward in the vicinity of the Marquesas Keys area (see Figure 32). The demonstration site area extends from the northwest corner of Middle Sambo Key toward the hardbottom areas just north of Middle Sambo Key. This provides some diversity in the bottom types and water depths from over 15 meters in the deepest parts of the channel to less than 5 m on the southern part of the study area. In 2007 the NOAA National Center for Coastal Ocean Science conducted shallow water bathymetric surveys of the Western Sambos Ecological Reserve. Bathymetric and imager data were collected with the Teledyne Benthos C3D Phase Differencing Bathymetric Sonar (PDBS), RESON Seabat 8125 multibeam echosounder and Odom Echotrac CV2 vertical beam echosounder (VBES). Data was used to update the nautical charts for this area in 2008 (Turner, 2007). The primary bathymetric survey and imagery system was the C3D sonar, which acquired 200% coverage over the study area. Although the C3D data did not meet NOAA charting standards due to issues with data quality, no navigation dangers were identified and no significant contacts were observed. Site bathymetry is shown in Figure 33.

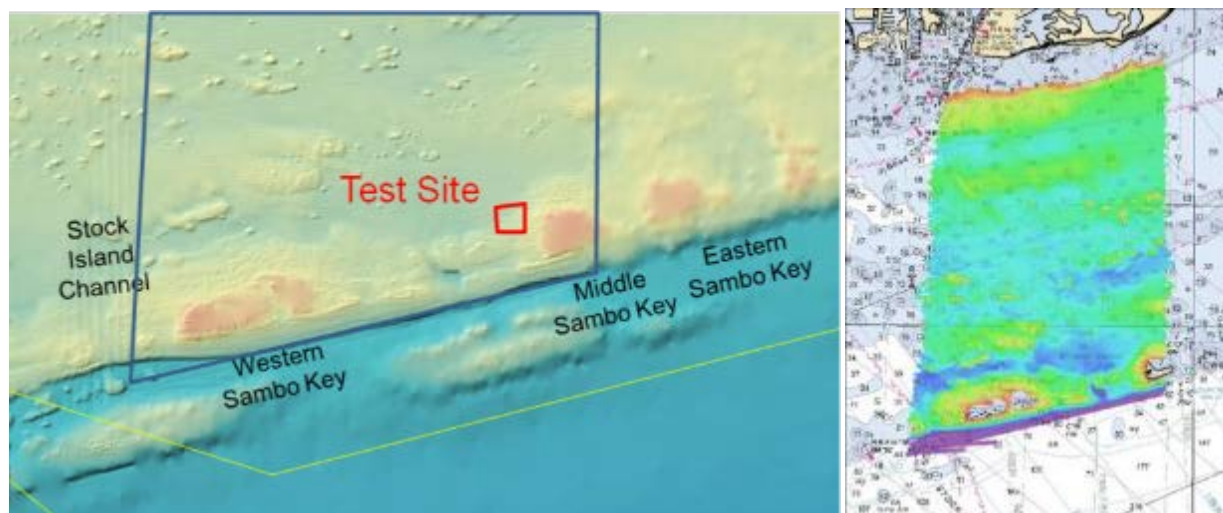


Figure 33. Left: Overview bathymetry of the Sambo Keys and Stock Island Channel portion of the outer reef between Hawk Channel and the Straits of Florida. Right: Extent of interferometric acoustic bathymetry data collected over the Western Sambos Ecological Reserve by NOAA in 2007. Our study area was just north and west of Middle Sambos Key, which is located in the southeast portion of the bathymetric survey area in water depths extending between 5 and 14 meters.

The Western Sambo Ecological Reserve is a 3,000 hectare rectangular shaped reserve extending from the shoreline around the Boca Chica Naval Air Station to the Western Sambo reef. The reserve is roughly 4 km wide at the air station and nearly 3 km wide at the reef track. In 2004, the Florida Fish and Wildlife Conservation Commission (FFWCC) conducted studies on the movements of spiny lobsters in the area. As part of that study, the FFWCC utilized a towed hydrofoil that was modified to accommodate GPS-tagged underwater video for habitat mapping. Poor visibility during surveys prevented integration of the underwater video with aerial photography, but nonetheless over 6,500 habitat classifications were generated. The predominant habitat was sand/mud (70%) followed by sea grass (21%) and patch reefs (3%) (Bertelsen et al., 2004).

Specific areas within our localized study site have been pre-surveyed that are relatively flat and featureless as a baseline against adjacent areas that have some varying relief and benthic conditions (sea grass, mixed carbonates, hard bottom). These areas have been identified and logged during preliminary ROV-EM surveys as well as from numerous recreational, research, and salvage diver logs from this area. Figure 34 and Figure 35 show underwater photographs of the study area taken by our dive team during preliminary site clearance activities.

The seafloor at this particular site has been extensively surveyed and has well known bottom conditions. The southern portion of the site area has been surveyed extensively by dive teams during dive operations, benthic habitat studies, and ecological surveys. This part of the site contains an undisturbed sands and hardbottom with shell and coral distributed throughout. Water depths are 17-44 feet (5-14 m) in this area and visibility is relatively clear for dive operations, target seeding, and underwater photography. Toward the southeast, the general site climbs steady to shallower water as the bottom conditions shift from primarily sandy sediments with areas of turtle sea grass to sparse areas of patch reef along the transitional ridge.



Figure 34. Underwater photographs of the mixed shell, sand, mud bottom during preliminary site clearance in the demonstration area.



Figure 35. Underwater photograph of the fine sandy carbonate sediments that cover dominate the demo area. Intermittent areas of sea grass and patch reef are also observed throughout the area.

General circulation over our study site is part of the southwest Florida shelf Loop Current, which enters the Gulf of Mexico through the Yucutan Straits and moves to the north as far landward as the 100-m isobath and turns clockwise directing it back south. Just southwest of the Dry Tortugas it becomes the Florida Current, which meanders through the Straits of Florida confined by 250-m and 500-m isobaths. Local circulation is dominated by wind and tides through the Hawk Channel. The study site is a wave dominated micro-tidal (-0.15 to 0.7 m maximum tide range; with 0.39 m mean tide range) environment with waves and storms representing the most significant coastal processes affecting seafloor sedimentation. Mean annual wave height is 17 cm (Davis et al., 1998). Salinity during April 2015 was in the range of 20.0 to 28.9 ppt (parts per thousand) and water temperatures were between 21 and 27 degrees Celsius. These values were estimated based on current and historical data from NOAA Oceanographic Station 8724580 near Key West, however, conditions at the study site may deviate to some degree. These salinity and temperature ranges corresponds to a minimum electrical conductivity of 3.34 S/m at 27°C and maximum of 4.14 S/m at 21°C.

Local NOAA and National Weather Data Buoys near Sand Key, Pulaski Light, and Key West provide marine weather and tide information (Figure 36). In addition, NOAA produces a Coastal Marine Zone Forecast. Our site lies within the zone designated as GM2-044, which extends along the Hawk Channel along the middle keys through our site area south of Boca Chica Key and west to Hamilton Shoal and the nearby reef. The outer zone, designated as GM2-054 is also relevant since it extends south of our site to 20 NMI.

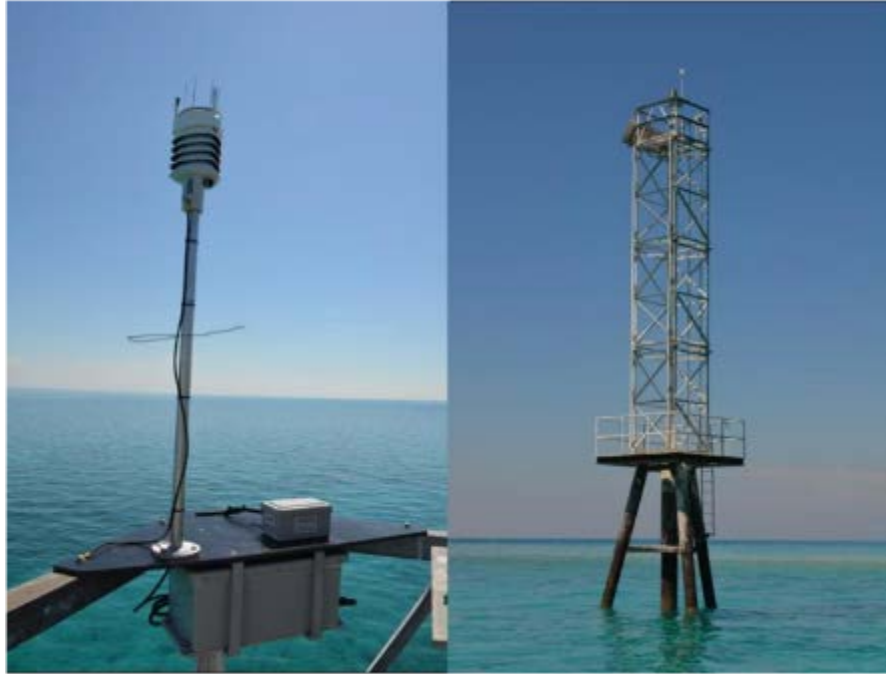


Figure 36. Photographs of the NOAA Sand Key National Buoy Station at 24.456 N 81.877 W . Data from the SANF1 buoy from our demonstration period (10-17 April 2015) revealed that wind conditions in the general study area was relatively constant. Figure 37 shows the wind speed, wind direction, and air temperature during our demonstration period.

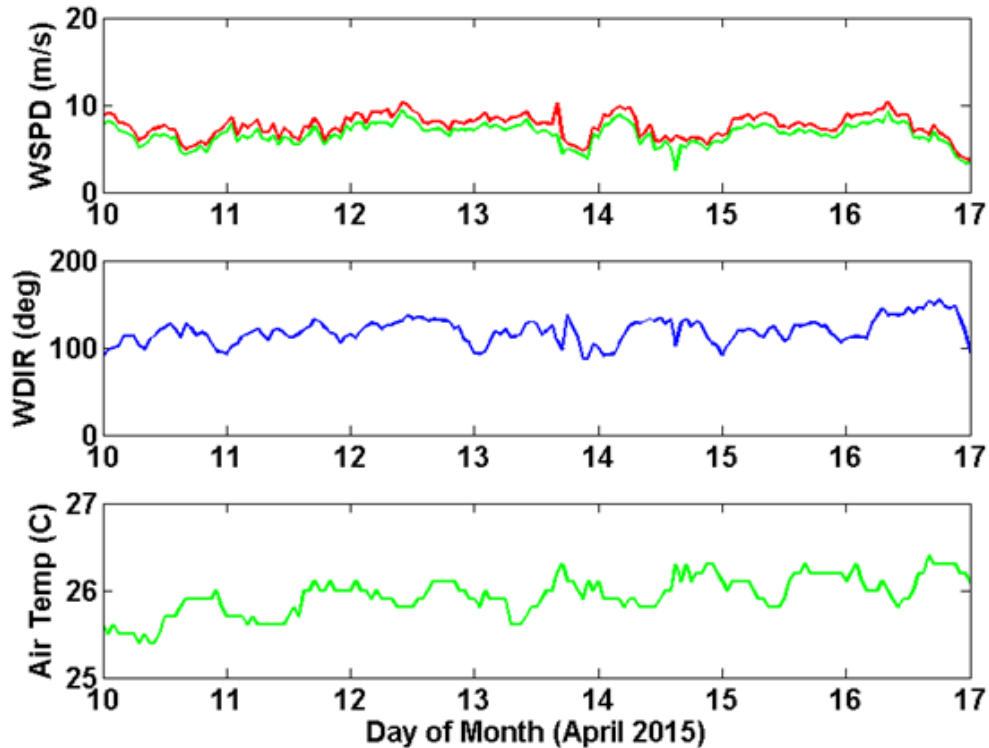










Figure 37. Surface METOC weather data from our demonstration period in April 2015: WSPD is wind speed, WDIR is wind direction relative to north, and the bottom plot shows the surface air temperature.

Tidal data from Key West tidal monitoring stations show that relatively small tidal variations were observed during our demonstrations. Table 2 shows the daily semidiurnal low and high tide mean water levels along with the moon phase for each day. The largest daily tidal variance during our demonstration was less than 75 cm.

Table 2. Daily tidal levels as measured from the Key West monitoring station during the demonstration period. The regular diurnal tidal variation was generally less than 1 m during April 2015.

DATE	High Tide Level				Low Tide Level				Moon
	AM	WL (ft)	PM	WL (ft)	AM	WL (ft)	PM	WL (ft)	
10 Sun	3:00	1.2	2:05	1.7	7:58	0.5	9:22	-0.1	
11 Mon	4:01	1.2	3:24	1.6	9:18	0.5	10:22	0.0	
12 Tue	4:5	1.4	4:52	1.5	10:41	0.4	11:19	0.1	
13 Wed	5:52	1.5	6:15	1.5	11:57	0.2			
14 Thu	6:40	1.7	7:26	1.5	12:12	0.1	1:02	-0.0	
15 Fri	7:24	1.9	8:27	1.4	1:00	0.2	2:00	-0.2	
16 Sat	8:07	2.1	9:21	1.4	1:46	0.2	2:53	-0.4	
17 Sun	8:49	2.2	10:10	1.4	2:30	0.2	3:43	-0.5	

4.2 SITE HISTORY

Both natural and cultural events have shaped this area of the lower Keys. Over the recent history, storm systems have arguably played the largest role in terms of acute events that affect the sea bottom in the area. During the winter months, large-scale mid-latitude cyclonic systems are transported over the Keys by fluctuations in the polar jet stream (Winsberg, 1990). These systems tend to occur on an average frequency of once per week. Although they are not associated with significant precipitation, they tend to effect the marine environment in terms of decreasing water temperature and increasing turbidity, nutrient and salinity levels. In addition, South Florida experiences more hurricanes and tropical depressions than any other area in the United States. Storms are most frequent between June and October, and statistically peaking in late September. On average there is a 14 percent probability of hurricane occurring in the Keys. However, with the exception of Hurricane Andrew in 1992 (a Class 4 hurricane on landfall), the Keys have only experienced two Class 1 hurricanes since 1966. Both tropical storms and hurricanes have had a significant effect on the natural environment in the lower Keys. These events tend to mobilize and alter sediment formations and restructure benthic habitats.

The site area has a rich maritime and ecological history including heavy use as a trade route in the 17th century primarily by Spain. In more recent times, the lower Keys became an attraction for visitors, divers, fisherman, and explorers. Beginning in 1957, environmental conservationists began working to preserve offshore areas around the keys by establishing state parks and marine conservation areas. After three large ships ran aground on the coral reef tract in the fall of 1989, the US Congress expedited the establishment of the Florida Keys National Marine Sanctuary (FKNMS; Florida National Marine Sanctuary and Protection Act of 1990: Public Law 101-605). The National Marine Sanctuary consists of 9,500 km² extending approximately 220 miles from the southern tip of the Florida peninsula along the 300-foot isobath to the Dry Tortugas. This encompasses our site area.

Prior to being designated a National Marine Sanctuary in 1990, FKNMS reefs in the lower Keys were drilled to explore for potential oil. Hydrocarbons are produced in the Lower Cretaceous limestone and dolomite that comprise the Sunniland Formation. Seventeen exploratory wells were drilled in south and central Florida in 1943, with all producing oil, but none economically feasible. All wells were left in place and contain steel casings that produce magnetic signatures. After establishment of the FKNMS, there was an immediate prohibition of oil drilling, including mineral and hydrocarbon leasing, exploration, development or production within the Sanctuary. The management plan for the Sanctuary contains 10 Action Plans: (1) channel and reef marking, (2) education and outreach, (3) enforcement, (4) mooring buoy, (5) regulatory, (6) research and monitoring, (7) submerged cultural resources, (8) volunteer, (9) water quality, and (10) marine zoning. The marine zoning plan represents a major departure from the traditional management actions in national marine sanctuaries (Keller and Causey, 2005).

Our specific study site area is primarily used for boating and diver recreation on the adjacent Sambo reefs and wreck sites and for fishing. The early history of the site area is not well documented prior to the U.S. taking possession in 1821 and the first U.S. colonization in 1822. Because this part of the lower Keys was located on the primary trade network for vessels traveling between Havana and St. Augustine, there is evidence of numerous ship wrecks and maritime events along the outer reef area. Historic trade vessels generally followed the Hawk Channel when traveling south to provide protection and to ride the 1-2 knot current flowing counter to the Gulf Stream (National Historic Center, 2003). After 1521, an increasing number of Spanish ships wrecked along this part of the lower Keys inviting salvagers and pirates. Hurricanes in 1622 and 1733 caused two great Spanish treasure fleet disasters. In the eighteenth century, the area's history was highlighted by conflicts between Spain and Britain and subsequently commercial fishing and salvage (and raiding) by Cuban "ranchos". After the American Revolution, Commodore David Porter established a naval base at Key West. This was the focus of operations in the area until the overseas highway was completed in 1938. In 1943, the Army transferred land containing an airport on Boca Chica Key to the Navy for the Boca Chica Naval Air Station (NAS). The Boca Chica NAS was originally used to train anti-submarine warfare and aircraft carrier flight operations (Windhorn and Langley, 1975).

The island of Boca Chica Key has been significantly altered by naval operations and infrastructure development. The area around the island has experienced many changes in modern history. Nautical chart 11445 shows three wrecks off the southern shore of Boca Chica Key including the Boca Chica Channel Wreck (designated 8MO1448), which is one of the most significant wrecks in that area. Additionally, two wrecks occurred on the Western Sambo reef: the *M/V Jacquelyn L.* in 1991 and the *M/V Miss Beholden* in 1993.

4.3 SITE GEOLOGY

The general area encompasses offshore areas south Boca Chica Key between the Hawk Channel and outer reef on the edge of the Florida Straits. This area is part of the Florida plateau, a large carbonate platform composed of varying types of marine sediments. Underlying the plateau are the crystalline and sedimentary basement rock of the South Florida Basin, which is a block-faulted feature associated with rifting of North America and Africa during the Mesozoic era. This block-faulting is also believed to have created the Straits of Florida. Subsequent sea level

transgressions flooded the area and initiated episodic reef building and marine deposition (Hoffmeister, 1968; Mueller, 1992). Sediments have been deposited in a series of bays and lagoons in and around the Keys, along with a large reef complex bordering the Atlantic Ocean to the east. Large areas in the region formed a series of cross-bedded carbonate (oolitic) sand bars as a result of tidal exchange between the Atlantic Ocean and the Gulf of Mexico.

The southern Florida Keys are the modern carbonate platform above the Pleistocene barrier outlier reefs that form a windward reef-rimmed bank margin. This shelf margin reef generally separates the inner Hawk Channel from the deeper Straits of Florida to the south and supports a variety of benthic habitats and sedimentary environments (Jaap, 1984; Lidz et al., 1985; Shinn et al., 1989). This area has been an important research site for classic studies in carbonate sedimentology dating back to Vaughn [1915; 1916] and remains one of the most popular sites for continued study.

Figure 38 shows a schematic cross section with the major terrestrial and submarine geomorphic features in the study area (from Lidz et al., 2003). There are also a number of different benthic communities along the seafloor around the study site. In general bottom habitats include sand, bedrock, gorgonian hardgrounds, seagrass beds, and coral reefs.

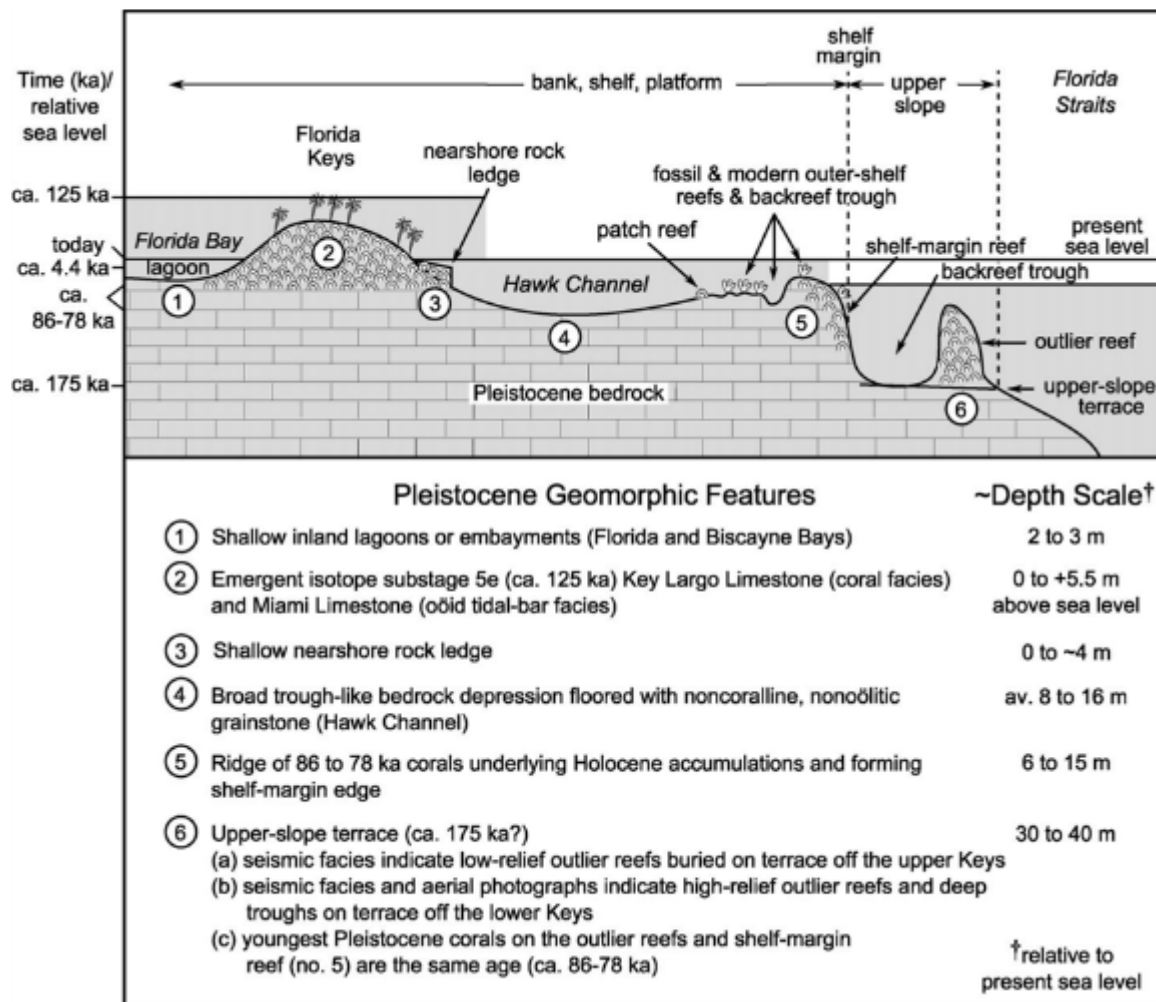


Figure 38. Schematic of the marine morphologic features in the study area (from Lidz et al., 2003).

The Holocene sediment thickness across the area was mapped by Lidz et al. [2003] using interpretations of geophysical data and probing with a rod in select areas. Figure 39 shows an isopach map of carbonate sediments over the study region. Colors represent thicknesses ranging from bare bedrock (white) to thin seafloor sediments (light pink) to the deepest sediment thickness (red to rust-color). Sediment thickness between 0 and 4 meters are present in and around the demonstration area.

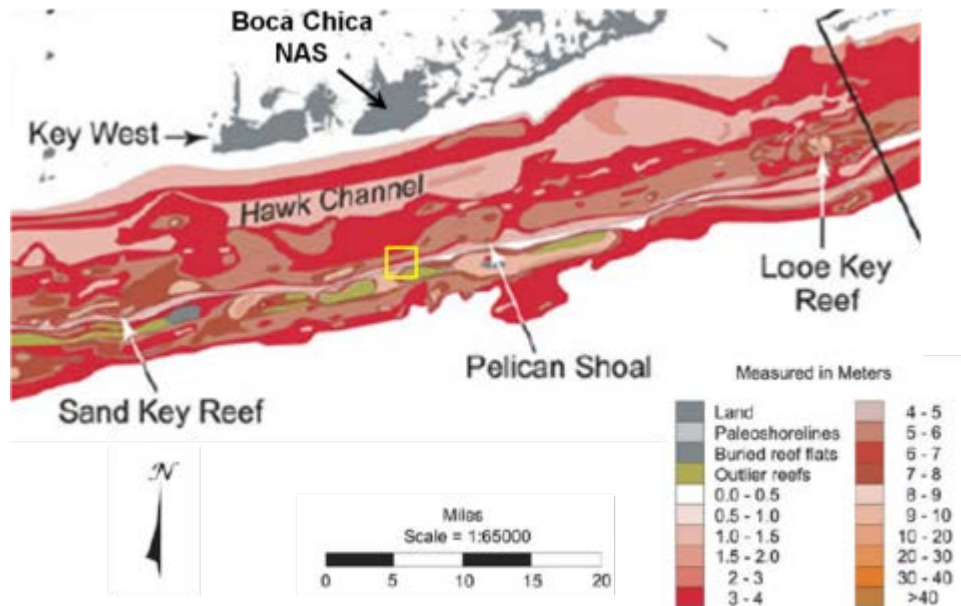


Figure 39. Isopach map of sediment thickness around the study site. A relatively large degree of variability in the sediment thickness is mapped around the study site - indicated by yellow outline (modified from Lidz et al., 2003).

Sediments in this area are characterized by submarine mega-ripples, small sand dunes, and tidal bars. Some submarine dunes overlie oolite and are primarily composed of Halimeda sands (Shinn and Japp, 2005). Tidal channels between the sand tidal bars are often populated with sea grasses. We did not find the Pleistocene bedrock exposed in any low areas in the tidal channels, but is assumed that it is exposed where thin layers cover low areas just outside of our study area.

A number of geotechnical and geophysical studies have detailed the sediments and morphology of the seafloor environment in this area (e.g., Lidz et al., 2003; Brandes, 2001; Incze, 1998; Lidz et al., 1997; Shinn et al., 1990). Most notable is series of high resolution seismic reflection surveys conducted by the USGS and NOAA in 1991 and again in 1997 (Lidz et al, 1997). These surveys and subsequent interpretations were focused on mapping the depth to bedrock and reef/sediment thickness in multiple areas along the length of the Florida Keys. A concentration of surveys in the area between Pelican Shoal and Sand Key Reef across the outlier reef was primarily used to generate the sediment thickness map in Figure 39. An example seismic reflection interpreted cross-section is shown in Figure 40.

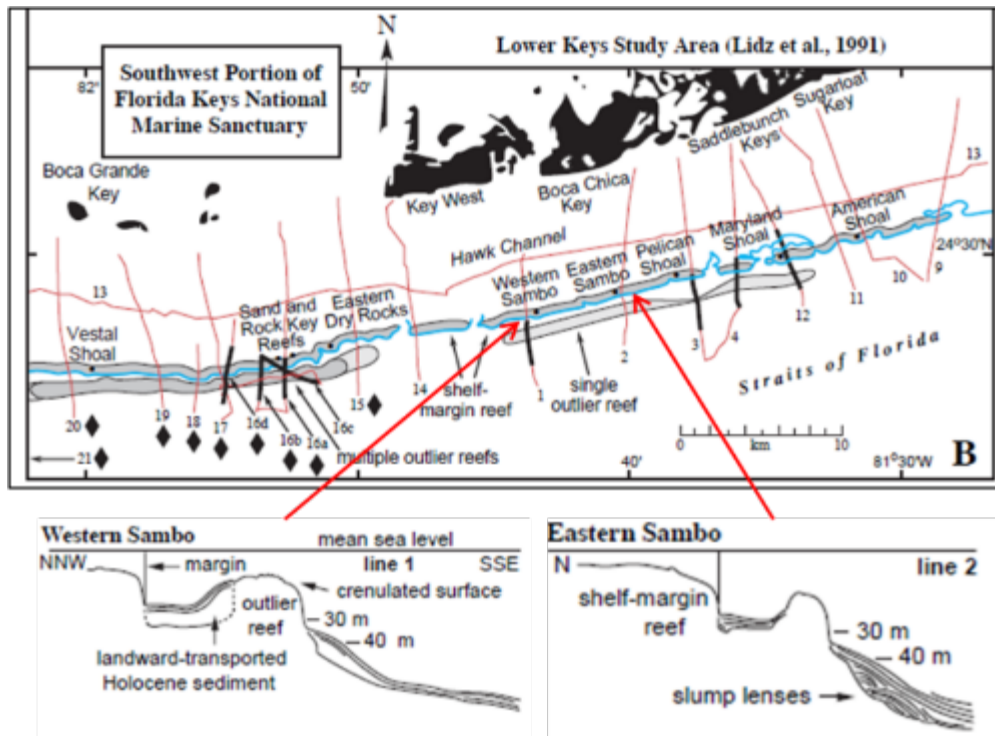


Figure 40. Data from the USGS/NOAA geophysical data collection campaigns in the study site area. Top : Map of the seismic profiles including the Lines 1 and 2, which correspond to the seismic profile interpretations shown in the Bottom figures (from Lidz et al., 1991).

4.4 MUNITIONS CONTAMINATION

Although our test area was not specifically selected based on proximity to known munitions areas, UXO contamination has been cited in the area. DOD currently maintains the largest unencumbered airspace for training on the East Coast. Large portions of the offshore (and some onshore) areas around the lower Keys are part of the Key West Range Complex, which is an active over-ocean multi-use training area. The Naval Air Station (NAS) Key West manages multiple areas in the range complex and operates with only a few environmental restrictions near the Dry Tortugas area. The complex is composed of the following ranges and target areas (as shown in Figure 41):

- Marquesas "Patricia" Target
- Key West Tactical Aircrew Combat Training System (TACTS)
- Warning Area W-174
- Warning Area W-465
- Key West Operating Area (OPERA)
- Bonefish Air Traffic Control Assigned Airspace (ATCAA)

The NAS outlines specific training activities and danger zones including aerial gunnery ranges, bombing and strafing target areas, and mine fields and special operations training sites. Of particular interest, military aircraft periodically use a designated bombing range located directly west of Marquesas Key, known as the Patricia Range. The range consists of a WWII vintage hulk that ran aground where aircraft are known to perfect air-to-sea delivery of ordnance.



Figure 41. Map of DOD training areas within the Key West Range Complex.

In addition, there is an abandoned sea mine field extending northeast from the Marquesas Keys area and two "Explosives Dumping Areas". These are deep water (>1000 ft) sites that the Navy may use to dispose of explosives. These can be located on the map shown in Figure 42. There are also a few onshore military facilities in the Keys, but none are known to have a munitions contamination issue.

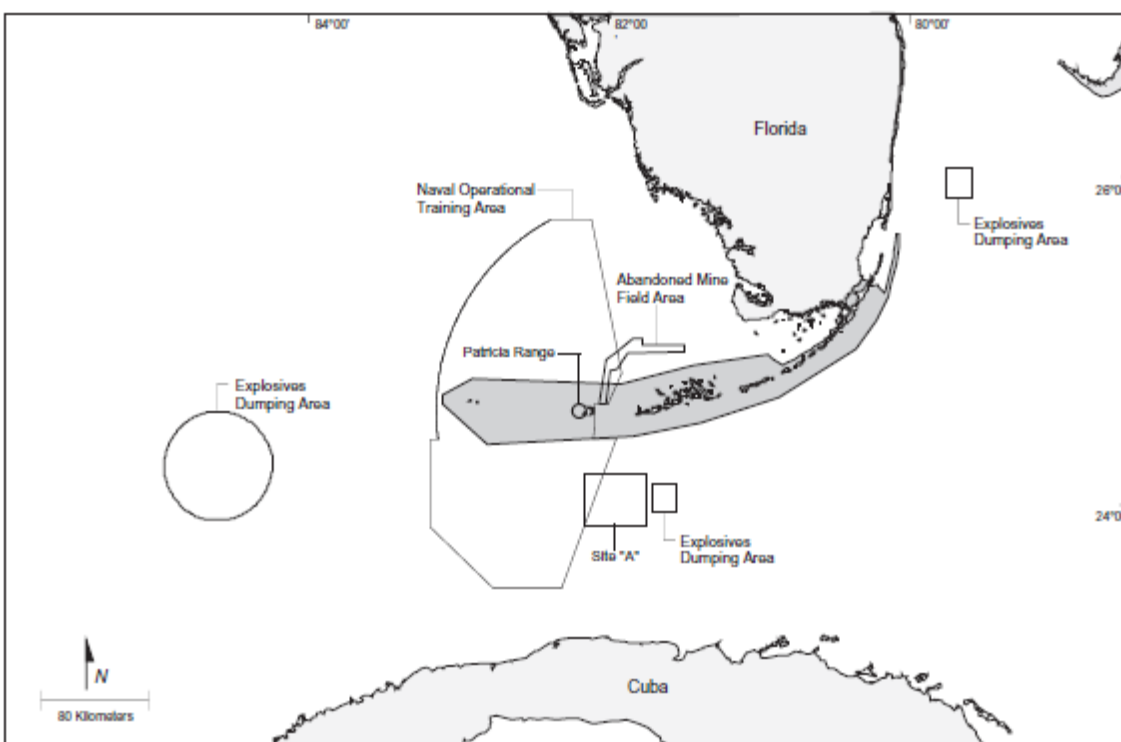


Figure 42. Map of DOD munitions dumping grounds and facilities in and around the Lower Keys.

Surveyors and salvage crews working in the area have recovered inert practice bombs, fragmentation, and numerous munitions remnants from the Quicksands areas west of the Marqueses Keys. Commonly found items in the area are AN-MK-5 and AN-MK-23 practice bomb targets as shown in Figure 43.



Figure 43. Photographs of AN-MK 5 Mod 1 practice bomb uncovered during salvage operations near our proposed site area. Left: Dummy bomb test item; Right: Tail section of dummy bomb detected with the ROV-EM system and recovered from the sea bottom.

Other potential munitions-related test items may be associated with current training activities as reported on in the U.S. Navy Atlantic Fleet Training and Testing (AFTT) Environment Impact Statement preliminary observations (Keith and Schnars, 2012). This document reports activities and potential military material that may be expended in the general area and is summarized in Table 3. The report notes a total of over 40,000 total military expended materials.

Table 3. Potential military expended material in the Key West Range Complex.

Military Activity	Expended Material	Military Platform	Location & Ordnance	
Air Combat Maneuver (ACM) Events	Flares and Chaffs	Fixed-wing (F/A-18, F-35, F-5)	W-174, W-465	no
Gunnery (Air-to-Air)	Projectiles, Casings	Fixed-wing (F/A-18, F-35)	W-174	maybe
Missile Ex (Air-to-Air)	Missiles, frag, flare casing, parachutes	Fixed-wing (F/A-18, F-35)	W-174	maybe
Flare Ex & Chaff Ex	Flares, chaffs	Fixed-wing aircraft & helicopter	W-174, W-465	no
Mine EOD	Target frag, mooring blocks	Helicopters, small boats	Demo Key	maybe
Combat Ship Qualification and Surface Warfare	Large caliber gun rounds, medium caliber rounds, munitions frag	Surface ships	Unknown	155mm, 5-in projectiles
Special Warfare	None	Surface craft, UUVs	Unknown	no
Other Activities	Ballast, "weapons"	Mixed	Unknown	maybe

5.0 TEST DESIGN

5.1 CONCEPTUAL EXPERIMENTAL DESIGN

The conceptual design of this demonstration focused on the collection of high quality EM sensor and navigation data using a hybrid AUV (HAUV) system. Specifically, we set out to demonstrate semi-autonomous means of maintaining one or more of the following ROV parameters: altitude, X-Y position, orientation, direction of travel, or speed of travel. The focus was on determining the ability of the integrated ROV-based EMI sensor system to perform these semi-autonomous behaviors applicable to UXO detection and characterization. These behaviors are required to complete three underwater UXO detection missions: 1) areal coverage and mapping, 2) cued anomaly characterization, and 3) reacquisition and persistent station keeping/sensing. Our tests were designed to capture the ROV's navigation and control accuracy and precision and the resulting quality of the EMI data acquired during execution of the semi-autonomous behaviors.

Our demonstration began with: 1) land-based target deployment preparation, 2) initial system setup, platform trimming, and operational checks while the R/V Dare was docked, and 3) mobilization of equipment to the site aboard the R/V Dare dive vessel. This was followed by integrated system deployment and background survey data collection. The purpose of this data collection was to test the functionality of the systems and to characterize the data collection area in terms of water column conditions, bottom types and location of EM clutter.

Concurrent with setup activities divers emplaced targets, spar buoys, and survey markers on the seafloor. Data collected over these targets formed the primary source of data for analysis and calculation of performance metrics. Installation of a target field took approximately six hours with an additional two hours to place and survey in spar buoys.

Approximately one day was spent collecting data while the HAUV exercised bottom following, line following, and station keeping behaviors. EMI array, navigation and control data, and USBL data were recorded during all exercises. One full (10-hour) day was also spent performing the anomaly characterization mission. Data collected during bottom following, line following, station keeping, and anomaly characterization tests were used to produce detection locations for comparison to the true locations.

5.2 SITE PREPARATION

Prior to deploying a target grid at the site, we worked to develop simple and straightforward method for deployment that did not overly rely on diver surveying or dead reckoning once on the seafloor. This led to the design of a 30 by 40 m target grid area within a larger north-south transecting profile. To ensure proper relatively positioning of targets and help to retain accuracy and integrity of groundtruth, we utilized a set of anchored seabottom lines to outline the grid. Divers deployed the lines with cement blocks anchoring the corner markers. The target placement along the bounding box lines and cross-lines were set and marked. The lines were then fixed to the pre-surveyed corner markers (see below for survey process of corner markers) and run along compass dead reckoning orientations to ensure right-angles and end-point

consistency. Figure 44 below shows a photograph of the dry-run layout. Divers were briefed on the layout and emplacement strategy and executed an end-to-end emplacement and survey process in a soccer field the day prior to at-sea target grid deployment on the seafloor.



Figure 44. Photograph of the dry-run target layout and planning with divers. Divers and crew practiced the deployment strategy in a soccer field the day prior to sea-based deployment in order to work out the best practices and process for deployment of the target grid.

The majority of the data collection was performed from surveys over targets emplaced and surveyed on the seafloor. Seeded items included Industry Standard Objects (ISOs; Nelson et al., 2009), ferrous ordnance simulants (Figure 45) of different sizes (60 mm to 155 mm), and clutter. ISO objects were the standard 2-inch (Medium) and 4-inch (Large) steel pipe sections normally used as ISOs.

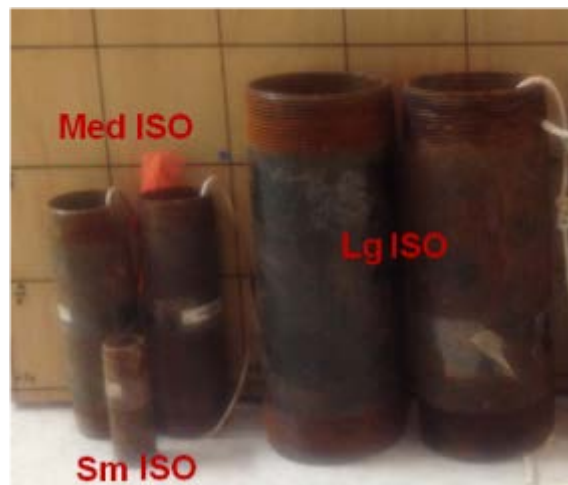


Figure 45. Photograph of our Industry Standard Objects, configured with floating marine rope lines for easy diver-based deployment and attaching to anchor systems or tie-downs.

Inert UXO simulant targets were also emplaced and surveyed using divers. UXO simulants consisted of inert simulant munitions from White River Technologies' inventory of munitions test items. Clutter items were acquired from the shipyard and from local archeological surveyors. These consisted of chains, shackles, aluminum plates and rebar. A composite photograph of the test items used in the target grid is shown in Figure 46.

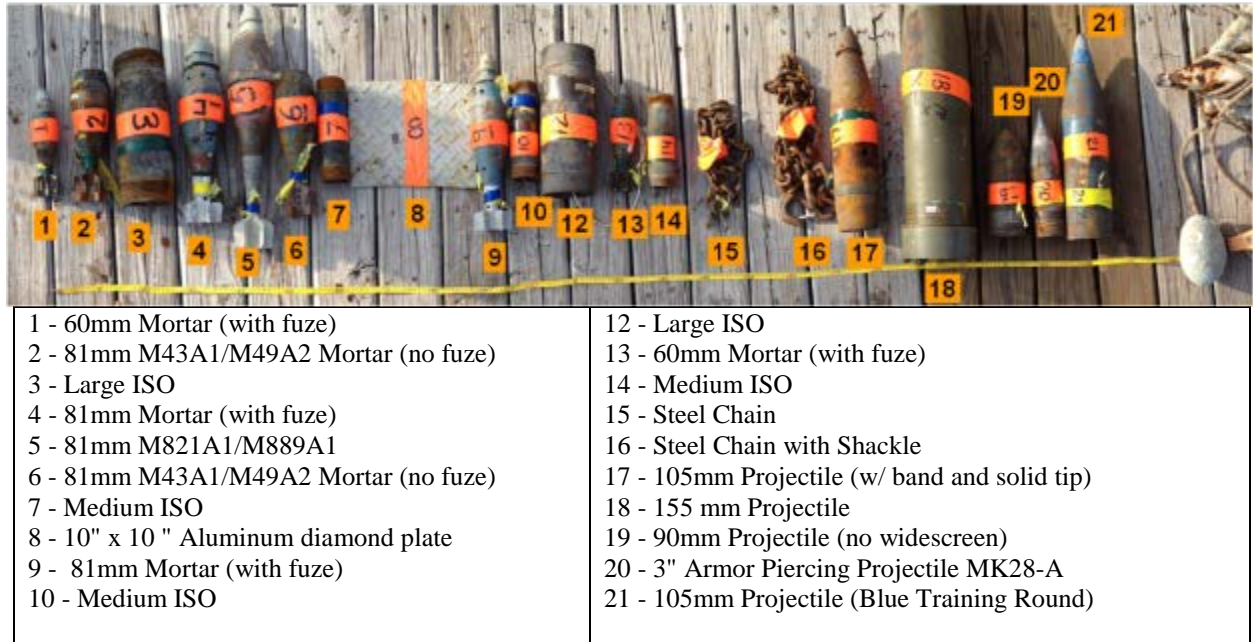


Figure 46. Photograph and table of the UXO stimulants and other targets used.

To establish global reference points for the survey area, we use the ship's Trimble SPS461 dual receiver GPS system located on a stern frame mount overhanging the diver platform. This GPS system is configured with two antennas located on port and starboard sides across the abaft beam to provide roll and heading information, Omnistar corrections, and global accuracy down to 20 cm. GPS position solution information indicated dilution of position of less than the following for each metric: PDOP<2.0, HDOP<1.0, VDOP<1.8, TDOP<1.1. A gravity line (rope with plumb weight on end) was attached to the frame directly under one of the two GPS antennas. The ship was maneuvered so that the gravity line was approximately (within +/- 2.5 meters of the desired GPS coordinates) centered over the corner location and 3-point anchor system was established to stabilize the ship. Once the ship was stabilized, the three-point anchor winch system was used to fine-tune the lateral position of the gravity line placement to within a 30 cm (+/- 15 cm) watch circle located approximately 1 meter below the water line. A diver near the water surface monitored the gravity line while another diver at the seafloor managed the endline weight and located the final surveyed location. The survey location was marked and anchored by cement blocks in order to establish each corner point of the grid. Figure 47 illustrate aspects of this survey process.

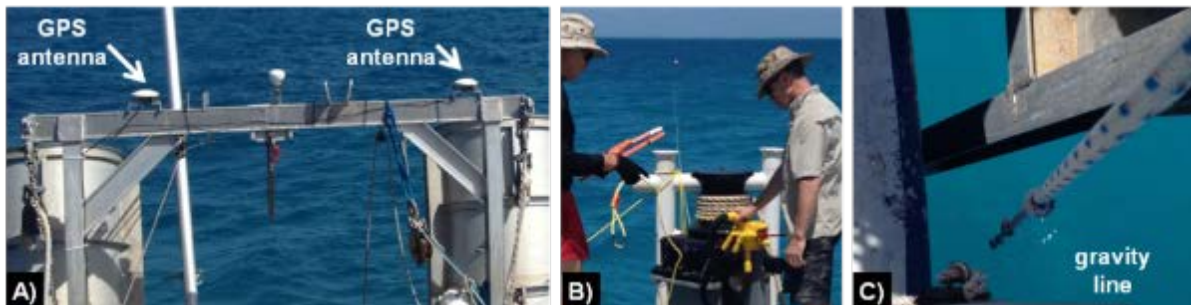


Figure 47. Photographs of the global positioning survey method for surveying in the grid corners and spar buoy locations. A) Trimble SPS dual antenna GPS system on the abaft beam, B) winch system for used for

establishing and fine maneuvering of the 3-point anchor system, and C) the gravity line extending down from below the GPS antenna.

Once the grid corners and spar buoy locations were established and surveyed, survey materials were lowered to the seafloor to establish that test grid. Divers used the grid corners along with a graduated dive reel to survey local positions of each target. When using the dive reel to survey local positions extra care was taken to maintain straight lines between each surveyed location and the local position. A ground truth target spreadsheet was created containing the target's type, latitude, longitude, orientation, and burial depth. Figure 22 below shows the layout of the target lines and targets used during the demonstration.

Prior to establishing the target grid, divers used handheld marine metal detectors to ensure the area was cleared of metallic debris or clutter. A general sweep was conducted over the entire study area and then a concentrated clearance was conducted over the survey lines to try to ensure that no target was placed near any unknown clutter item. Figure 48 shows a photograph of divers clearing the seafloor.

The layout of the overall test area is shown in Figure 49 below. Divers installed the spar buoy at the end of the primary survey line 45 meters north of the grid corner "A". The spar buoy is constructed of 4" schedule 40 PVC and is weighted down onto the seafloor with 4 concrete blocks. The spar buoy established a "home base" for long transect surveys.



Figure 48. Photographs of divers clearing the grid area prior to target installation.

The target grid was used for local area testing and cued reacquisition and station keeping data collections. The grid corners were surveyed relative to its center using dive reels and fixed length ropes. Divers used float bags to transport targets to the sea floor and distribute them along the grid. We utilized 12 UXO simulant targets including 37mm projectile, 60mm mortars, 81mm mortars, 105mm projectiles, 90mm projectile, and 155mm projectiles as well as 5 ISO targets and 4 clutter items in the grid (total of 21 targets). ISO targets were the standard large (4" pipe by 12" length, McMaster-Carr part 44615K137) and medium steel pipe sections (2" pipe by 8" length, McMaster-Carr part 44615K529). Additionally, a 2.5" solid steel sphere and a Mk118 Rockeye simulant were emplaced on the spar buoy line as additional targets outside of the primary target grid. Pictures of the spar buoy, 60 mm target, and 155 m target installations are shown in Figure 50.

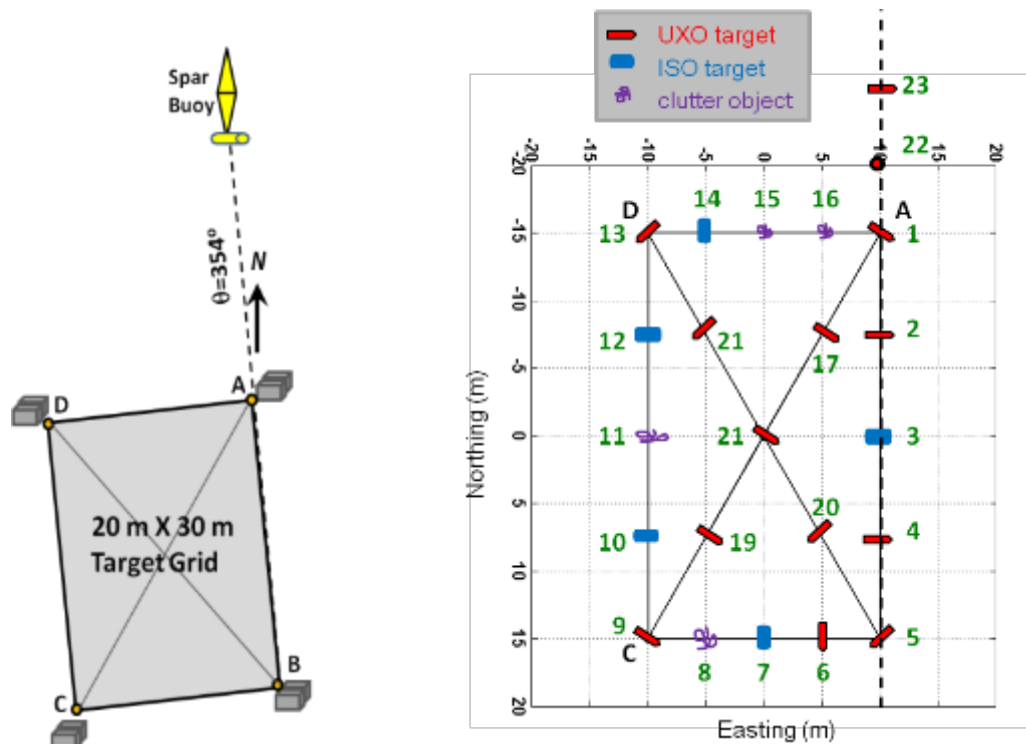


Figure 49. Target grid layout with UXO simulants, ISO and clutter objects oriented along perpendicular transects. Targets are spaced along grid points and surveyed using the grid corners as a global reference. This set up contains 17 distinct targets, with 12 UXO simulants, 5 ISOs, and 4 clutter objects.

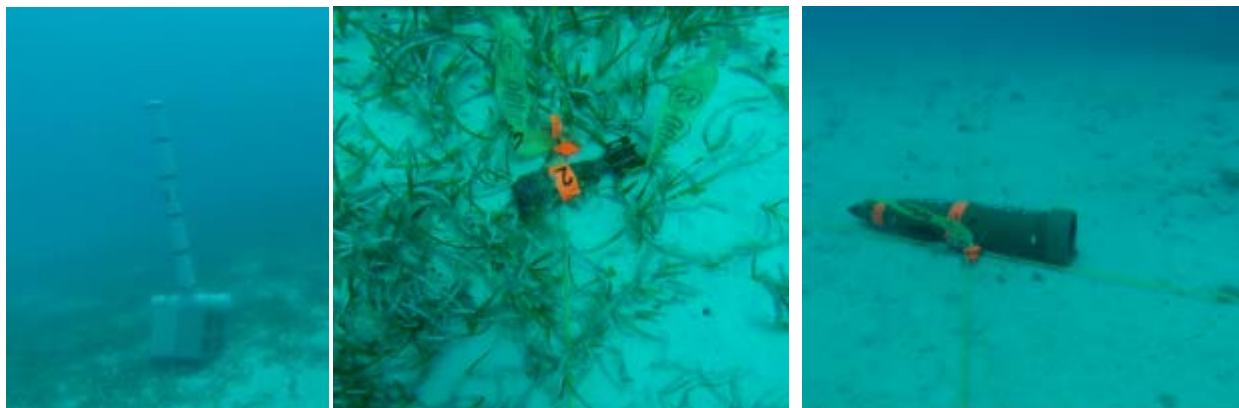


Figure 50. Left-to-Right: Photographs of the spar buoy, a 60mm simulant target, and 155mm projectile installed in the target grid.

5.3 SYSTEM SPECIFICATION

The complete system used in our demonstration included the multi-frequency EM sensor array (MFDA), inertial navigation and control system, the Dolores HAUV-1000, subsea data acquisition system, ship-based GPS to provide global position information, and a USBL positioning system. Specifications for each subsystems are described below.

5.3.1 Multi-Frequency Digital Array (MFDA) EM Sensor

The MFDA sensor head was mounted in front of and slightly below the bow of the ROV so that the operator may view the coil during operation. A single cable connects the sensor head to the sensor electronics. The MFDA electronics receive power and an Ethernet connection to the vehicle data network through the central sensor manifold provided on the HAUV. A topside computer running a software application interface communicates with the MFDA electronics through the vehicle network. Data is acquired in a polled mode at a rate of approximately 10 Hz. The topside MFDA computer will time-stamp the polled data and send streaming messages to the NCS for logging and display of MFDA data. To assure minimum latency the Navigation and Control system and MFDA data acquisition computers will be time synced using the Network Time Protocol (NTP) computer synchronization protocol. The MFDA sensor array is mounted such that it is 48 cm below the HAUV and 65-95 cm forward from the nose. This ensures constant bottom lock with the DVL system when the array is sitting on the seafloor. The forward offset was set to 71 cm in the current configuration based on platform noise signature studies described in the Year 1 report. The mounting arrangement is adjustable to accommodate different forward and vertical offsets of the array relative to the HAUV.

The MFDA frequency set utilized during testing was determined using two methods: 1) An automated noise cancelling routine that selects the frequency set least affected by environmental noise; and 2) analysis of data samples taken using each of the frequency sets. Our nominal frequency selection is constrained to following: [FREQ 1: 1.216-1.693 kHz; FREQ2: 3.743-5.126 kHz; FREQ3: 10.90-15.10 kHz; FREQ4: 32.78-45.56 kHz], but may extend outside this range if significant interference is observed during noise cancelling or discrete frequency selection analysis for a particular site. We utilized frequency set 1 for our demonstrations, which contains the lowest value for each FREQ1-4 listed above.

5.3.2 Navigation and Control System

The navigation and control system comprises a modular unit installed in the HAUV consisting of a small pressure housing and a topside operator interface. The aiding sensors that compose the total navigation suite form the subsystem and are largely defined by two embedded software applications running on the same processor in the subsea pressure housing: one application providing an interface to the navigation sensors and outputting a navigation solution, and one application interfacing with the operator control panel, calculating a control solution, and outputting thruster commands to the HAUV.

The subsea housing contains an embedded processor module, a signal interface module, a magnetic heading reference, a MEMS-based inertial measurement unit (IMU), and a depth sensor. The housing is rated to 500 m seawater depth and provides three connectors: one for power and Ethernet to the ROV manifold and two for aiding sensors. The housing is mounted under the foam pack on the HAUV.

The INS employed DVL and GPS aiding sensors for the navigation solution. USBL data was displayed and logged but was not integrated into the real-time navigation solution. The USBL interfaces with the system through the primary communication channel over Ethernet. This

update rate is approximately 2 Hz and provides positioning of the vehicle based on acoustic tracking. For this demonstration, we used the Tritech MicronNav USBL. The USBL subunit consists of a remote head operating in responder mode and a topside transducer mounted to a rigid pole on the ship. The USBL system provides absolute positioning information of the HUAUV by applying the measured range and bearing between the topside transducer and the ROV to the GPS position of the topside transducer. We also used the Linkquest Micro 600p DVL for this demonstration. The DVL measures vehicle velocity with respect to the bottom in three axes: x, y, and z. The update rate of the DVL is approximately 1 Hz.

The HAUV control system was provided by a separate application from the navigation system, however it runs on the same embedded processor in the subsea pressure housing. This control system provides significantly more control features and better performance characteristics than the standard ROV control system. It accepts operator input from the joystick controls as well as the Graphical User Interface, calculates a control solution based on the current commanded control mode, and outputs thruster commands to the HAUV. The control system used for this demonstration provides open and closed-loop attitude control (heading and roll), open and closed-loop positioning control (x, y, depth, and altitude), as well as several autonomous control modes for path planning, target acquisition, station-keeping, and dynamic positioning.

5.3.3 Remotely Operated Vehicle

The ROV used for this demonstration is the hybrid-ROV/AUV manufactured specifically for Cobalt Marine LLC (Sugarloaf Key, Florida). The HAUV-1000 is larger than the inspection-class ROVs previously demonstrated with the MFDA technology (Seabotix LBV or vLBV) and provides a stable overall design and significantly increased payload capacity over standard small inspection ROVs (e.g., LBV and vLBV units). The HAUV-1000 has two vectored thrusters for axial maneuvering and two vertical thrusters for vertical control. The vehicle provides a mechanically-scanned forward looking sonar as well as a payload capacity supporting up to three additional serial sensors and three additional Ethernet sensors.

The HAUV was configured with the MFDA coil such that the coil is visible in the camera by the pilot. The coil electronics housing will be installed in the forward instrument bay on the HAUV. The HAUV was deployed trim and neutral for operation in nominal seawater for our study area and site conditions (salinity and temperature).

5.3.4 Ship-based Positioning

The host vessel has a Trimble SPS461 dual receiver GPS system permanently installed and dedicated to the HAUV system. This GPS and heading receiver is DGPS capable and utilizes L1/L2 carrier GPS, Satellite-Based Augmentation System (SBAS), Minimum Shift Keying (MSK) beaconing, and OmniSTAR receivers for 25 cm horizontal accuracy and 50 cm vertical accuracy as quoted on the manufacturer specification documents. With the dual antenna solution differential corrections also provide heading accuracy of 0.05 degrees RMS. Coupled the stable 90 ton vessel, the "Dare", we anticipate adequate global georeferencing from this system. The host vessel is an 84-foot aluminum "swiftship" that has been modified for salvage/dive

operations and dedicated ROV surveying. It also contains a 3-anchor mooring system with hydraulic winches and a 2-ton marine crane and smaller davits for operations.

5.4 CALIBRATION ACTIVITIES

Calibration of the MFDA array is generally not needed. If the sensor needs to be calibrated, a built-in procedure measures the characteristics of the front-end electronics and uses this information to calibrate the reference signals. This takes approximately 30 seconds and is necessary to perform when one of the following has occurred:

- the system micro-controller has just been programmed (or re-programmed)
- a sensor array or coil of different dimensions is being used
- the sensor coil array or PCB has undergone a large temperature change

Once the sensor is calibrated, a noise cancellation procedure can be conducted to allow the sensor to automatically search through a number of frequency sets and select the set that is not affected by any external electromagnetic interference. This is an automated process that requires about 20 seconds of stable deployment to complete. In addition, the sensor can be "zeroed" to achieve a stable in-air absolute calibration. This operation internally "zeros" all DC components of the receiver signals and ensures that all previous instrument calibrations are applied properly and cross-validated.

During surveys, we also performed calibrations to check our navigational and positioning system functionality and accuracy. Two ISO targets, separated by 5 m and contained in the survey line between spar buoys, were used to calibrate the EMI array and navigation and positioning system at the beginning and end of each data collection day. The SNR values of EMI sensor data collected over each target were compared to the SNR of data collected previously in a controlled setting. The EMI sensor passes calibration if the SNR is within +/-20% of the controlled SNR. For these calculations SNR was computed based on linear scaling of the signal and not in decibels. The distance traveled using the navigation solution will be compared to the known separation (5 m) of the two targets. The success criteria for the navigation and control system is achieved if the distance traveled is within +/- 5% of the known separation of the targets (5 m). Standard pre-deployment functional checks of Dolores HAUV thrusters, sensors, and topside communication are also performed prior to deployment of the system.

5.5 DATA COLLECTION PROCEDURES

The data required for creation of the metrics detailed in Section 3 are raw MFDA data, raw navigation sensor data, and the processed navigation solution. These data types are time-stamped and logged in the NCS topside data acquisition computer during testing. Unless the ROV speed is the variable being tested, the mission control and/or ROV operator attempted to maintain a speed of approximately 1 knot (~0.5 m/s) resulting in approximately 5 cm sampling of the seafloor by the MFDA operating at 10 Hz. Data are stored locally on the topside 'copilot' control computer. At the end of each day the data was backed up on a second hard drive for redundancy.

Over the course of the demonstration a total of 4315.8 linear meters were surveyed with an average sample distance of 3.35 cm. During data collection several QC procedures were utilized:

- 1) The topside computer acquiring the raw MFDA data printed messages to the computer's console every time a sample was acquired. The constant movement of these messages assured regular receipt of MFDA data.
- 2) A color-coded waterfall plot displaying the sum of the I and Q values across the four frequencies was displayed on the topside ROV control GUI. This waterfall continues to update only upon receipt of correctly formatted data to provide verification of data updates.
- 3) Data logged by the topside ROV control GUI was periodically checked using software QA routines. Checks included sample distance metrics and I and Q noise metrics for each coil and frequency.

During data collection we maintained a spreadsheet containing metadata describing each data collection. Metadata fields included the file collection date, name, description, and comments for each file. MFDA data was collected in a comma separated value format or CSV file while all navigation and control information was recorded to a binary file. The binary file was then converted to individual CSV files labeled with the data type contained within the CSV file. Each CSV file contained a common time stamp for data synchronization in post-processing. Separate CSV files were created for the following individual sensor data:

- ROV compass
- ROV control messaging
- DVL
- ROV GPS
- ROV IMU
- ROV navigation solution
- ROV pressure sensor
- Thruster commands and status
- Topside compass co-located with USBL transducer
- USBL
- Topside GPS

These data are stored on local hard disk drives and a Network-Attached Storage (NAS) device and are organized by data collection date and mission type.

5.5.1 Basic Operational Test Instructions

The following instructions provide a basic set of procedures we followed for each mission type.

Bottom Following

1. Enter the start and stop line waypoint into the navigation software.
2. The ROV operator will manually position the ROV at the desired altitude above the start point of the data collection line.
3. Engage the Bottom Following ROV control

4. Start logging data.
5. The ROV operator will travel along the line at approximately 1 knot while operating only the horizontal thrusters to maintain heading and speed.
6. Stop logging data when the ROV reaches the end of the line.

Station Keeping

1. The ROV operator will manually position the ROV so that the MFDA sensor is directly above the target of interest.
2. Engage the Station Keeping ROV control
3. Start logging data.
4. Stop logging data after an elapsed time between 2 and 5 minutes.

Station Keeping tests were performed over multiple targets at sensor array altitudes of 25 and 50 cm.

Waypoint Mission Control

1. Enter the waypoints into the navigation software.
2. The ROV operator will manually position the ROV near the first waypoint.
3. Engage the waypoint following ROV control
4. Start logging data.
5. Stop logging data when the ROV reaches the end of the line.

5.5.2 Quality Checks

Periodically throughout each data collection day the MFDA data is processed to assure data quality. Quality control metrics produced will include the standard deviation of each channel to illuminate noisy data channels. Previous experience with the MFDA sensor have revealed the presence of the intermittent, short duration noise consisting of I or Q data spikes with values at the limits of the ADC (± 32768 counts). These noise events are typically for a single data sample and are removed during filtering and despiking employed in post-processing algorithms. During post-processing analysis, the display of the raw I/Q values at all frequencies will alert the user to these noise events. In real-time, these noise events may cause a discrete jump in the waterfall display followed by a return of the waterfall to the mean level as the data propagates through the real-time filtering software. Throughout development and testing we have observed slightly higher noise levels from I and Q data for all frequencies tested in receive coil #3 compared with receive coils 1 and 2. The cause of this noise is not known. Due to data filtering this noise is not visible during real-time viewing. In post-processing, an increase in noise in one coil reveals itself during review of profile plots or single-pass coverage maps. The sample time of each data collection was also reviewed to assure no gaps in sampling. The real-time NCS navigation display flashes indicators if data quality of any sensor is not met including loss of bottom-lock by the DVL.

5.5.3 Characterization of Background Water Column Parameters

In order to continuously monitor properties of the water column during tests, we mounted a small PVC housing containing a conductivity, salinity, and temperature (CST) logger to the ROV. The CST logger used was the Onset HOBO U24 logger, a self contained sensor unit that measures electrical conductivity and temperature and is suitable for use in seawater. This system is used with the U12 pressure logger and/or U26 dissolved oxygen logger. It is capable of logging data on-board continuously for up to 3 years at sample rates that range from 1 second to 18 hour intervals. We used sampling rates of 30-60 seconds during each submersion of the ROV-EM system. The data logger is contained in a sealed pressure housing rated to 100 m saltwater depth. The logger was then placed inside the flooded PVC housing to further protect it from any impact. A photo of the logger and housing are shown in Figure 51.



Figure 51. Photograph of the Onset HOBO environmental monitoring device used to sample background water column conductivity and temperature during ROV-EM tests.

Sample data from two ~6 hour testing periods during the afternoons of 14 and 15 April are shown in Figure 52. This data reveals relatively constant conductivities despite variation in the position of the ROV-EM system in the water column and over the site footprint. Observed conductivities were between 3.1 and 3.8 S/m during our demonstration period. Temperature also remained relatively constant during tests with only some small perturbations during changes in the tidal current. The spikes at the beginning and end of the data collection reflect re-equilibration during launch and recovery.

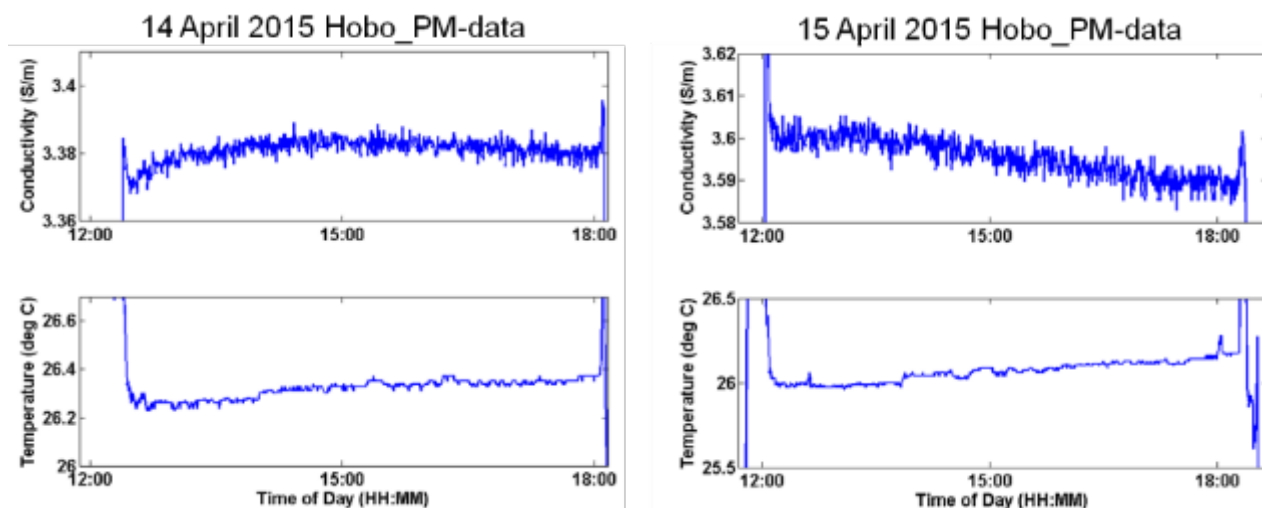


Figure 52. Sample of background water column property observations during ROV-EM tests. Left: 14 April 2015 data; Right: 15 April 2015 data.

6.0 ANALYSIS AND DATA PRODUCTS

Data analysis was performed using a custom preprocessing, detection, and target characterization software environment originally developed using MATLAB, which was converted to a Windows PC executable. We also utilized the openSEA (OPEN Software and Equipment Architecture) software to post process and analyze navigation and control information archived during tests.

6.1 DATA PREPROCESSING

6.1.1 MFDA Data

The preprocessing of MFDA data includes median filtering of each in-phase (I) and quadrature (Q) data channel to remove intermittent spikes found in the raw data. Each I and Q channel's raw data drifts over time. To remove the drift the data are sent through a linear piece-wise detrending algorithm the output of centers the noise of the data at an amplitude of 0. Navigation and MFDA data are correlated in time through spline interpolation of the MFDA data producing MFDA data with time samples that match the navigation data.

6.1.2 Navigation and Control Data

No preprocessing of the navigation and control data is required. A custom Matlab application imports the raw log files (LCM format) recorded during surveys and analyzes the data to produce statistics describing the noise and bias of the individual sensors, the vehicle navigation, and the control system performance.

6.2 DETECTION

The detection signal is $(I^2 + Q^2)^{0.5}$ across one or more frequencies following data preprocessing. A threshold is applied to this statistic to produce target detections. Historic data collected using the sensor and data collected during preliminary tests in Florida, Massachusetts (test stand data), and North Carolina (see Appendix) was used to set detection thresholds. A baseline SNR detection threshold was set to 9 dB based on statistical estimation of a non-fluctuating target in Gaussian noise at an operating point associated with a relatively conservative 0.01 probability of false alarm.

6.3 PARAMETER ESTIMATION

For each detection an estimated correspondence position is determined using a custom algorithm that searches for the zero crossing between the two peak response typically produced by the MFDA quadrupole receiver coils. The location corresponding to the zero crossing is the estimated location of the target.

6.4 TRAINING / DISCRIMINATION

Although, our demonstration did not explicitly endeavor to assess the discrimination potential of this ROV-based EM system, we did investigate a preliminary version of a polarizability inversion methodology using MFDA array data. Utilizing only the angular offset with the single axis transmitter of the MFDA we configured an inversion algorithm to extract target polarizabilities. This combined models that account for the physics of the underwater environment (e.g., such as those developed under SERDM MR-1632 and MR-1714 projects) with proven least squares inversion methods from terrestrial live site software environments. (such as those demonstrated under ESTCP projects MR-201101, MR-201225, and MR-201227).

Further characterization of suspected target anomalies was determined through the inversion of data from regions of interest (ROIs) around a target detection. ROIs are effectively masks over the data acquired within some distance from a target detection pick location. All post-processed data from an ROI is forwarded to an inversion module for determination of the frequency-dependent polarizability of the object.

To prepare the EM sensor data for input into feature extraction and classification routines regions of interest (ROIs) are created using detector output and integrated EM sensor and position data. For each detection an ROI is created containing the EM sensor data within a specified spatial extent. The ROI data is then inverted through comparison to forward model realizations created using different input parameters. The outputs of the inversion are features for target discrimination and classification. Figure 53 shows a graphical representation of the processing flow.

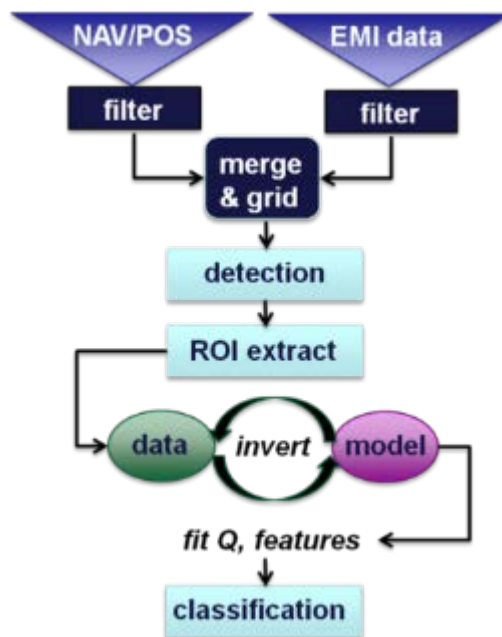


Figure 53. Processing flow used to create target classification features from raw EM sensor and navigation data.

Classification features are extracted from the forward model realization most closely matching the observed data. Figure 54 shows two comparisons of the forward model output to the observed data.

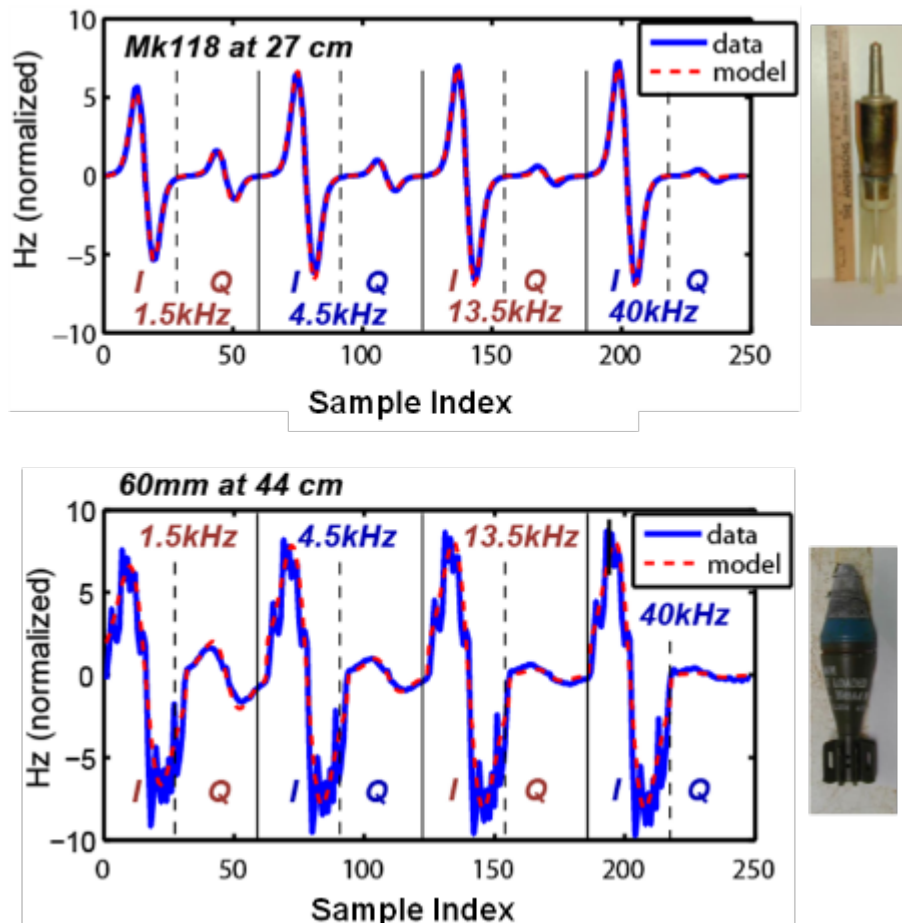


Figure 54. Comparison of the forward model output to observed data at each of the four EM sensor frequencies for a MK118 rocket (top) and a 60 mm mortar (bottom). The sample index represents a non-sequential data scan number. Each frequency I and Q value is demodulated and digitally acquired simultaneously so that the first 62 sample indices associated with 1.5 kHz I and Q values correspond to those acquired at the same time for the other 3 frequencies (i.e., samples 63-124 for 4.5 kHz data, samples 125-186 for 13.5 kHz, and samples 187-248).

Figure 55 shows an example of inverted polarizabilities derived from application of the ortho-normalized volume magnetic source (ONVMS) model that we modified to accommodate the conductive seawater environment. For this example, we see that it is possible to generate polarizabilities for the axial components that reflect the symmetric nature of the 3" spherical steel target. Multiple data points are concatenated together and used in the inversion to generate the frequency-domain polarizabilities. This was required in order to facilitate angular illumination and consequently constrain the axial moments of the target so as to produce representative polarizability values.

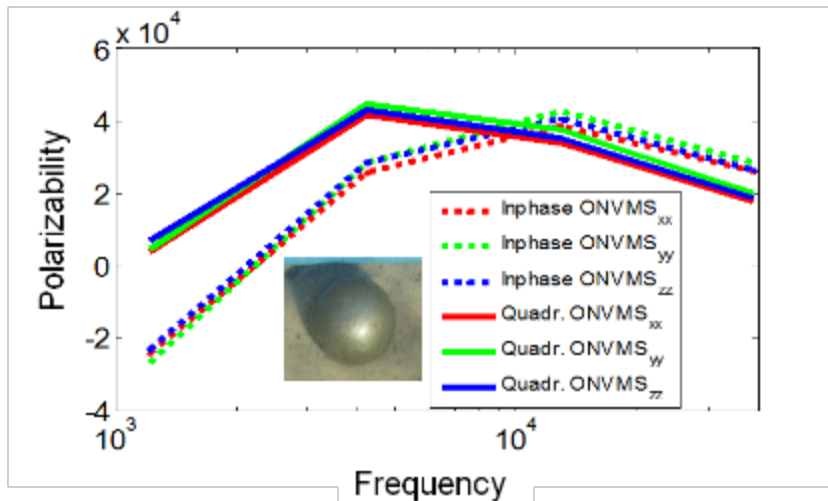


Figure 55. Example of frequency-domain inverted polarizabilities using the orthonormalized volume magnetic source model that was modified to address EM propagation through a conductive seawater medium. This example shows that nearly identical axial polarizabilities for both In-Phase and Quad-Phase components are derived as expected for the axisymmetric sphere target tested.

6.5 DATA PRODUCT SPECIFICATION

Data products will consist of calculated metrics as well as figures to illustrate the data used to calculate the metric.

6.5.1 Bottom Following, Waypoint Mission Control, and Station Keeping

Metrics emanating from these tests result from the comparison of a true value to a value estimated by the navigation system. These can be represented by plots of time versus the navigation system data and time versus the ground truth data or desired data. For altitude (bottom following) data the navigation output will be compared to the desired height above sea floor. For northing and easting data the navigation output will be compared to target ground truth and the northings and eastings of the target lines.

6.5.2 Detection Accuracy

The estimated detection location (N, E) will be compared to the ground truth location of the target interrogated. This will result in a two-dimensional location error plot (Figure 56) showing the location of the estimate versus the ground truth to reveal error trends and bias. Halos of different sizes are shown to illustrate scale.

6.5.3 EMI Sensor Data

Data from the MFDA will be periodically checked including all data channels comprising 3 receivers with I and Q component data at each of the 4 frequencies. An example of this is shown in Figure 57.

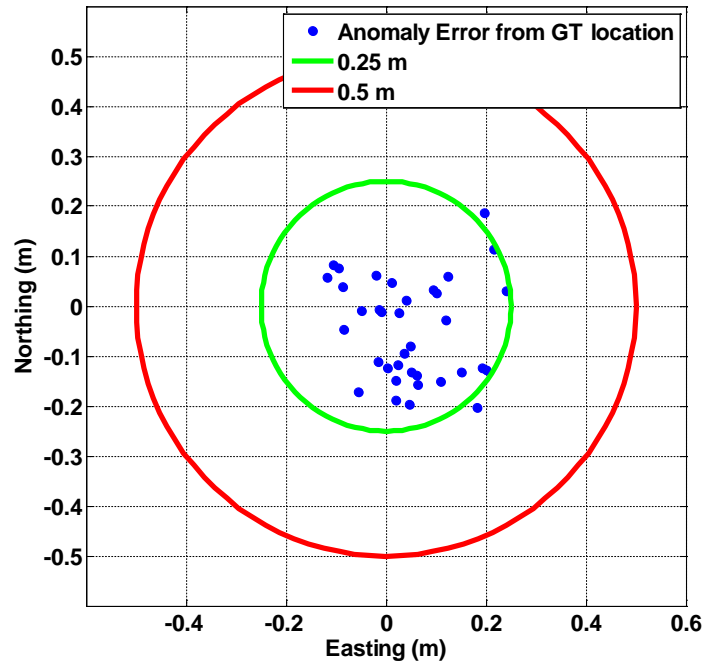


Figure 56. Example data product to be supplied along with the detection location accuracy metric.

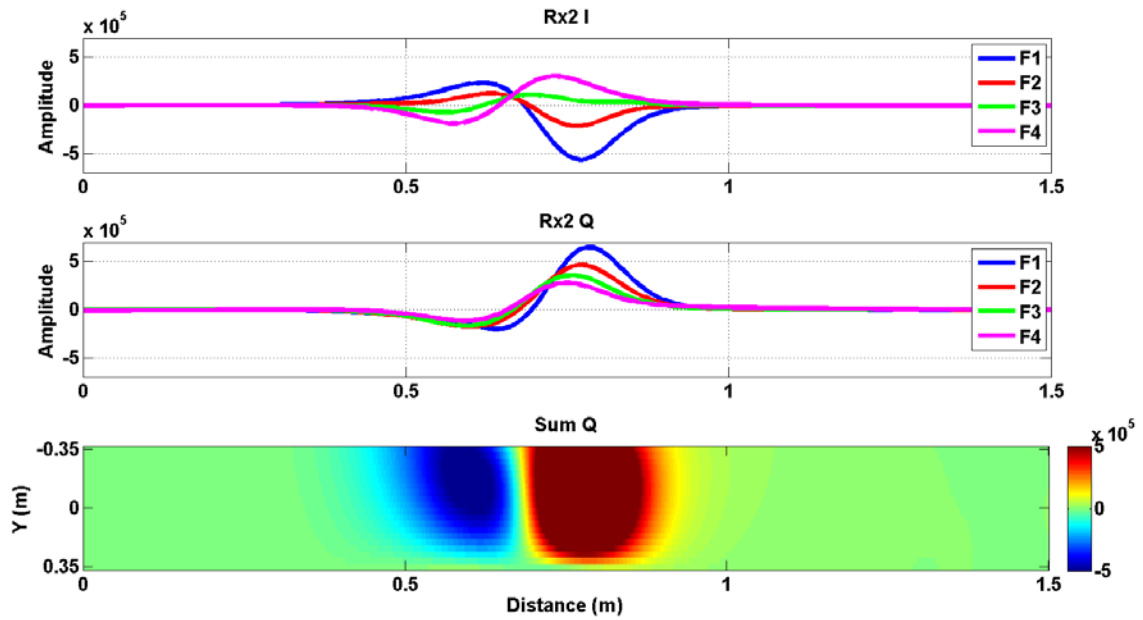


Figure 57. Example data product to be supplied along with the EMI array data quality checks.

7.0 PERFORMANCE ASSESSMENT

We assessed performance using the previously defined test objectives and associated metrics shown in Table 4. These include quantitative metrics related to navigation and control and detection/localization as well as qualitative metrics such as those associated with launch and recovery (LAR) and ease of use. An assessment of each objective is provided in the following sections.

Table 4. Summary of target objectives, metrics, and results.

Performance Objective	Target Metric	Result
Bottom Following	$\Delta A < 0.15 \text{ m}$ $\sigma A < 0.15 \text{ m}$	$\Delta A = 0.1 \text{ m}$ $\sigma A = 0.03 \text{ m}$
Station Keeping Accuracy and Precision	$\Delta N \text{ and } \Delta E < 0.35 \text{ m}$ $\sigma N \text{ and } \sigma E < 0.35 \text{ m}$ $\Delta A < 0.15 \text{ m}$ $\sigma A < 0.15 \text{ m}$ $\Delta H < 1 \text{ degree}$ $\sigma H < 2 \text{ degree}$ $\Delta R < 1 \text{ degree}$ $\sigma R < 2 \text{ degree}$ $\Delta P < 1 \text{ degree}$ $\sigma P < 2 \text{ degree}$	$\Delta N = 0.13 \text{ m}, \Delta E = 0.12 \text{ m}$ $\sigma N = 0.07 \text{ m}, \sigma E = 0.06 \text{ m}$ $\Delta A = 0.03 \text{ m}$ $\sigma A = 0.01 \text{ m}$ $\Delta H = 0.86 \text{ degree}$ $\sigma H = 0.61 \text{ degree}$ $\Delta R = 0.31 \text{ degree}$ $\sigma R = 0.08 \text{ degree}$ $\Delta P = 0.27 \text{ degree}$ $\sigma P = 0.09 \text{ degree}$
Waypoint Mission Control	$\Delta D = (\Delta N^2 + \Delta E^2)^{0.5}$ $\Delta D < 1.5\% \text{ distance travelled}$ $\sigma D < 0.5 \text{ m}$	$\Delta D_{\text{waypoint}} = 0.26 \text{ m}$ $\sigma D_{\text{waypoint}} = 0.29 \text{ m}$ $\Delta D_{\text{line}} = 0.7 \text{ m}$ $\sigma D_{\text{line}} = 0.53 \text{ m}$ Typical Distance traveled approx. 40 m; $\% \Delta D_{\text{waypoint}} = 0.65\%$ $\% \Delta D_{\text{line}} = 1.75\%$
Detection of all munitions greater than 60 mm	$\text{SNR} > 9 \text{ dB}$ $\text{Pd} > 0.95$ (assuming a nonfluctuating target and Gaussian noise a 0.95 Pd at 9 dB corresponds to a pFA of approximately 0.01)	All target SNRs $> 20.7 \text{ dB}$ $\text{Pd} = 1.0$
Detection Location Accuracy and Precision	$\Delta \text{TN and } \Delta \text{TE} < 1.0 \text{ m}$ $\sigma \text{TN and } \sigma \text{TE} < 1.0 \text{ m}$	$\Delta \text{TN} = 0.29 \text{ m}$ $\Delta \text{TE} = 0.22 \text{ m}$ $\sigma \text{TN} = 0.42 \text{ m}$ $\sigma \text{TE} = 0.51 \text{ m}$

Ease of use	Ease of use comparable to alternate standard marine surveying procedures	ROV control and navigation GUI very user friendly. Lack of real-time fusion of USBL position with INS/DVL position made true ROV location difficult to determine within GUI. Procedures put in place to minimize error between USBL and DVL/INS position.
Mission Assisted Autonomy	Value of assisted autonomy functions	Very valuable especially during line following operations. Auto-heading, auto-depth, and auto-velocity critical during line following operations.
Integrated System Stability	Valuation of time and effort to stabilize	Integrate EM / ROV system stabilized in less than 30 minutes using 1 or 2 lb dive weights

7.1 BOTTOM FOLLOWING

Bottom following capability was assessed by analyzing navigation and control observations for traverses of the ROV-EM system between prescribed waypoints. Images of the HAUV captured during bottom following tests are shown in Figure 58.

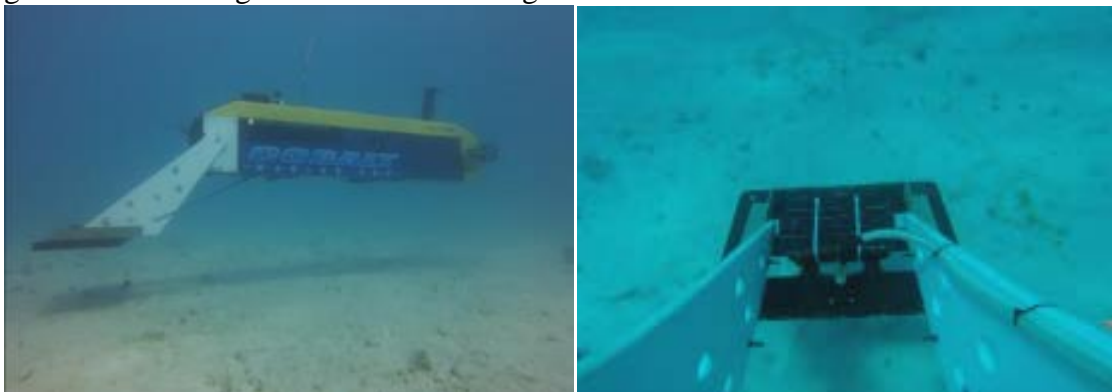


Figure 58. Still shots of the integrated ROV-EM system (left) and the EM sensor (right) performing bottom following operations.

We calculated bottom following metrics using data collected while the ROV-EM system collected EMI sensor data at commanded sensor altitudes between 10 and 60 cm. The average altitude error over 18 transects each of which were approximately 50 m in length (total distance approximately 900 m) was 10 cm while the standard deviation of the altitude was 3 cm. These

metrics were lower than the average and standard deviation objectives of 15 cm and 15 cm, respectively. Figure 59 shows the desired versus actual altitude, roll, and pitch data collected during one of the transects.

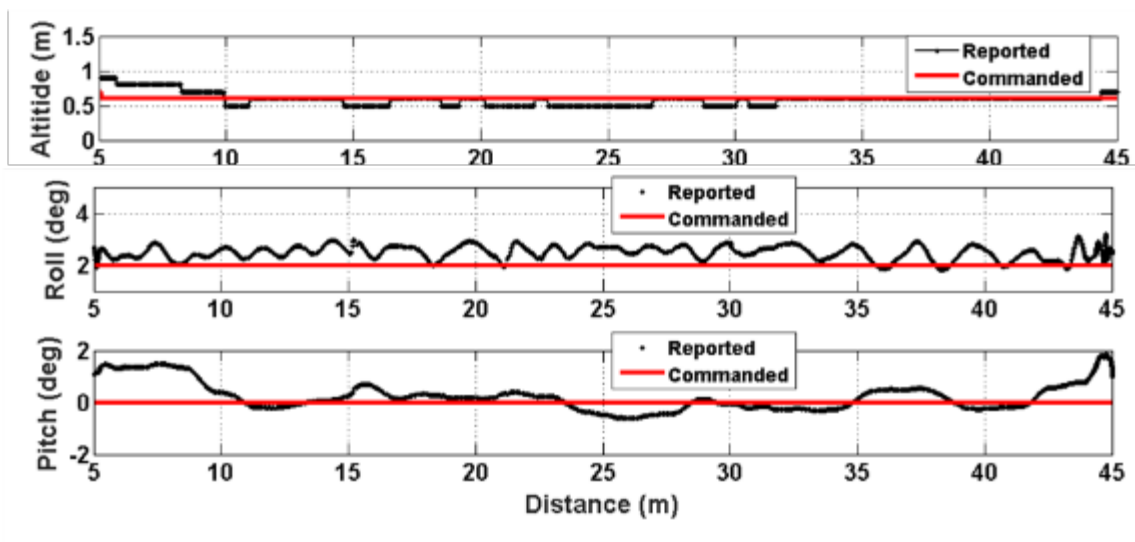


Figure 59. Plots showing desired versus actual ROV altitude, roll, and pitch during a 45 m transect.

The commanded versus reported altimeter, roll, and pitch error mean and standard deviation for the 18 transects used to create the coverage map are shown in Figure 60.

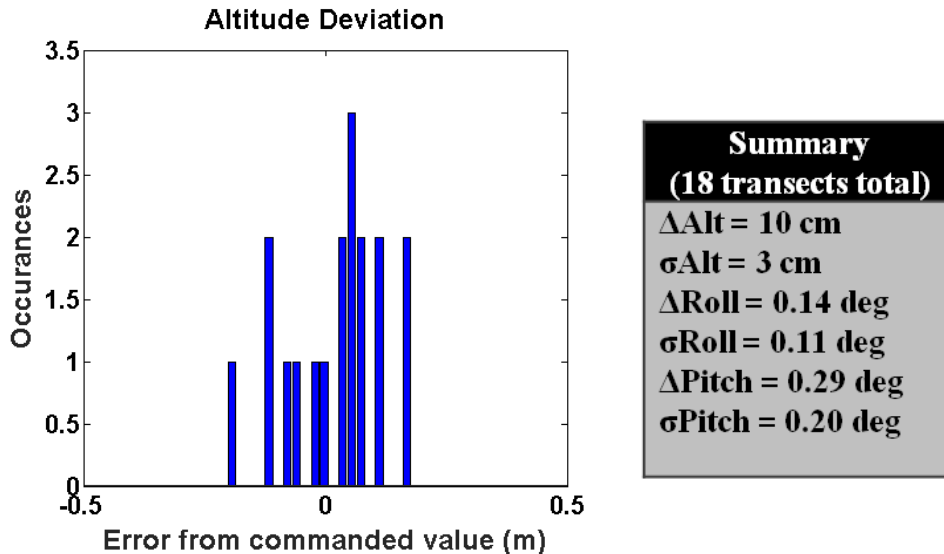


Figure 60. Summary of altimeter, roll, and pitch control errors.

Achieving the bottom keeping objectives and maintaining roll and pitch errors less than half a degree indicate vehicle stability sufficient for near bottom (< 0.5 m) surveys. An average forward pitch error of 0.29 degrees was confirmed using underwater pictures of the vehicle taken by divers while the vehicle was in motion. Midwater tests of the vehicle at higher speeds showed a tendency of the vehicle to dive with increased speed. Possible contributors to the pitch

error include current, tether drag, and downward force imparted on the vehicle when in motion due to the mounting of the EMI sensor forward and underneath the vehicle.

7.2 STATION KEEPING

Station keeping objectives focused on maintaining position of the sensor array over a commanded location, in our case over an individual target in the deployed target grid or over a grid corner marker. We calculated metrics by comparing the ROV's northing and easting positions and altitude from the navigation solution to the commanded position and altitude. Our objective was to stay on average within 35 cm of the commanded northing and easting coordinates with northing and easting position standard deviations less than 35 cm. The altitude objective was to be within 15 cm of the commanded altitude with altitude standard deviation less than 15 cm. We commanded the ROV-EM system to maintain position for periods between 1 and 5 minutes over several target items to provide data for calculating station keeping metrics. Examples of data collected from one of the station keeping data collections are shown in Figure 61, Figure 62, and Figure 63. All of the stated station keeping objectives were achieved.

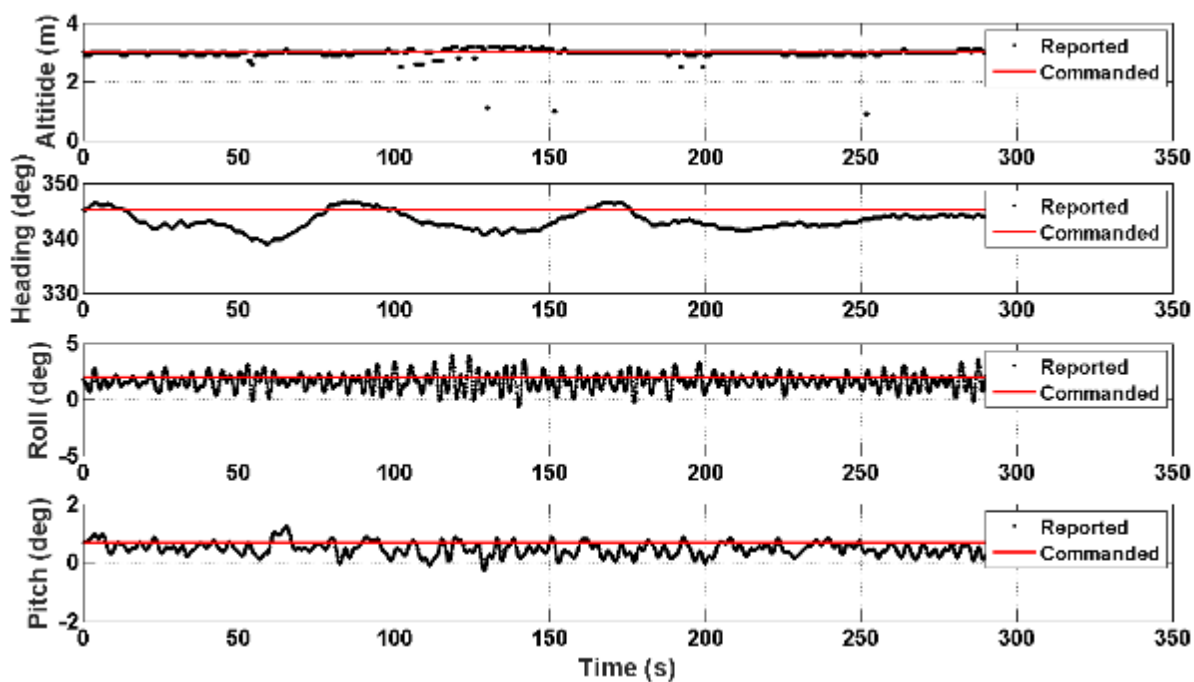


Figure 61 Example of station keeping data collected while keeping station for 5 minutes over an individual target. Data zoom-in plots show the local position error found by subtracting the commanded northing and easting position from the northing and easting position reported by the navigation system.

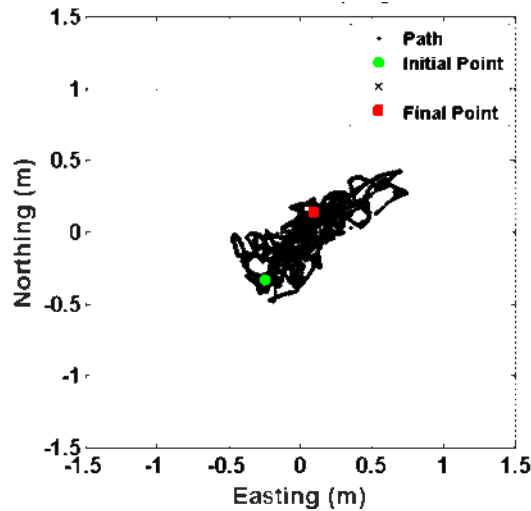


Figure 62 Reported Easting and Northing data over the 5-minute station keeping data collection.

Summary (13 stations)
$\Delta E, \Delta N = 12 \text{ cm}, 13 \text{ cm}$ $\sigma E, \sigma N = 5.7 \text{ cm}, 6.7 \text{ cm}$
$\Delta \text{Alt} = 2.5 \text{ cm}$ $\sigma \text{Alt} = 1.3 \text{ cm}$
$\Delta \text{Yaw} = 0.86 \text{ deg}$ $\sigma \text{Yaw} = 0.61 \text{ deg}$
$\Delta \text{Roll} = 0.31 \text{ deg}$ $\sigma \text{Roll} = 0.08 \text{ deg}$
$\Delta \text{Pitch} = 0.27 \text{ deg}$ $\sigma \text{Pitch} = 0.09 \text{ deg}$

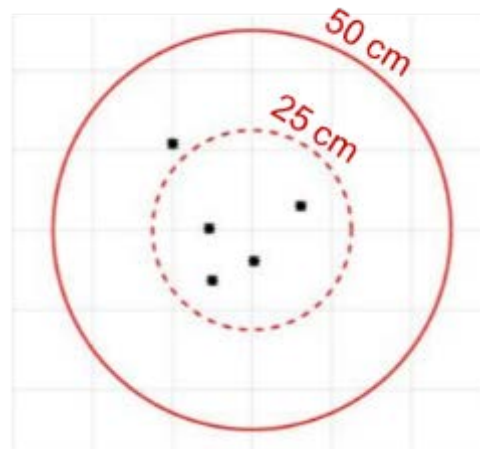


Figure 63 Left: Summary of station keeping stability and accuracy. Right: Example bullseye plot of the station keeping error from groundtruth locations from the four corners and center of our test grid.

7.3 WAYPOINT CONTROL

The ROV-EM system was tested on its ability to transit from one point to another and follow a given line. The operator can pre-plan and load mission control waypoints in the user interface software as shown in Figure 64. ROV-EM performance of this task affects the quality and completeness of UXO survey map data collected by the EMI array mounted to the ROV. We compared the desired position (northing, easting) of the system at a number of co-linear waypoints to the measured position reported by the navigation and control system.



Figure 64. User interface for waypoint mission control. The center portion of the screen illustrates the waypoints input by the user to which the ROV-EM system is commanded to navigate. Multiple waypoints can be entered to configure a multi-point mission plan.

The stated metric was to achieve distance errors less than 1.5 percent distance traveled. Average northing and easting error is defined as the mean of reported position minus the nearest desired position. Northing, Easting, and distance error metrics were created for the waypoints and for the line connecting the waypoints. The waypoint error indicates how accurately the ROV's final position was to the desired waypoint. The line error indicates how accurate the ROV followed the line between the two waypoints. Heading, roll, and pitch reports were also analyzed to shed light on trends in the position data. Table 5 contains the measured performance of the waypoint and line following behaviors.

Table 5. Waypoint and line following performance in meters.

Metric	Waypoint	Line
ΔD (m)	0.26	0.7
σD (m)	0.29	0.53
ΔN (m)	0.15	0.13
σN (m)	0.23	0.16
ΔE (m)	0.04	0.62
σE (m)	0.28	0.59



The waypoint errors were less than the line errors indicating the navigation and control system's ability to maneuver to a specified waypoint. Line error metrics, specifically the ΔE value of 0.62 m, indicate the ROV was more than 60 cm from the desired line for the majority of the time spent performing the coverage transects. This is to be expected since the version of the navigation and control software used during this demonstration contained control feedback specific to reaching the next waypoint and did not have a true line following capability, i.e., no control feedback existed to maintain the ROV's proximity to the line. Future versions of the navigation and control software will have a line following capability. The procedure for following a line consisted of: 1) orienting the vehicle at the specified line heading and altitude at a waypoint location approximately 5 meters from the start of the line, and 2) engaging waypoint navigation from the current location to the starting location of the line to the end location of the

line. Figure 65 below shows the location of each waypoint, the straight line between waypoints, and the reported ROV position while traveling between waypoints for 5 North heading transects and one Eastward transect. Even without a true line following capability the consistent ROV location offset from each line when heading North make full coverage of the target area feasible.

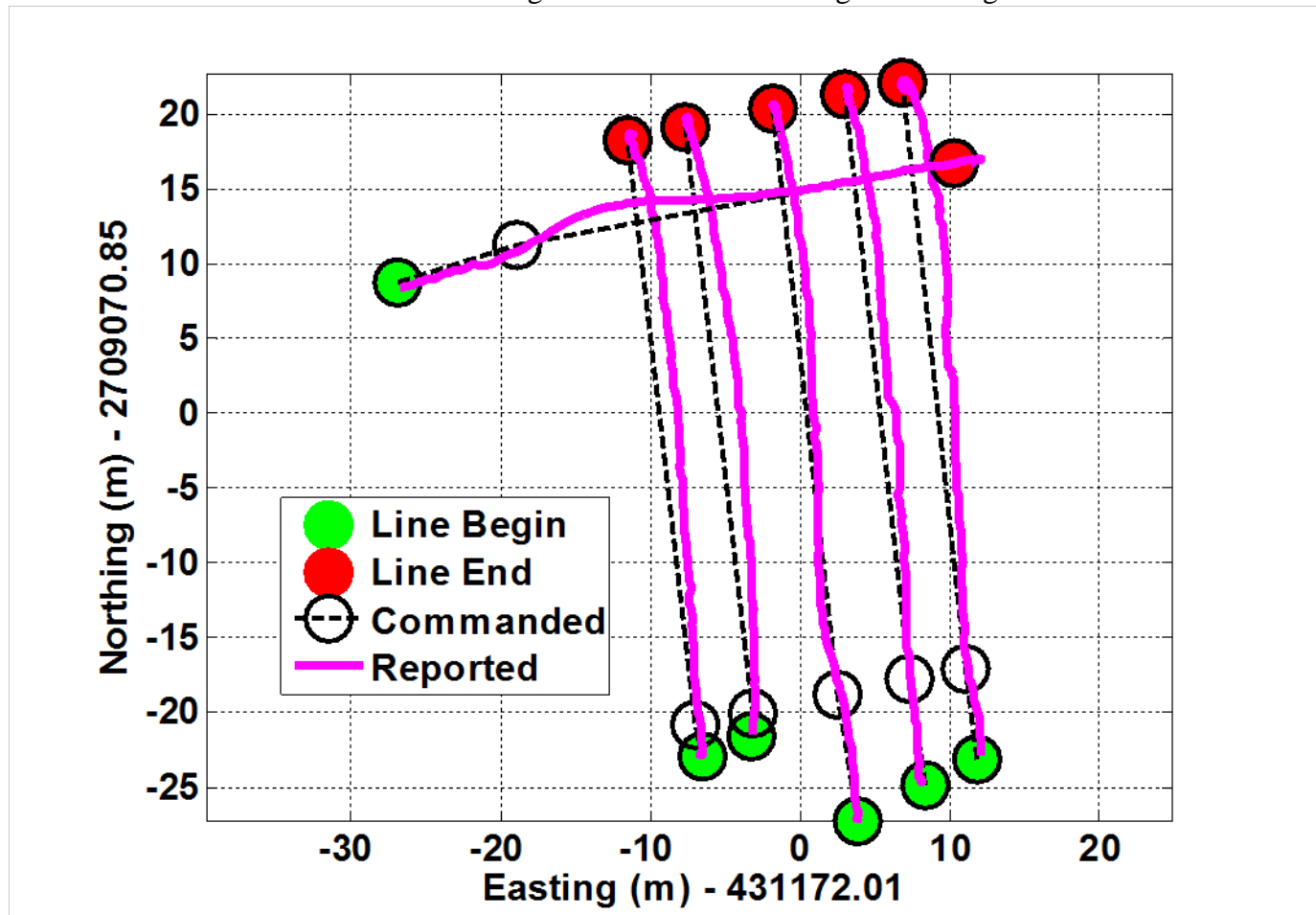


Figure 65 Desired line defined by waypoints (black circles), line beginning (green) and line ending (red) waypoints, and the reported location (magenta) of the ROV as it traveled between waypoints.

The summary performance of the waypoint navigation control as a function of approximate distance travelled reveals that the waypoint accuracy was within 0.65% distance travelled and the line following was approximately 1.75% distance travelled.

7.4 DETECTION

Detection metrics were calculated using the SNR and location of detections output from the detection processing and ground truth information. The target detection objective was target SNR greater than 9 dB for all targets greater than 60 mm in size. We achieved the objective with SNR greater than 20.7 dB for all targets including data from sensor altitudes between 20 cm and 60 cm. The largest detection SNR value was 84 dB for the large ISO and the smallest was 20.7 dB for the 60mm mortar.

Detections were scored as TOI detections if the detection location was within a radius of 1.5 m of the TOI ground truth location. Five non-TOI alarms were generated at SNR values greater

than 9 dB; three were from emplaced clutter targets and 2 were from natural clutter within the survey area. Table 6 shows the SNR and offset from the estimated target location to the ground truth location for all of the TOI.

Table 6. Detection performance results.

ID	Target	Detected?	SNR (dB)	Offset (m)
1	60 mm	Detect	20.7	1.23
2	81 mm	Detect	22.1	0.56
3	Large ISO	Detect	83.6	0.26
4	81 mm	Detect	65.9	0.43
5	81 mm	Detect	54.1	0.58
6	81 mm	Detect	60.4	0.12
7	Medium ISO	Detect	38.5	0.80
9	81 mm	Detect	37.5	0.50
10	Medium ISO	Detect	48.1	0.40
12	Large ISO	Detect	76.9	0.40
13	60 mm	Detect	25.7	0.33
14	Medium ISO	Detect	38.3	0.71
17	105 mm	Detect	25.8	1.07
18	155 mm	Detect	61.6	0.91
19	90 mm	Detect	33.4	0.37
20	3" Round	Detect	52.6	0.90
21	105 mm	Detect	69.5	0.32

7.5 LOCALIZATION ACCURACY

We calculated two estimates of ROV location. The first estimate was based on USBL data only. The second estimate fused USBL and INS data. Localization processing consisted of the following:

1) Calibrate USBL Easting and Northing reports using GPS-surveyed control points.

We analyzed USBL data collected while the ROV hovered above GPS-surveyed locations to estimate a range and bearing error from the USBL data and GPS-surveyed data. USBL data were calibrated in range by reprocessing the raw USBL data with an adjusted sound speed to equal the range from GPS-surveyed locations. A bearing calibration was applied to center the USBL reports on the GPS-surveyed locations. Figure 66 below shows the raw and calibrated (filtered) USBL measurements.

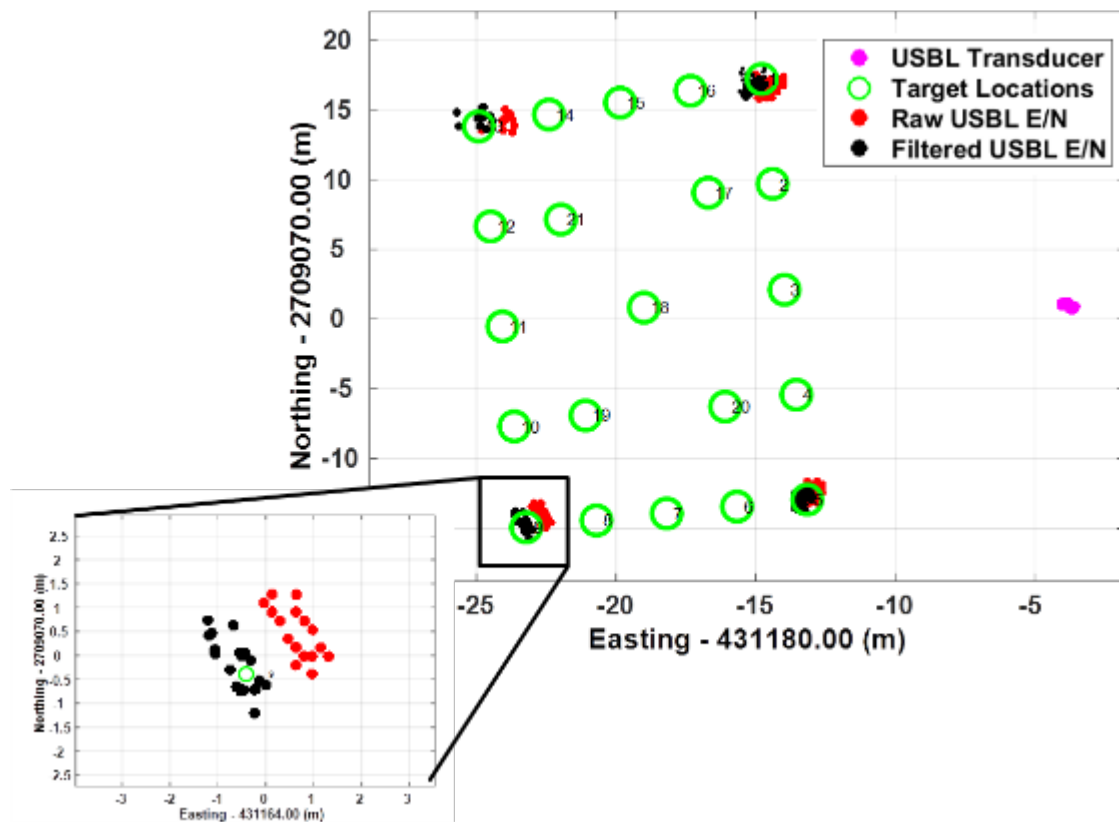


Figure 66. Raw (red) and calibrated (black) USBL Easting and Northing locations are shown. Each corner target location (green circle) were DGPS surveyed. The USBL transducer locations (magenta) are also shown. The zoom-in on the bottom left shows the effect of the calibration. Calibrated locations are centered around the surveyed location.

2) **Filter raw USBL range and bearing data to remove outliers.** Raw USBL reports output from the USBL sensor are unfiltered and calculated independently from measurement to measurement. Filtering was performed via outlier removal. Outliers were identified based on range and bearing transitions that were impossible based on the ROV's maneuverability, e.g., the bearing to the ROV at a range of 25 m cannot change from 10 degrees to 35 degrees within one second of ROV travel.

USBL and INS fusion processing involved the addition of the following processing steps:

1) **Recalculation of USBL range using depth from INS solution instead of depth reported by USBL system alone.** USBL systems utilize precise timing to determine the waveform propagation time between the USBL transducer and pinger. The sound speed is then applied to create a slant range between the two sensors. The horizontal and vertical angle of arrival are derived using phase delay estimation using data from tightly spaced acoustic elements in the USBL transducer. The horizontal angle of arrival translates directly to a bearing estimate. The vertical angle of arrival along with the slant range provides the required information to estimate the depth and horizontal range between the transducer and pinger. This standard USBL processing is prone to error from multipath effects especially in shallow water. Using the more reliable depth from the INS onboard the ROV we recalculate the horizontal range using the INS depth and slant range from the USBL. Figure 67 below shows the geometry involved.

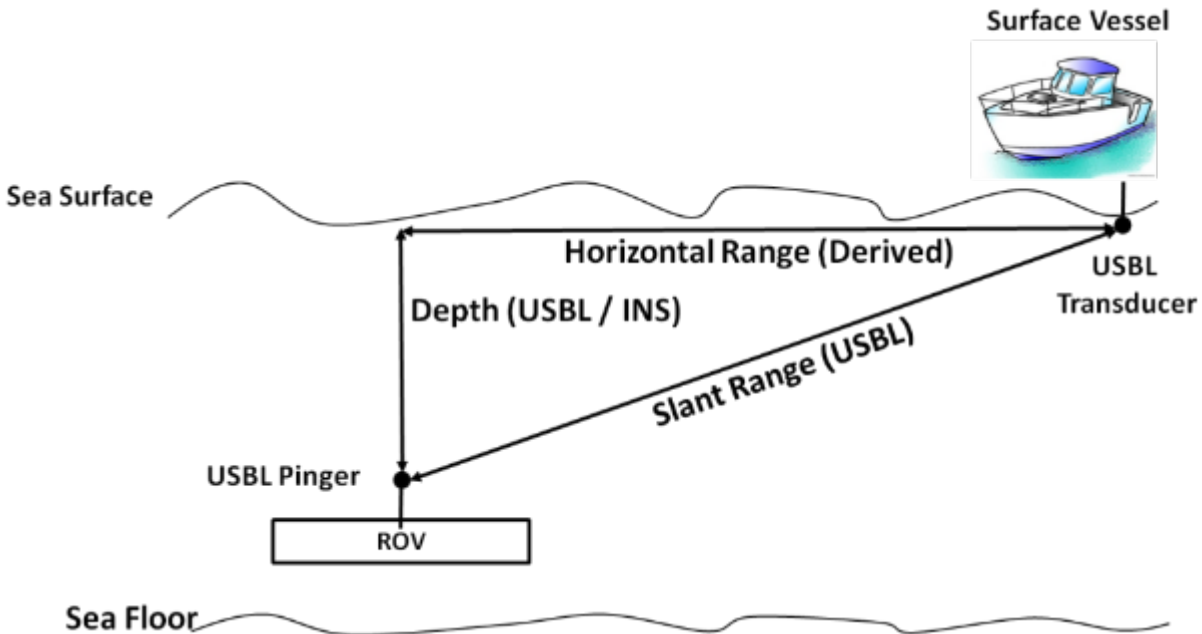


Figure 67 The slant range is provided by the USBL. The USBL estimates a depth estimate using the slant range and the vertical angle of arrival. The USBL depth and slant range are used to estimate the horizontal range. Horizontal ranges were adjusted using the more accurate depth estimate from the INS sensor onboard the ROV along with the USBL slant range.

2) Translate and rotate INS data using USBL start and end locations. The goal of the fused processing is to capitalize on the local accuracy of the INS and the global accuracy of the USBL. Figure 68 below shows an example of the USBL and Fused location estimates for a transect with large target responses in the center of the EMI sensor indicating ROV travel directly over the target locations.

We applied both the GPS-calibrated USBL positions and USBL-INS fused position estimates to the grid survey trackline data to compare and assess performance for localizing UXO targets. All tracklines exhibit a slight bend as a result of the cross-current during surveys. Although, the HAUV tried to track between waypoints, cross-currents, especially during periods of maximum tidal current, cause the system to veer off the linear transect and correct back around to achieve the ending waypoint. We utilized multiple waypoints in the HAUV mission planning to help mitigate this arching track effect with some success.

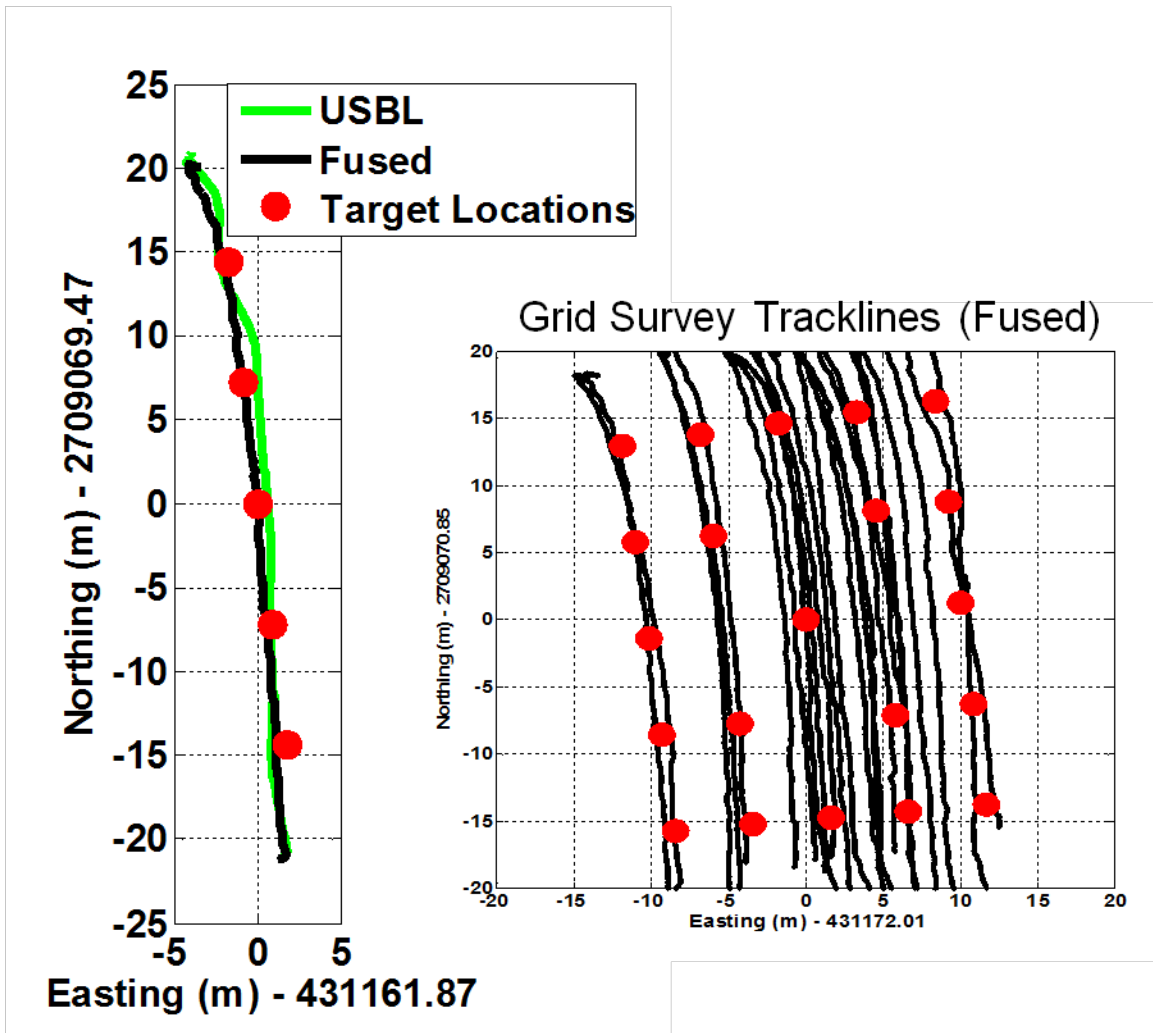


Figure 68 USBL (green) and Fused (black) position estimates for a transect with large target responses in the center of the EMI array indicating ROV travel directly over the targets. In this example the Fused locations provide a better estimate of the true ROV position during the transect.

USBL-INS fused locations were merged with magnetic field data from the EMI sensor to create a coverage map over the survey area. Figure 68 shows the coverage map created using this approach. Full coverage over the western portion of the grid was not possible due to limitations of the ROV positioning data on some of the traverses in that area. We were able to compile and grid EM data over traverses that encountered every target in the grid, thus enabling us to perform an analysis of detection and localization performance over every target.

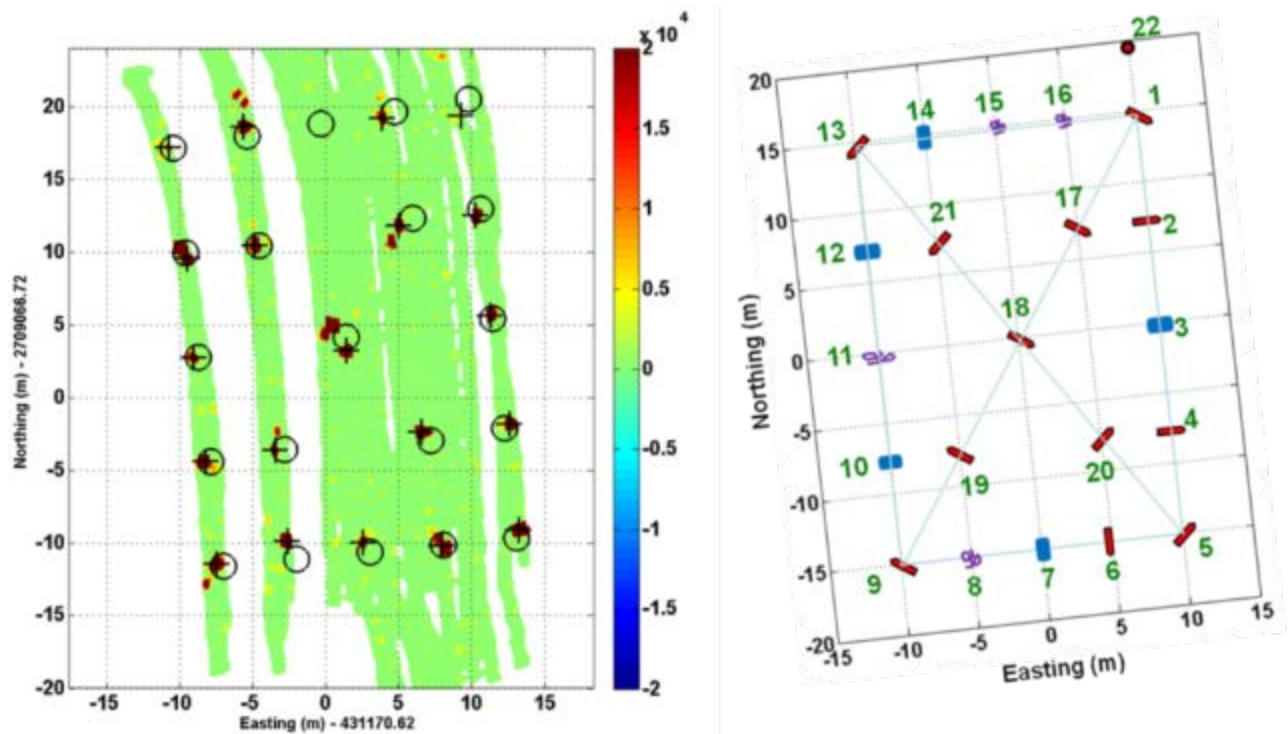


Figure 69. Coverage map created using EMI data integrated with filtered USBL position information.

USBL and USBL-INS Fused detection location accuracy metrics are compared in Table 7. Overall the USBL and Fused approaches yielded similar results with an average offset of 0.67 m and 0.66 m, respectively. The

Table 7. USBL and Fused detection location accuracy metrics

	USBL	Fused
ΔR (m)	0.67	0.66
ΔN (m)	0.29	-0.03
σN (m)	0.42	0.56
ΔE (m)	-0.22	-0.35
σE (m)	0.51	0.33

Overall, the performance objective of mean and standard deviation of Easting and Northing estimates less than 1 m were achieved. The detection location errors for both processing methods are show in Figure 70 below. The "bullseye" plot shows a slight westerly bias to the location errors, although no quantifiable statistical bias was established. Retrospective analysis revealed that heading errors from the INS data were likely the largest factor affecting the overall localization accuracy. For our waypoint-to-waypoint linear survey transects, there did appear to be any improvement when we included INS measurements in the navigation solution relative those without it. Other sources of error included those from the ship GPS, those associated with USBL range and bearing accuracy, across-track resolution of the EM receivers, and errors in the actual groundtruth locations.

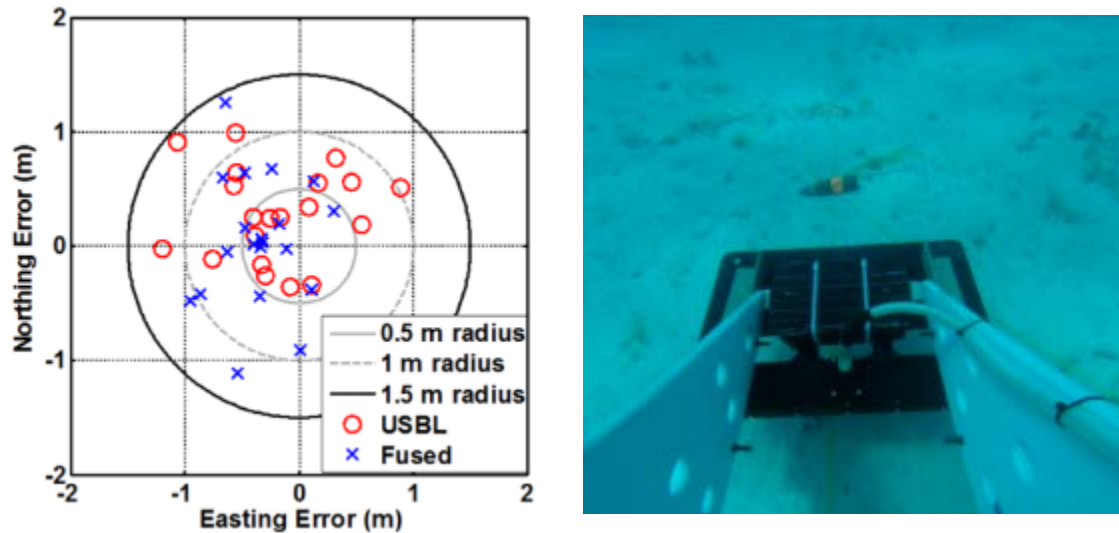


Figure 70. Detection location errors for USBL (red circle) and Fused (blue x) location estimates.

7.6 INTEGRATED SYSTEM STABILITY

The integrated system proved to be very stable in the water. Initial trimming of the system took approximately 30 minutes and consisted of adding 1 and 2 pound dive weights to the platform to make it level in the water. After system deployment, bubbles were released from under the system by a diver manually rocking the system back and forth on the water surface. This was all that was required after deployment in the water to permit operations.

7.7 OPERATIONAL EASE OF USE

We determined the ease of use of the system by overseeing and reviewing ROV-EM operations including system deployment, recovery, and data collection. Our deployment and data collection with the mid-sized integrated Dolores HAUV and integrated EM array provided information on launch and recovery (LAR) requirements, topside support, and data processing and analysis toward survey map and detection list production. The Dolores HAUV weighs over 500 pounds in air and thus requires a hoist for LAR and sufficient deck space for storage and maintenance. Figure 71 shows launch and recovery and desk operations of the system.

Since most of the system components are commercially available or otherwise supported line-replaceable units, the overall system has a great deal of modularity. This holds promise for future streamlining of integration, operations, maintenance, and sustainment. The ROV system is composed of bulk components that are highly modular. These include the ROV platform structure (frame, flotation, and mounting points) and its propulsion system (thrusters and actuators) as well as its tether and topside control system. The navigation and control system is the other key element pre-integrated with the ROV. This includes navigation and positioning sensors (inertial core/IMU, DVL, pressure sensors, altimeters, GPS or USBL, and other orientation sensors) and the control processors and tether management systems (power distribution and modem).

Launch and recovery (LAR) is an important factor in implementation infrastructure and associated cost and level of effort required to deploy the ROV-EM system. We found that even with the smallest mini-ROV systems, LAR will likely require some small davit to support sea-

based deployment. While the integrated system can be configured in a man-deployable form factor, it may not be worth the limitation in hydrodynamic mobility and control once the system is in the water. Even through our demonstration configurations were too large and cumbersome to alleviate the need for a davit for LAR, we found that the process given an appropriate deck configuration and vessel size (approximately >25 foot length) was not a significant factor for operational considerations. The difference between the required winch and deck support for LAR of a mid-size (Dolores) ROV in comparison with that for a smaller inspection ROV (vLBV) was not likely to play an important role in configuring the overall system.



Figure 71. Dolores HAUV-1000 integrated ROV-EM system launch and recovery operations. The system requires sufficient deck space and hoist capability to deploy over the side of the vessel.

Personnel required for ROV-EM operation using the Dolores platform and MFDA EM sensor includes: 1) ROV pilot, 2) Co-pilot to assist in sensor monitoring and data logging, and 3) a minimum of one person to monitor the tether and aid in deployment and recovery of the ROV-EM platform. The pilot planned missions and performed command and control of the ROV through the pilot user interface (UI). This interface has a number of features for planning missions, viewing and controlling the ROV configuration, creating real-time event markers (aka, Man Over Board), logging and playing back system data, displaying and logging EM data and sonar data and controlling the ROV subsystems such as thrusters, lights, cameras, sonar systems, and other auxiliary sensors. The UI was found to support more than enough functionality to fully operate the ROV-EM system. Figure 72 below shows some examples of the UI.

We developed a Standard Operating Procedure (SOP) and QuickStart guide for operational users conducting geophysical surveys with the system. The guidance documentation is meant to provide single button access to run EMI array command and control and data acquisition when performing marine operations with the integrated ROV-EM system. Three software executables were also provided: one for starting and logging synchronized MFDA data files during HAUV operations (mfdaLOG.exe), one for local logging and system diagnostics independent of the HAUV (for example, for deck checks or system calibration checks; mfdaRT.exe), and one for raw serial data communication troubleshooting (this allows direct access to the MFDA microprocessor configuration; mfdaSerialCom.exe). The combination of the SOP documentation, software executables, and associated software QuickStart guides successfully

enabled non-expert operators to acquire data with the system without White River Technologies expert users and analysts on-site. This has resulted in over 800 hours of operations with the ROV-EM system without expert technical staff on-board the host vessel and represents the potential for transition of the technology to operational application.

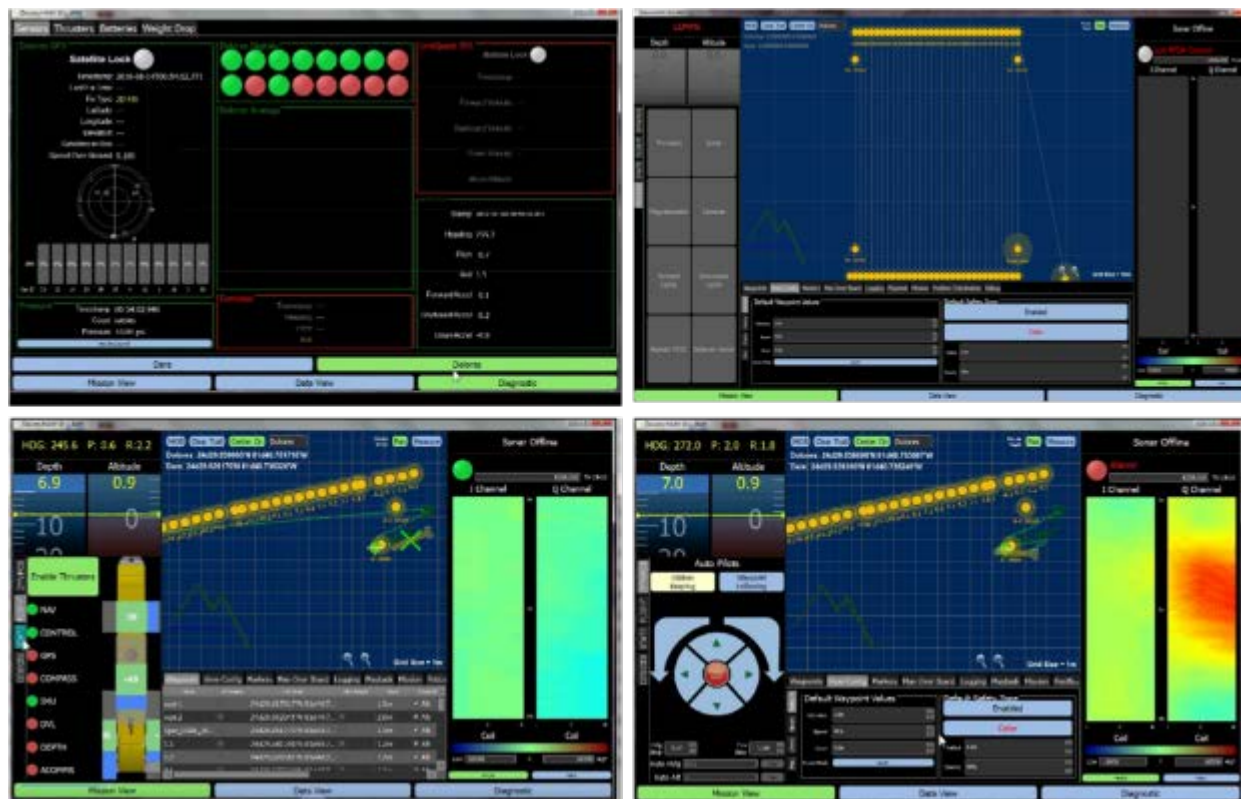


Figure 72. Various screen captures of the integrated HAUV-EMI graphical user interface. The top left image shows one of system configuration windows. The top right shows system configuration information and map display of waypoints set up during mission planning of grid surveying. The bottom left image shows a screen grab during operation waypoint missions with system configuration and status information on the left, waypoint map information and mission plan data in the middle, and MFDA real-time data display on the right. The bottom right image shows a similar view with a different set of real-time system data displayed on the lefthand portion of the UI.

Regarding the collection of data with the ROV-EM system, we determined that the UI used during these data collections contained all of the information display and control functionality required for efficient ROV-EM operations in UXO remediation applications. A single operator was capable of setting and invoking navigation, positioning, and autonomy parameters as well managing the data collection. During relatively dynamic conditions when numerous tasks are being observed or managed by an operator, it may be prudent to divide ROV system management and sensor data acquisition management amongst two operators. The Dolores GUI consists of a pilot CPU providing control of the ROV and display of all ROV vehicle, position, sensor, and mission information. A co-pilot CPU provides a co-pilot access to the same GUI as the pilot with complete functionality with the exception of ROV control. In dynamic situations or when multiple sensors require monitoring simultaneously, the co-pilot may offload the pilot's workload by monitoring separate sensors and data. The co-pilot functionality is particularly

useful in sensor troubleshooting and data collection activities. In these situations the pilot is able to focus on ROV control while the co-pilot relays position and sensor information to the pilot.

Commanding/piloting, monitoring, and setting data acquisition of the ROV-EM system is conducted from the main control cabin. An ethernet network enables all system data that is managed by a Linux server CPU system to be distributed to additional computers or transmitted over the TCP/IP communications external network. In general, the pilot commands the ROV or adjusts waypoint and mission plans via the UI as needed during operations. A co-pilot may support in data acquisition logging, monitoring ROV cameras for obstructions or anomalies, or managing auxiliary sensor equipment as needed. The control cabin on the Dare contains 5 large screen monitor displays and 8 smaller computer monitors to accommodate multiple system operators, observers, or analysts. Figure 73 shows the general configuration of the control cabin and system monitors, joystick and UI control interfaces and topside computing system components.

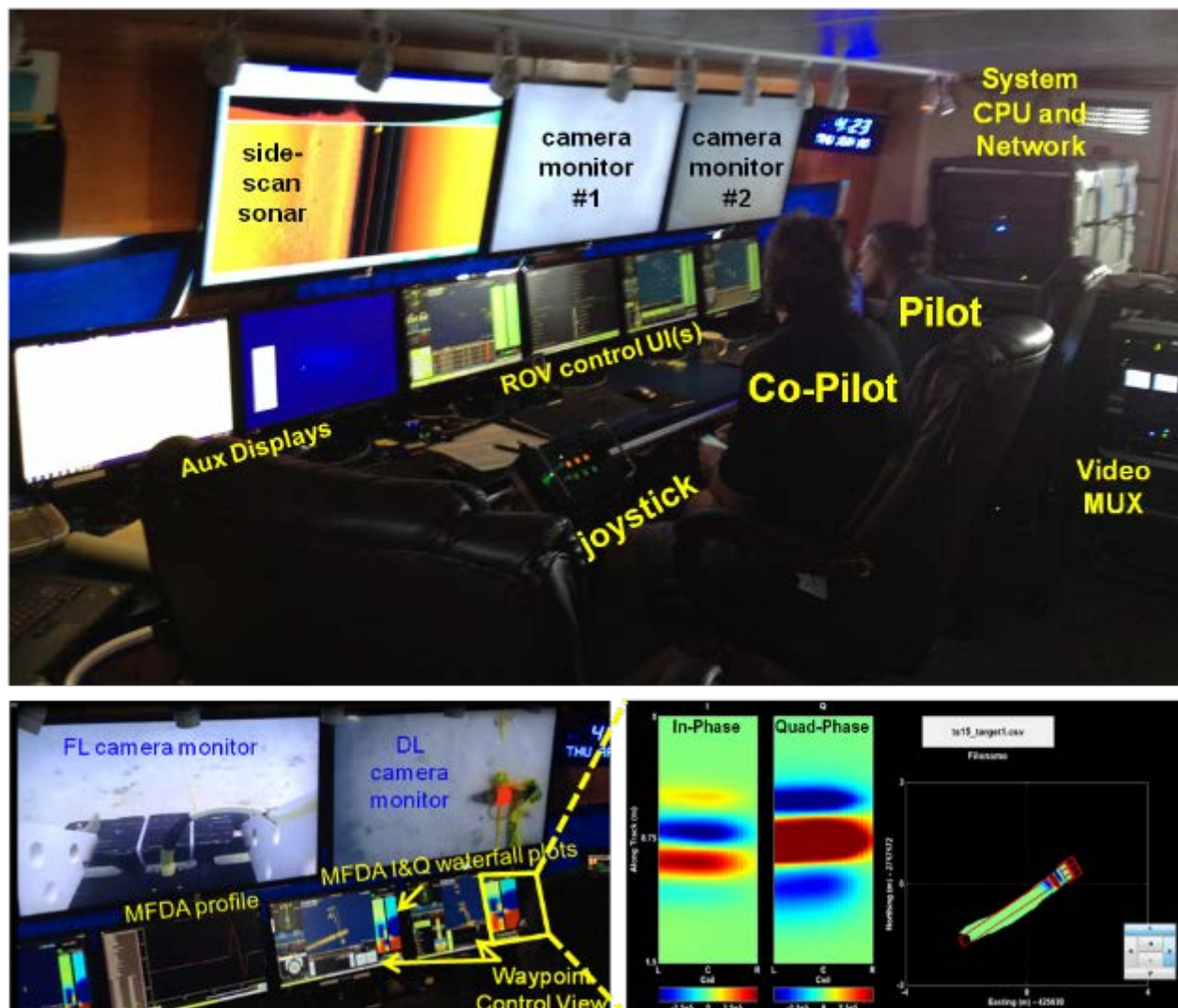


Figure 73. Photograph of the main control cabin are showing the layout of joystick control and flat panel displays for real-time awareness during operations. The bottom images show the myriad of camera, data, and user information displays and zoom-in of the MFDA data display and map tracking UI.

7.8 ASSISTED AUTONOMY

The assisted autonomy objective was to determine the improvements in the execution of ROV-EM applications using automated ROV behaviors such as altitude, heading, bottom following, station keeping, and waypoint navigation. Autonomous behaviors were critical to efficient calibration and operation of the ROV-EM system. The station keeping behavior allowed the collection of positional data while the ROV hovered over points of interest such as the GPS-surveyed coverage area corner locations. Manual attempts at station keeping are difficult due to onerous conditions imparted by current and tether drag. Autonomy was also critical for the EM mapping application that requiring accurate navigation along closely-spaced lines. Manual attempts at controlling ROV altitude, heading, and line following resulted in lower quality data requiring additional time compared to autonomous data collections. The additional time was due to abandoning numerous transects due to observed drifts in sensor altitude and drifting position from the desired altitude and line position.

8.0 COST ASSESSMENT

8.1 COST MODEL

The cost elements that were tracked during the demonstration in Florida are detailed in Table 8. The provided cost elements are based on a simple and incomplete cost model developed for the Dolores HAUV-1000-based ROV-EM system used in our demonstrations. The integrated ROV-EM system does not yet have a price developed for purchase or lease. Therefore, some aspects of the price elements must be estimated for the purposes of cost assessment.

Table 8. Cost Model for a Detection/Discrimination Survey Technology

Cost Element	Data Tracked	Estimated Costs
Instrument cost	N/A (See description below)	All major equipment and instrumentation are on-loan to the project by participating performers; estimated costs of the MFDA or similar array are \$150/day or \$750/wk
Support equipment lease rates	Lease rates for major components <ul style="list-style-type: none">• Engineering estimates based on current development• Lifetime estimate• Consumables and repairs	Vessel Charter: \$ 8,400/wk HAUV w/ Operator: \$ 5,500/wk EM array and NCS: \$ 1,200/wk USBL: \$ 700/wk RTK-GPS: \$ 1,200/wk
Mobilization and demobilization	Cost to mobilize to site <ul style="list-style-type: none">• Derived from demonstration costs	Equipment Prep (est.): \$ 950 Shipping (NH-FL-NH): \$ 3,810 TOTAL Mob/Demob: \$ 4,760
Site preparation	Time and cost to setup test site (relates to seafloor IVS set up)	Test Target Prep: \$ 350 Dive Ops Site Prep: \$ 1,300

Instrument setup costs	Unit: \$ cost to set up and calibrate Data requirements: <ul style="list-style-type: none"> • Hours required • Personnel required • Frequency required 	ROV Control Setup: \$ 525 EM Array Setup/QA: \$ 275 RTK-GPS Setup: \$ 175 TOTAL Setup: \$ 975
Survey costs	Unit: \$ cost per acre Data requirements: <ul style="list-style-type: none"> • Hours per acre • Personnel required 	1.1 acres/hour at 100% coverage 100% coverage (\$/acre): \$ 571 50% coverage (\$/acre): \$ 286 25% coverage (\$/acre): \$ 143
Detection data processing costs	Unit: \$ per hectare as function of anomaly density Data Requirements: <ul style="list-style-type: none"> • Time required • Fixed costs and Personnel required 	Fixed Costs: \$ 1,250 1 person (analyst at \$100/hr) 2 mins. / anomaly (average) Per anomaly (100/acre): \$ 3.33 Per acre (100/acre): \$ 333

Instrument Cost: There are four primary components of the demonstrated technology: 1) ROV including all power supply, propulsion, and tether subsystems; 2) DVL/IMU navigation sensors; 3) EM sensor; and 4) integrated navigation, control, and EM software. The ROV, navigation and control system, and EM sensor were on-loan to the project so no project cost was incurred for use of these components during this demonstration. To estimate cost for commercial use of this system the cost estimates for each component follow.

Remotely-operated vehicles vary in size, power, payload capacity, and sensor integration capability. For ROV-EM operation the size and power of small inspection-class vehicles such as the Seabotix vLBV ROV is the minimum required. Larger inspection and midsize class ROVs that provide more power but remain deployable using a davit and not requiring other specialized launch and recovery equipment are also appropriate for ROV-EM operation. Table 9 shows specifications, purchase and lease costs for several applicable ROVs.

Table 9. ROV lease and purchase data.

ROV System	Class (weight air)	Lease (\$/wk)	Price (est.)	LAR required	Support (hr/wk)
Seabotix VLBV	Inspection (22 kg)	\$ 3,500 / wk	\$ 100K	sm. davit	2
Saab Seaeye Falcon	Inspection (55 kg)	\$ 5,250 / wk	\$ 220K	med. davit	4
Teledyne Stingray	Inspection (32 kg)	\$ 4,500 / wk	\$ 160K	med. davit	2

The cost and accuracy of inertial navigation DVL/IMU sensor is primarily determined by the type of IMU used. Microelectromechanical systems (MEMS) IMUs are typically the least accurate and least expensive IMUs. Fiber optic gyro (FOG) based units are next in cost and accuracy. The most expensive and most accurate are Ring Laser Gyro (RLG) based units. Table 8 shows the specified accuracy and estimated purchase price of several DVL/INS navigation sensors.

Table 10. Inertial core navigation systems.

DVL/IMU System	IMU Type	Specified Accuracy (%DT)	Purchase (est.)
Greensea Bolton	MEMS	0.5	\$ 45K
CDL TOGS/NAV	FOG	0.1	\$ 105K
Kearfott KN-6053	RLG	0.05	\$ 230K

Figure 74 shows the estimated error over a 50 m distance traveled for the DVL/INS sensors in Table 10 above as well as a modestly-priced USBL system (Tritech MicronNav) and a more expensive, more accurate USBL unit (IXSEA GAPS).

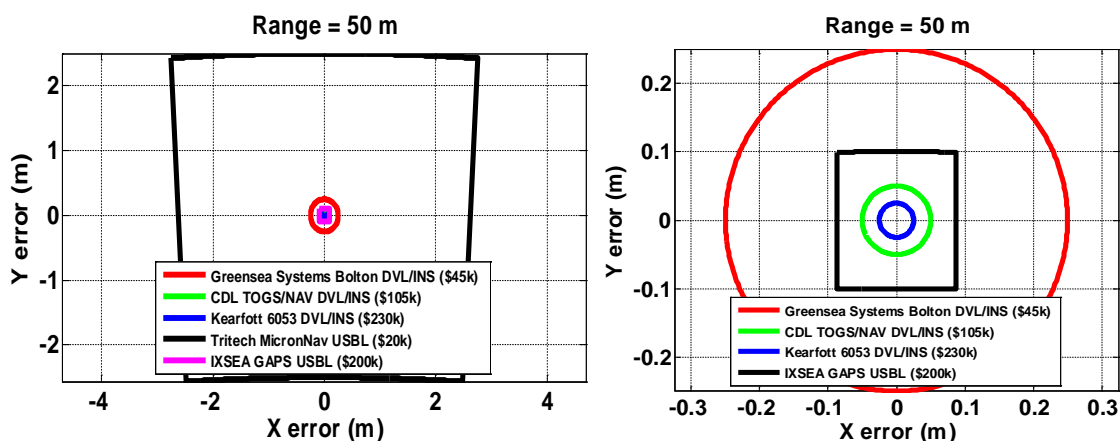


Figure 74. Left is the estimated error after 50 m distance traveled for DVL/IMU systems with a MEMS IMU (Greensea Bolton), FOG IMU (CDL TOGS/NAV), and a RLG IMU (Kearfott 6053). Also included for comparison are the Tritech MicronNav USBL system and the IXSEA GAPS USBL system. Right is the same figure with the Tritech MicronNav removed.

Key DVL specifications include the maximum altitude, minimum altitude, size weight and power (SWAP), and long term accuracy specifications. A 600 kHz unit with a minimum altitude of approximately 30 cm fits ROV-EM requirements. The DVL/INS sensor used in our test consisted of a Crossbow MEMS IMU and a Linkquest Navquest 600 Micro DVL with a specified 0.5% distance traveled accuracy

EM sensors applicable for underwater UXO applications vary in size and complexity. Although we do not have lease prices for the MFDA sensor, we estimate costs based on the commercially available Geonics EM-61S sensor. The EM-61S has a daily rate of \$95 and fixed mobilization charge of \$125.

Support Equipment Lease Rates: Since all major equipment and instrumentation were on-loan to the project by participating performers there are no capital equipment costs to record. Estimates of equipment lease rates were derived based on current published rates or requested quotations. In addition purchase price estimates were derived from quotations and published prices.

Support equipment such RTK-GPS, vessel, and environmental monitoring instrumentation have associated lease rates that were tracked independently (Table 11). This equipment is categorized as preferred, required, or not needed for UXO operations. All associated labor costs were tracked and aggregated to form the cost element assessment.

Table 11. Support Equipment Costs

Equipment	Lease cost	Purchase Cost	Category
RTK-GPS	\$1200 per week	\$40k	Required
USBL	\$700 per week	\$22-200k	Required
Vessel	\$8400 per week	N/A	Required
Conductivity Sensor	N/A	\$920	Preferred

Required RTK-GPS equipment consists of a GPS base station and rover with internal 450 MHz radios, survey controller hardware, and tripods. If there survey location is greater than approximately 1 km from the base station location an external high power radio will be required to achieve RTK accuracy.

USBL systems vary by accuracy and price from a modestly priced system like the Tritech MicronNav system used during our testing to a higher price, more accurate system such as the IXSEAP GAPS with a purchase price of approximately \$200K.

The vessel required to conduct ROV-EM operations must include:

- A winch system (or hand-operated davit) for launch and recovery of the vehicle
- Adequate deck space for launch, recovery, and storage of the system while in transit.
- Adequate cabin space for setup and operation of the ROV control station and navigation, control, and EM sensor data acquisition computer.
- Generator or battery power sufficient to provide power to the ROV and ROV control and data acquisition computers.

The conductivity and salinity sensor utilized on this project was a Hobo U24 conductivity data logger which logged data independent of ROV operation. COTS conductivity sensors are available for ROV integration. This sensor is in the preferred category because it is not necessary for ROV-EM operation but it does provide useful information regarding the local EM environment to be used during the data processing stage.

Mobilization and Demobilization: The cost for mobilization and demobilization activities are derived from actual costs including packing and shipping from Lebanon, NH to Key West, FL. The number of personnel and labor hours were tracked for specific mobilization /demobilization tasks. We estimate the total cost to mobilize the system inclusive of shipment via commercial carrier for our demonstration to be approximately \$4,760. The total labor and materials cost estimated for preparation of the system for mobilization is \$950. The breakdown of shipping costs yielded \$3,810 for shipping to and from the demonstration site.

Site Preparation:

The cost for site set up and preparation including target seeding were tracked based on actual labor hours and logistical costs associated with this cost element. This included the use of a 2-

person dive team for at least one full day to deploy underwater infrastructure. During testing we utilized members of our team that were certified divers for target deployment thereby reducing the costs incurred during testing.

We obtained a quote for \$75/hour from a local dive crew in order to estimate the anticipated dive crew costs. This \$6,000-weekly cost is for a two person (non-EOD trained) dive team. Non-EOD trained divers are used for operations such as calibration target deployment and setup of any other underwater infrastructure. It is unlikely that a dive crew will be required for the duration of a ROV-EM UXO remediation operations. Instead, they will be used only during the initial and final stages of the operation to install and remove underwater infrastructure such as the target calibration string. We estimate 6-10 hours of total dive operations that may be required for ROV-EM deployment activities, and thus \$900-1500 in dive operations for site preparation in addition to another 12 full-time equivalent man hours or an estimated \$1,440 in additional labor. All materials are assumed to be allocated through other mean (government-provided test objects).

Instrument Set Up Costs: The cost for preparation and set up of instrumentation including the ROV-based EM system, topside control components, launch and recovery, and supporting equipment. Time associated with non-recurring engineering or additional set-up required for engineering analyses was not included. We estimate 4-5 hours of labor for initial setup of the ROV control station including ROV unpacking and assembly, DVL/INS sensor mounting and cabling, and USBL setup. We estimate 2-3 hours labor for EM array setup and QA including EM array mounting and cabling. Configuration, setup, and checkout of the RTK-GPS system will take approximately 2 hours. Overall, this results in an estimated instrument setup cost of \$1,100.

Survey Costs: Because our test objectives involve individual mission scenarios beyond those associated purely with survey coverage, we segment survey costs as a separate mission. Waypoint mission control and survey coverage were estimated based on the actual time spent in survey mode normalized by the area covered. Costs are estimated from the incurred cost of labor and equipment (based on day-rate lease estimates) during survey mode operations. Area was calculated based on data acquired from the system navigation data. Based on estimates from the testing reported in this document 100% area coverage will cost \$571 per acre, 50% area coverage will cost \$286 per acre, and 25% coverage will cost \$143 per acre.

Detection Data Processing Costs: Detection-level processing costs will be pro-rated based on the prescribed data flow and standard procedures that are being demonstrated. Since different survey operations have different requirements, we will attempt to segment costs for separate mission scenarios. Costs will be estimated based on individual labor hours and any required fixed costs (e.g., for software licensing). Our estimate for data processing costs are \$333 per acre assuming approximately 100 anomalies per acre.

9.0 IMPLEMENTATION PROSPECTUS

The overarching goal of this demonstration project was to evaluate innovative technologies required for deploying underwater EMI sensors from ROVs in order to overcome limitations of current diver-deployed, towed, and unmanned integrated underwater UXO detection systems. The demonstration we conducted was the first that we are know of in which a full marinized multi-sensor EM array was tightly integrated with a HAUV system capable of controlled maneuvers close to the seafloor. The tests and analyses we conducted were intended as a through shakedown and preliminary evaluation in preparation for follow-on demonstrations at a current or former DoD underwater test range. Since the nature of the testing activities involved engineering integration, iterative evaluations and adjustments to optimize the system, we have did not attempt to assess capabilities and limitations of the system in a full-scale live site demonstration. Despite the preliminary nature of our assessment, we were able to evaluate the prospects and potential challenges for directly transitioning and implementing the system and related procedures for operational use in MMRP production environments.

Our demonstration sought to assess three primary types of survey activities that are relevant to underwater UXO detection and remediation operations: 1) Local Area Search Missions to detect, locate, and digitally mark UXO on or beneath the seafloor within a pre-defined munitions response area, 2) Anomaly Characterization to provide high resolution (i.e., full coverage) mapping, target localization, and potential classification analysis (via dynamic one-pass classification methods), and 3) Re-acquisition and Cued Classification Surveying to acquire stationary target confirmation and/or classification data for dig/no-dig assessment (Figure 75). Implementation issues and opportunities are discussed for each of these survey applications that we assessed.

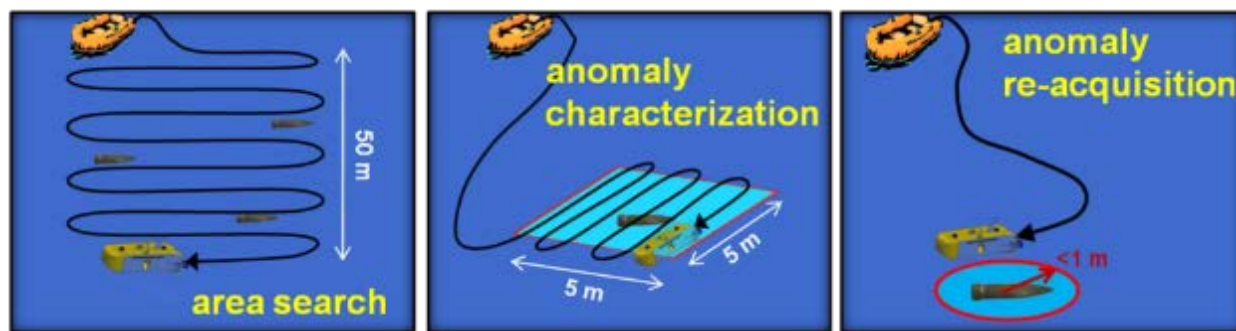


Figure 75. Survey activities relevant to underwater UXO detection include local area search (left), anomaly characterization (center), and anomaly re-acquisition (right).

8.1 LOCAL AREA SEARCH MISSIONS

Local area search missions include continuous mapping over areas of the seafloor on the order of 2000 to 10,000 m² (0.5 to 2.5 acres) for a given surface vessel anchoring site. For our demonstration we limited surveys to our grid area, which was 30 m by 40 m or 1600 m² (0.4 acres). Local search areas of this size are constrained by the range of the ROV system (typically 100-500 m) and degradation of positioning accuracy with range from the surface deployment vessel. These range-dependent local positioning accuracy issues appear to dominate the overall performance of the ROV-EM system. Overall the ROV-based EM technology we demonstrated was *generally effective* for local area search missions with clear limitations and associated opportunities for operational improvement.

Local positional accuracy metrics are specified differently for each type of system based on the localization algorithms and sources of error specific to each system. Local USBL positional accuracy is estimated by the range from transceiver to transponder and a bearing error. Therefore, as the range from the USBL transceiver (typically located on a surface vessel) and the USBL responder / transponder (located on the underwater asset to be tracked) increases the positional accuracy decreases. Local INS positional accuracy is typically specified as a percentage of distance traveled due to the accumulating error found in the inertial measurement unit (IMU) sensor inside the INS. Local LBL localization accuracy is dependent on the configuration of the LBL beacons on the seafloor. With proper configuration and calibration of the LBL beacons within a survey area, centimeter level accuracy may be obtained across the entire survey area. Figure 76 shows the positional accuracy of a USBL, INS, and LBL positioning system with respect to our 30 m by 40 m survey area.

Global position estimation based on a local position requires transformation of the local reference frame to a global reference frame. The first step in this process is the rotation of the local frame to a global frame using local heading information provided by an IMU. IMU heading measurement errors result in errors in global position estimates. Next, a translation from local (X,Y) to global UTM coordinates (Easting, Northing) requires GPS data. The error in the local position measurement and the error in the GPS measurement, on the order of +/- 1 m in non-RTK DGPS systems, contribute to the error in the translated global position.

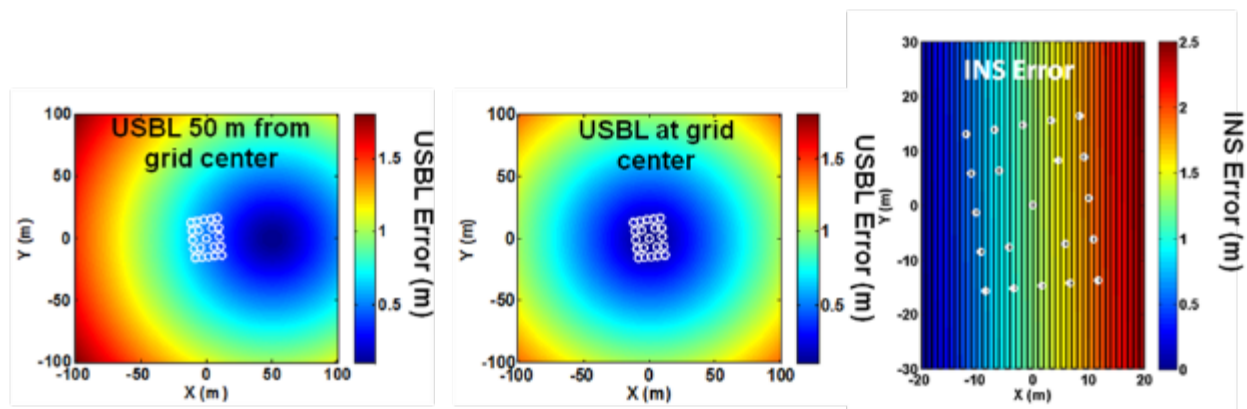


Figure 76 Positional accuracy estimates over a 50 m x 50 m survey area (black square) for four scenarios. Top left: USBL system with the USBL transceiver (white circle) located 50 m East of the center of the survey area. Top right: USBL system with the USBL transceiver (white circle) positioned directly over the center of the survey grid. Note the improved accuracy over the survey area due to the reduced ranged from the USBL transceiver to the survey area. Bottom left: INS position system accuracy on a survey platform starting the survey in the southwest corner of the survey area and following 1 m spaced lines (white) in a lawn mower pattern across the survey area. Without calibration from a secondary positioning system INS error increases with distance traveled. Bottom right: LBL error is constant across an area encompassed by calibrated LBL transceivers (white circles).

Another key function we assessed during local area search missions was bottom following control in order to enable the ROV to keep the EM array in close proximity to the seafloor. This is essential to providing close range to targets (<1.5 m) and associated SNR. We found that bottom following control was effective regardless of distance travelled or type of environment

over which the system was traversing. We note that our demonstrations were somewhat limited in bottom condition variability and that challenges expected in more varied terrain. Specifically, it is anticipated that the DVL bottom-lock consistency and altitude accuracy will degrade in areas with dense, high, or highly variable benthic vegetation such as sea grass. Another potential limitation of bottom following control during local area surveys may be due to sudden or frequency changes in bottom morphology (i.e., rugosity) over reefs or reef patches. In these cases, additional information from acoustic altimeter (pinger), forward looking sonar and/or pressure depth gauges could be utilized to fuse with DVL data and provided to the altitude estimation and bottom following control algorithm (B. Kinnaman, pers. comm.).

A clear limitation of the ROV-EM system we demonstrated in terms of survey coverage efficiency is due to the limited size of the EM sensor array used and potential to hold positioning accuracy over time. Through utilization of the USBL system and survey of local fiducials using boat-mounted GPS, our system requires no periodic activity for resetting accumulating navigation errors. Data collection of USBL data while the system hovers above the surveyed fiducials at the beginning and end of each day is the only additional time required to maintain accurate navigation estimates throughout the survey day. This procedure does accrue additional costs that are not accounted for in our estimates provided in Section 8.

Full coverage over a site requires 1 transect every 50 cm. Therefore, at an estimated 1 knot (0.51 m/s), our estimated survey coverage efficiency is approximately 4.4 hours per acre (requiring 8192 m of linear line transect surveying). Including turnaround time and daily IVS and related QA checks, this is equivalent to approximately 1.5-2 acres per day. The survey efficiency simply scales linearly with array survey coverage swath width or areal coverage planned. Thus, a 2 m wide array would likely cut the current survey time in half and increase the production rate to 3-4 acres per day. Commensurately, a 50% coverage requirement would result in the same areal coverage efficiency. This assumes best case conditions; hydrodynamics and site/survey complexity may degrade maneuverability, survey production efficiency, and, correspondingly, coverage rates.

8.2 ANOMALY CHARACTERIZATION

Anomaly characterization over relatively small areas of the seafloor may be useful to conduct when the ROV-EM system is cued to the area by previous surveys or other information (e.g., wide area magnetometer mapping or acoustic mapping survey data). In this case, the ROV-EM operator may wish to survey at high resolution over a limited area on the order of 10-50 m² (5m x 5m area, for example). This type of close-in high surveying requires lateral and vertical control that is accurate and precise enough to produce densely sampled high-quality EM data. This type of survey mission may ultimately be used for dynamic classification data acquisition and thus must have the control and stability to acquire data for inversions. Because of the stability of the platform and associated ability to acquire relatively high SNR data over small areas, we found the overall anomaly characterization application to be *very effective* for ROV-based EM.

Another potential application may be to refine localization of potential target based on data from a prior wide area assessment surveys. For these missions, we found the use of integrated real-time video and sonar data very informative for referencing points on the seafloor, general

context, and spatial awareness. The real-time awareness is facilitated by continuous connection subsea-to-topside via the fiber optic tether system. This is in contrast to a fully autonomous unmanned vehicle such as the torpedo-like form factor AUVs utilized for more covert military sensing operations. The point-to-point relative position accuracy appears to be good enough over these small areas to perform dynamic or multipoint inversion to aid in characterizing and discriminating targets. This may provide a useful mechanism for future dynamic classification methods for marine UXO.

8.3 RE-ACQUISITION AND CUED CLASSIFICATION

Reacquisition surveys based on predefined coordinates may be important for visual inspection, marking, detailed confirmation data collection with EM, sonar, or a combination of them, as well as for potential static cued data collections for advanced classification data collection. The ROV-EM system may also be utilized in reacquisition surveys in collaboration with other ROV-based systems in order to guide them to a location for remediation operations. In this case, the ROV-EM system would act as the anomaly location system and would guide another ROV equipped with additional equipment such as an excavator, manipulator or robotic arm, or perhaps an explosive charge for blow-in-place operations.

For this mission, the ROV-EM system we demonstrated was *generally effective*, but had limitations associated with navigation and positioning accuracy that increase with range in the case of inertial navigation with or without USBL integrated. Overall, the reacquisition capability allowed for anomalies to be localized to within an approximate 1 m circular error probability.

Furthermore, the station keeping control capability was very effective at holding position to within ~25cm over a target position for minutes at a time in low to moderate current conditions. Some adjustments may be required and degradation experienced in current conditions exceeding the maximum 1.8 knot currents we experienced during our demonstration. The ability to hover and hold position over a cued point may be a necessary feature for ROV-EM if used for cued EM classification surveys. Although, we did not explicitly test this functionality, the ROV-EM system is projected to be relatively effective at the controlled data collection required to successfully operate in this mode. The MFDA array we used was not suitable for either dynamic or cued classification due to its inability to produce multi-angle EM excitation and effectively elucidate all three components of the magnetic polarizability of targets under the array.

10.0 REFERENCES

- Brandes, H.G., 2001, Geotechnical properties of marine sediments from acoustic measurements, Proc. International Offshore and Polar Engineering Conference (2001), 482-487.
- Bruschini, C., 2004, On the low frequency EMI response of coincident loops over a conductive and permeable background reduction schemes, IEEE Geoscience and Remote Sensing, 42, 1706-1719.
- Davis, A., Huws, D., Pyrah, J., and Haynes, R., 1998, New geophysical technologies applied to the quantitative evaluation of seabed properties related to mine burial prediction, In Coastal Benthic Boundary Layer (CBBL) Research Program Final Reports, NRL/MR/7430--98-8213 by Richards, M.D., 386 pps.
- Hoffmeitster, J.E., and Multer, H.G., 1968, Geology and origin of the Florida Keys, Geologic Society of America Bulletin, 79, 1487-1502.
- Incze, M.L., 1998, Petrophysical properties of shallow-water carbonates in modern depositional and shallow subsurface, University of Miami, PhD Thesis, 405 pp.
- Jaap, W.C., 1984, The ecology of the south Florida coral reefs: A community profile, U.S. Department of the Interior, Fish and Wildlife Service and Minerals Management Service Publication FWS/OBS 82/08 and MMS 84-0038, 138 pp.
- Jackson, P.D., Briggs, K.B., Flint, R.C., Hoyler, R.J., and Sandidge, J.C., 2002, "Two- and three-dimensional heterogeneity in carbonate sediments using resistivity imaging", Marine Geology, 182, 55-76.
- Keith and Schnars, 2012, Preliminary Draft of the Atlantic Fleet Training and Testing Environmental Impact Statement, U.S. Navy Fleet Force Command, 27 pp.
- Keller, B.D and Causey, B.D, 2005, Linkages between the Florida Keys National Marine Sanctuary and the South Florida Ecosystem Restoration Initiative, Ocean and Coastal Management, 48, 869-900: doi: 10.1016/j.oceanaman.2005.03.008.
- Lavoie, D.L., Richardson, M.D., Holmes, C., 1997, Benthic boundary layer processes in the Lower Florida Keys, Geo-Marine Letters, 17, 232-236.
- Lidz B.H., Reich, C.D., and Shinn, E.A., 2003, Regional Quaternary submarine geomorphology in the Florida Keys, GSA Bulletin, 115, 845-866.
- Lidz, B.H., Robbin, D.M., and Shinn, E.A., 1985, Holocene carbonate sedimentary petrology and facies accumulation, Looe Key National Marine Sanctuary, Florida, Bulletin of Marine Science, 36, 672-700.
- Lidz B.H., Shinn, E.A., Hine, A.C., Locker, S.D., 1997, Contrasts within an outlier-reef system: Evidence for differential Quaternary evolution, south Florida windward margin, J. Coastal Res., 13, 711-731.
- Lidz, B.H., Shinn E.A., Hansen, M.E., Halley, R.B., Harris, M.W., Locker, S.D., and Hine, A.C., 1997, Sedimentary and biological environments, depth to Pleistocene bedrock, and Holocen sediment and reef thickness from Molasses Reef to Elbow Reef, Key Largo, south Florida, U.S.G.S., Survey Miscellaneous Investigations Series Map I-2505, Scale 1:24,000, 3 sheets.

- Mueller, E., and Winston, G.O., 1992, Geologic history of the Florida Keys, In J. Gato Eds, The Monroe Country Environmental Story, Big Pine Key, FL, Monroe Country Educational Task Force, 370 pp.
- National Historic Center, Underwater Archeology Branch, 2003, The Boca Chica Channel Wreck: A site assessment, Washington, D.C., B00FOBL2B6, 166 pp.
- Nelson H.H., Bell, T., Kingdon, J., Khadir, N., and Steinhurst, D.A., 2009, "EM61-MK2 Response of Three Munitions Surrogates", NRL Report NRL/MR/6110--09-9183.
- Peery G.M., Lidz, B.H., Wiese, D.S., 2002, Archive of seismic reflection data collected during USGS cruise 97KEY01, upper and middle Florida Keys, 12 October - 1 November, 1997"U.S.G.S. Open File Survey Report 02-421 (DVD and CD ROM).
- Richardson, M.D., 1996, Coastal Benthic Boundary Layer research program: A review of the third year, NRL Report NRL/MR/7431--96-8001, 242 pp.
- Richardson, M.D., Lavoie, D.L., Briggs, K.B., 1997, Geo-acoustic and physical properties of carbonate sediments of the Lower Florida Keys, Geo-Marine Letters, 17, 316-324.
- Schultz, G., Shubitidze, F., Miller, J., Evans, R., 2011, Active source electromagnetic methods for marine munitions, in Detection and Sensing of Mines, Explosive Objects, and Obscured Targets XVI, Proceedings of SPIE, Vol. 8017-17.
- Schultz, G., 2013, "MR-201233 Demonstration of ROV-based Underwater Electromagnetic Array Technology", ESTCP Interim Report for Project MR-201233, 95 pp.
- SERDP, 2007, SERDP & ESTCP Workshop on Technology Needs for the Characterization, Management, and Remediation of Military Munitions in Underwater Environments, 45 pp.
- Shinn E.A., Lidz, B.H., Holmes, C.W., 1990, "High-energy carbonate sand accumulation, the Quicksnads, southwest Florida Keys", Jour. Sediment. Petrol., 60, 952-967.
- Shinn, E.A., and Japp, W.C., 2005, "Field guide to the major organisms and processes building reefs and islands of the Dry Tortugas: The Carnegie Dry Tortugas laboratory centennial celebrations (1905-2005)", U.S.G.S. Memoir, Key West, 13-15, October 2005, 53 pp.
- Shinn, E.A., Lidz, B.H., Hudson, J.H., Kindinger, J.L., and Halley, R.B., 1989, "Reefs of Florida and the Dry Tortugas", IGC Field Trip Guide T176, Washington D.C., American Geophysical Union, 53 p.
- Stamatescu, L., and Schultz, G.M., 2007, Minelab's advanced EMI array, UXO & Countermine Range Forum 2007, Orlando.
- Stamatescu, L., and Nesper, O., 2012, Multi-frequency Transmitter for a Metal Detector, USPTO Patent 81259225 B2, Filed June 2009, Published April 2012.
- Stephens, K.P., Lavoie, D.L., Briggs, K.B., Furkurawa, Y., Richardson, M.D., 1997, Geotechnical and geoacoustic properties of sediments off south Florida: Boca Raton, Indian Rocks Beach, Lower Tampa Bay, and the Lower Florida Keys, NRL Report NRL/MR/7431--97-8042, 314 pp.
- Turner, P.T., 2007, Western Sambos Ecological Reserve reconnaissance: Descriptive report to accompany hydrographic survey H11658, NOAA 76-35A, H11658 Report, Project M-H910-NRT7-07 NOAA Vessel Survey NRT-7, S3004, 26 pp.

- Vaughn, T.W., 1915, The geologic significance of the growth rate of the Floridian and Bahaman shoal-water corals, Jour. Wash Acad Sci, 5, 591-600.
- Windhorn, S. and Langley, W., 1975, Yesterday's Florida Keys, Langley Press: Key West.
- Winsberg, M.D., 1990, "Florida weather", Orlando, FL, University of Central Florida Press, 171 pp.

Relevant website addresses related to referenced material in this plan:

pubs.usgs.gov/pp/2007/1751/professional-paper/
www.link-quest.com/html/intro_nq.htm
www.minelab.com/usa/consumer/knowledge-base/minelab-technologies#FBS
www.moog.com/news/operating-group-news/2011/moog-announces-undersea-integrated-control-interface-navigation-system
www.necc.navy.mil/
www.seaeye.com/falcon.html
www.trimble.com/trimbler8.shtml
www.tritech.co.uk/product/usbl-tracking-system-micronnav
www.xbow.com/products/inertial-products

APPENDICES

Appendix A: NOAA FKNMS Access Permit for AUV Testing.



UNITED STATES DEPARTMENT OF COMMERCE
National Oceanic and Atmospheric Administration
NATIONAL OCEAN SERVICE

Florida Keys National Marine Sanctuary
33 East Quay Road
Key West, FL 33040

April 28, 2015

Mr. Kim Fisher
Motivation, Inc.
200 Greene Street
Key West, FL 33040

Dear Mr. Fisher:

The National Oceanic and Atmospheric Administration, Office of National Marine Sanctuaries (ONMS) has approved the issuance of permit amendment number FKNMS-2006-052-A6 to conduct AUV testing activities in Florida Keys National Marine Sanctuary (sanctuary). This amendment supersedes all previous permits or amendments for this activity. Activities are to be conducted in accordance with the permit application and all supporting materials submitted to the sanctuary, and the detailed terms and conditions of permit number FKNMS-2006-052-A6 (enclosed).

You are responsible for reviewing and understanding all terms and conditions of this amendment. However, the changes made in this amendment from the previous permit or amendment can be summarized as follows:

This permit has been amended to include the placing of temporary targets on the sand bottom for use in the testing of tethered hybrid AUV equipment within in the specific location identified within this permit. Deploying targets and testing tethered hybrid AUV equipment may be conducted periodically for the duration of this permit and within specified location only. All targets must be removed at the end of each test.

Reporting requirements under Special Condition #10 have changed. Permittees shall send notification via e-mail to FKNMSPermits@noaa.gov each day when engaging activities under FKNMS historical resource permits.

Your permit contains specific terms, conditions and reporting requirements. Review them closely and fully comply with them while undertaking permitted activities.

If you have any questions, please contact Brenda Altmeier at Brenda.Altmeier@noaa.gov. Thank you for your continued cooperation with the ONMS.

Sincerely,

Sean Morton
Superintendent

Enclosure



Appendix B: ESTCP MR-201233 Year 1 Engineering Test and Demonstration Interim Report.